Institut für Wasserbau · Universität Stuttgart

Mitteilungen

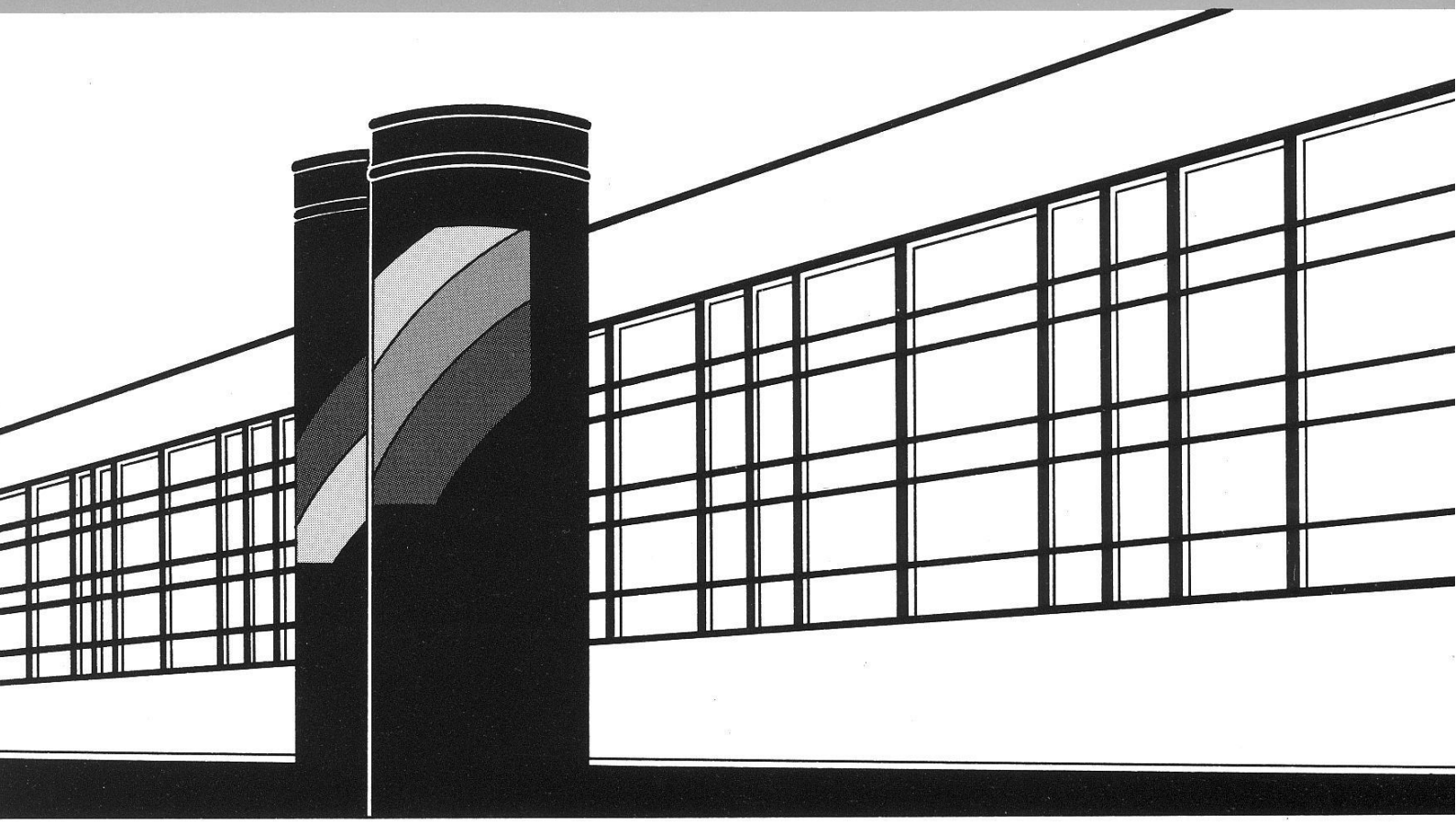

Heft 162

Tesfaye Kebede Gurmessa

Numerical Investigation on Flow and Transport Characteristics to Improve Long-Term Simulation of Reservoir Sedimentation

Numerical Investigation on Flow and Transport Characteristics to Improve Long-Term Simulation of Reservoir Sedimentation

Von der Fakultät Bau- und Umweltingenieurwissenschaften der Universität Stuttgart zur Erlangung der Würde eines Doktor-Ingenieurs (Dr.-Ing.) genehmigte Abhandlung

Vorgelegt von
Tesfaye Kebede Gurmessa
aus Ambo, Shoa, Äthiopien

Hauptberichter:	Prof. Dr.-Ing. habil. Bernhard Westrich
Mitberichter:	Prof. Dr. rer.nat. Dr.-Ing. habil. András Bárdossy
Mitberichter:	Prof. Gerhard H. Jirka, Ph.D.

Tag der mündlichen Prüfung: 21. Juni 2007

Institut für Wasserbau der Universität Stuttgart
2007

Heft 162

Numerical Investigation on Flow and Transport Characteristics to Improve Long-Term Simulation of Reservoir Sedimentation

von
Dr.-Ing.
Tesfaye Kebede Gurmessa

Eigenverlag des Instituts für Wasserbau der Universität Stuttgart

D93 Numerical Investigation on Flow and Transport Characteristics to Improve Long-Term Simulation of Reservoir Sedimentation

Titelaufnahme der Deutschen Bibliothek

Kebede Gurmessa, Tesfaye:

Numerical Investigation on Flow and Transport Characteristics to Improve Long-Term Simulation of Reservoir Sedimentation / von Tesfaye Kebede Gurmessa. Institut für Wasserbau, Universität Stuttgart. Stuttgart: Inst. für Wasserbau, 2007

(Mitteilungen / Institut für Wasserbau, Universität Stuttgart: H. 162)
Zugel.: Stuttgart, Univ., Diss., 2007
ISBN 3-933761-66-2
NE: Institut für Wasserbau < Stuttgart >: Mitteilungen

Herausgegeben 2007 vom Eigenverlag des Instituts für Wasserbau
Druck: Sprint-Druck, Stuttgart

Preface

Planning, construction and maintenance of water reservoirs become increasingly important, in particular in countries and regions which are vulnerable to climate change. Therefore reservoir sedimentation and sustainable sediment management is an important issue in water resources engineering and management. Reservoir sedimentation has great technical, economic and social implications. It is a challenging task for hydraulic and environmental engineers to develop appropriate methods and tools to perform a long term prediction of reservoir sedimentation, in order to develop mitigation measures, extend the reservoir life time and enhance the benefit of the storage capacity.

The presented work is an in depth investigation on sedimentation processes of medium size reservoirs by using a 2-dimensional physically based numerical model. Reservoirs of typical size and shape have been analyzed focussing on their response to temporal variation of inflowing discharge and suspended sediments as well as reservoir operation. The numerical investigation provides basic information and a deep insight into the overall sediment trapping characteristics of reservoirs under unsteady discharge and suspended sediment input conditions. The results show the key role of the shape and mean residence time of the reservoir on the damping of the amplitude and the modification of the frequency of inflowing discharge and suspended sediment concentration, in particular for highly unsteady flood events. Some important criteria for long term numerical simulation are developed resulting in an aggregation of input data and a combined quasi-steady and unsteady numerical modeling. The modeling strategy was successfully applied to a daily storage reservoir in South of Germany to predict the sedimentation for some future decades.

Furthermore, the candidate Mr. Kebede Gurmessa has shown that if a good database is available the application of a multiple regression based on the principle component analysis allows a reliable medium-term prediction of the development of the deposited sediment volume including the spatial distribution of the deposits.

The thesis is an important scientific contribution to the engineering modeling of non-stratified reservoirs that undergo long-term sedimentation processes. The combined approach of both mathematical-numerical modeling of the unsteady reservoir flow and sediment behavior and of multivariate statistical techniques has yielded useful insights on how these systems can be predicted efficiently in order to manage their long-term behavior. The guidelines developed therein have important implications for engineering practice.

Bernhard Westrich

Acknowledgment

Above all, I am very grateful to Prof. Bernhard Westrich, the head of Versuchsanstalt für Wasserbau at the Universität Stuttgart for taking the position of an advisor in this research. He followed the work closely and gave me invaluable suggestions and critiques without any hesitation. He also provided me with necessary research facilities and encouragements during the period of this work.

I would like also to extend my thank to Prof. András Bárdossy, chair of Lehrstuhl für Hydrologie und Geohydrologie, and director of the Institut für Wasserbau at the Universität Stuttgart, for taking the position of internal co-advisor. His guidance was very crucial particularly in the second part of this work.

I would also very much thank Prof. Gerhard H. Jirka, director of Institut für Hydromechanik at the Universität Karlsruhe for overtaking the position of external co-advisor. He gave me both critical oversight and words of encouragement.

There are a number of people to mention in the IWS who were helpful in the process of the research: Prof. Helmut Kobus gave critical remarks during the doctoral seminars of the ENWAT program. Dipl.-Ing. Joachim Karnahl, Dr.-Ing. George Jacoub, and Dipl.-Ing. Sven Würms with whom I made discussions relevant to the TELEMAC modeling system. Dipl.-Phys. Gerhard Schmid supported the research in providing all necessary computational facilities. He also helped in organizing field sample collection and laboratory analysis on sediment samples, on which two other colleagues, Dipl.-Geoökol. Thomas Jancke and Herr Werner Bareth took part. Dr.-Ing. Yeshewatesfa Hundecha Hirpa deserves my thanks for valuable discussions relevant to the work. I would also like to thank Mr. Jeffrey Tuhtan for proofreading the work. I also thank Dr.-Ing. Sabine Manthey for her suggestions on editorial aspects. The lecturers of the Fakultät Bau- und Umweltingenieurwissenschaft at the Universität Stuttgart from whom I learned valuable ideas also deserve my thank.

There are also people to mention from various organizations which deserve my thanks: Mr. Pierre Lang from SOGREAH/LHF gave me advices on the TELEMAC modeling system. Dr.-Ing. Roberto Kohane from Lahmeyer International, Herr Ralf Klocke from Lech Elektrizitätswerk, and Herr Thomas Köhler from Bayerisches Landesamt für Umwelt provided me with the data used in this research. Dipl.-Ing. Thomas S. Hille, from the university of technology of Delft, made proofreading of some part of the work as well as translation to the Deutsche Zusammenfassung in which Dipl.-Ing. Sven Würms had a share.

My thank extends to the IPSWaT program initiated by the German Federal Ministry of Education and Research for supporting me financially in the period of the research. I would also like to thank all my friends and my family. Finally, I would like to give thank to the almighty God for giving me health and strength to accomplish this work successfully.

Stuttgart, April 2007 Tesfaye Kebede Gurmessa

Contents

List of Figures

List of Tables

List of Abbreviations

Symbol	Definition	Dimensions
A_s	surface area of reservoir	$[L^2]$
$\mathbf{b}$	external forces in the momentum equations	$[L/T^2]$
b_i	external forces in the direction i of the momentum equations	$[L/T^2]$
$\mathbf{C}$	covariance matrix	$[L^2]$
$\mathbf{C}$	the convection/advection matrix in the finite element	$[var]$
C	depth averaged suspended sediment concentration	$[M/L^3]$
$\bar{C}$	the mean of the depth-averaged sediment concentration	$[M/L^3]$
C'	the fluctuation of the depth-averaged sediment concentration	$[M/L^3]$
C_{sf}	bottom concentration of deposited sediment	$[M/L^3]$
C^*	depth integrated sediment carrying capacity	$[M/L^3]$
c	instantaneous concentration	$[M/L^3]$
$\bar{c}$	mean part of the instantaneous concentration	$[M/L^3]$
$c^{'}$	fluctuating term of the instantaneous concentration	$[M/L^3]$
c_{b*}	equilibrium concentration above saltation layer	$[M/L^3]$
C_d	drag coefficient	$[-]$
c_i	input suspended sediment concentration	$[M/L^3]$
c, c_o	output/reservoir suspended sediment concentration	$[M/L^3]$
D_b	deposition flux of the sediment fraction n	$[M/L^2T]$
DQ	differential discharge as used in the regression models	$[L^3/T]$
d	sediment grain size	$[L]$
$\mathbf{E}$	spatio-temporal reservoir bed evolution	$[L]$
E	bed evolution at the numerical grid points	$[L]$
E_b	erosion flux	$[M/L^2T]$
$\mathbf{E}_n$	reconstructed bed evolution in using the regression models	$[L]$
$f(\mathbf{x})$	values at any point over a finite element domain	$[var]$
$f^e(\mathbf{x})$	the finite element approximation	$[var]$
$\hat{f}_i(\mathbf{x})$	the nodal values in the finite element calculations	$[var]$
g	acceleration due to gravity	$[L/T^2]$
H	average water depth of a reservoir	$[L]$
h	depth of water at the numerical grid points	$[L]$
$\mathbf{K}$	the dispersion matrix in the finite element	$[var]$
K_{st}	Manning-Strickler coefficient	$[L^{1/3}/T]$
k	kinetic energy of fluctuating motion	$[L^2/T^2]$

M	erosion coefficient	$[M/L^2T]$
$\mathbf{M}$	mass matrix in the finite element	$[var]$
m_i	inflow sediment mass into a reservoir	$[M]$
m, m_o	mass of sediment in a reservoir as a suspension	$[M]$
m_d	mass of sediment deposition in a reservoir	$[M]$
N_i	interpolation function	$[-]$
N_j	weighting function	$[-]$
P_e	Peclet number	$[-]$
p	instantaneous pressure	$[M/LT^2]$
$\bar{p}$	mean of the instantaneous pressure	$[M/LT^2]$
$p^{'}$	fluctuating part of the instantaneous pressure	$[M/LT^2]$
Q	discharge	$[L^3/T]$
q	source/sink term in the continuity equation	$[L/T]$
Q	daily averaged discharge as used in the regression model	$[L^3/T]$
$\bar{Q}$, Q_{avg}	mean discharge in a period T	$[L^3/T]$
Q_o	initial discharge in the period T	$[L^3/T]$
Q_p	peak discharge in the period T	$[L^3/T]$
q_{bx}, q_{by}	component of the total-load transport in x and y directions	$[M/LT]$
$\mathbf{R}$	correlation matrix	$[-]$
R	Reynolds number	$[-]$
R	multiple linear correlation coefficient	$[-]$
r	simple linear correlation coefficient	$[-]$
s	volumetric source and sink term of the sediment	$[M/L^3T]$
SS	imposed suspended sediment concentration at the upstream BC	$[M/L^3]$
SS	daily average input concentration in the regression models	$[M/L^3]$
t	time	$[T]$
t_{th}	theoretical residence time	$[T]$
$\bar{t}$	mean residence time	$[T]$
T	period of input functions	$[T]$
$\mathbf{u}$	velocity vector	$[L/T]$
$\mathbf{U}$	scores of the principal components	$[L]$
$\mathbf{U}$	depth averaged velocity vector	$[L/T]$
U	depth averaged velocity in longitudinal direction	$[L/T]$
V	depth averaged velocity in lateral direction	$[L/T]$
V	volume of a reservoir	$[L^3]$
$\mathbf{u}$	velocity vector	$[L/T]$
u_i, u_j	instantaneous velocity in the direction i, j	$[L/T]$

$u_i^{'}$, $u_j^{'}$	fluctuating term of the velocity in the direction i, j	$[L/T]$
$\bar{u}_i^{'}$, $\bar{u}_j^{'}$	mean part of the velocity in the direction i, j	$[L/T]$
u_{cd}	critical deposition velocity	$[L/T]$
u_{ce}	critical erosion velocity	$[L/T]$
u_o	bottom shear velocity	$[L/T]$
$\mathbf{u}_t$	partial time derivative of the velocity vector	$[L/T]$
v_s	settling velocity	$[L/T]$
v_{sn}	settling velocity of class n in non-uniform sediment	$[L/T]$
$W(t)$	periodic loading into the reservoirs	$[M/T]$
z	free surface elevation	$[L]$
z_b	bottom of the domain	$[L]$
α	eigenvectors of the principal components of the bed evolution	$[-]$
α_n	eigenvector of the reconstructed n^{th} principal component	$[-]$
β, β_s	transfer function of the steady state stirred reactors	$[-]$
β_p, β_{sp}	transfer function of the steady state plug flow reactors	$[-]$
β_{om}, β_{qm}...	the regression parameters in the regression models	$[-]$
$\triangle Q$	amplitude of the discharge in the periodic inputs of period T	$[L^3/T]$
$\triangle T$	quasi-steady time step	$[T]$
$\triangle t$	discretization time step	$[T]$
ϵ	rate of dissipation of turbulent kinetic energy	$[L^2/T^2]$
ε	residual error in the FE calculation	$[var]$
ε_s	depth integrated sediment turbulence diffusivity	$[L^2/T]$
Γ	turbulent diffusivity of mass	$[L^2/T]$
θ	implicity value	$[-]$
λ	diffusivity of mass	$[L^2/T]$
λ_k	the eigenvalue of the k^{th} principal component	$[L]$
ρ	density of water	$[M/L^3]$
ρ_s	density of sediment	$[M/L^3]$
$\rho^{'}$	sediment porosity	$[-]$
σ_t, σ_c	turbulent Schmidt number	$[-]$
σ	standard deviation of the residence time distribution	$[T]$
τ_{cd}	critical shear stress for deposition	$[M/LT^2]$
τ_{ce}	critical shear stress for erosion	$[M/LT^2]$
τ_o	bottom shear stress	$[M/LT^2]$
ν	kinematic viscosity	$[L/T^2]$
ν_t	turbulent viscosity	$[L/T^2]$
$\tilde{\nu}_t$	depth averaged turbulent viscosity	$[L/T^2]$

Spatial Differentiation

$\boldsymbol{\nabla}()$	gradient of a variable which is given as $\left[\frac{\partial}{\partial x_1}\ \frac{\partial}{\partial x_2}...\frac{\partial}{\partial x_n}\ \right]^T$
$\boldsymbol{\nabla}\cdot()$	divergence of a variable is given as $\left[\frac{\partial}{\partial x_1}+\frac{\partial}{\partial x_2}...+\frac{\partial}{\partial x_n}\ \right]$

Abbreviations

BC	Boundary Condition
CSTR	Continuously Stirred Reactors
DNS	Direct Numerical Simulation
EOF	Empirical Orthogonal Function
FDM	Finite Difernce Method
FEM	Finite Element Method
FVM	Finite Volume Method
GMRES	Generalized Minimum Residual
HC	Head Controlled Boundary Condition: Variable Head
HCC	Head Controlled Boundary Condition: Constant Head
IWS	Institut für Wasserbau
LES	Large Eddy Simulation
LEW	Lech Elektrizitätswerk
QC	Discharge Controlled Boundary Condition
QS	Quasisteady Approximation
PCA	Principal Components Analysis
PCR	Principal Components Regression
PCs	Principal Components
PFR	Plug Flow Reactors
RANS	Reynolds-averaged Navier-Stokes Equation
RTD	Residence Time Distribution
SUPG	Streamline-Upwind Petrov-Galerkin
SETEG	Ein Strömungskanal zu Ermittlung der tiefenabhängige Erosionsstabilit ät von Gewässersedimenten
VCA	Variance Covariance Analysis

Abstract

Sediment management plays an essential role in planning water storage facilities, navigation and irrigation channels, and flood protection works. It is also very important in water quality and ecosystem management.

Long-term prediction of the quantity and spatial distribution of sedimentation is required in the planning and management of reservoirs. Numerical models, conceptual models, empirical models, scale models, or a combination of them can be used in order to predict long-term sedimentation of reservoirs. Some approaches are complex while others tend to oversimplify addressing practical questions related to sediment management.

This work has attempted to address simplified methodologies to predict the amount and spatial distribution of reservoir sedimentation. Two complementary approaches were specifically assessed: the numerical and the data-driven modeling approaches.

Numerical modeling of long-term sedimentation processes involve model, parameter, and data uncertainties and often require very high computational costs. Model conceptualization and solution procedures involved in long-term simulation of sedimentation processes of riverine systems are challenging.

The first part of the study deals with the investigation of simplification of numerical simulations. The study begins with investigations made on the basic system response of reservoirs to unsteady inputs. By making use of hypothetical domains and periodic inputs, efforts were made to try to specify the theoretical concepts. The response of the reservoirs was investigated by using aggregate parameters such as theoretical residence time, critical erosion discharge, amplitude and the frequency of inputs. The analytical solutions of ideal continuously stirred reactors and/or plug flow reactors as compared with the real two-dimensional advection-dispersion numerical solutions of the TELEMAC modeling system were evaluated. Criteria for the refinement of quasisteady steps were investigated revealing the importance of reservoir shape, range of discharges, and residence time.

The work then continues by investigating into long-term simulation and simplification strategies. A thorough evaluation of hydrological, topographical, and sediment data was conducted on the Lautrach reservoir of River Iller. Using the two-dimensional depth-integrated TELEMAC modeling system, sensitivity studies were conducted with relevance to data aggregation, temporal and spatial discretization, coupling methods, turbulence models, and sediment gradation.

Based on the simplifications from the preliminary studies, long-term reservoir sedimentation was calibrated and validated with fully unsteady simulation. The validated morphological simulations were tested for the extent of the applicability of quasisteady approximation considering large steady time steps. It was found out that except for extreme discharges and low flows with high sediment concentrations, the quasisteady approximation with large time steps can be successfully applied without major discrepancy from the fully unsteady simu-

lation. Comparisons of the prediction of bed evolution were made using complete unsteady, mixed-unsteady-quasisteady, and steady approximations.

In the second part of the work, a new approach on the use of principal component regression in modeling the spatio-temporal bed evolution processes of riverine system was developed. The principal component analysis made on long-term bed evolution simulation indicated that only the first four principal components represent some 95 percent of the variance. This indicated that a significant simplification and representation of the spatio-temporal simulated data can be made in a condensed form. Multiple regression models were then investigated between the first four principal component scores and the flow and the sediment inputs, resulting in a very good correlation.

The reconstruction of reservoir bed evolution resulted in an excellent agreement when multiple regression was used between the principal component score and the time series of discharge, change in discharge, and suspended sediment concentration. The model was also reasonably validated with acceptable uncertainty for ranges outside the period of reconstruction. It was found that the regression parameters are dynamic due to the dynamic nature of reservoir bed as well as flow and sediment parameters.

Furthermore, a multiple regression model was developed for the rate of sediment mass deposition that performed very well on the step of reconstruction. For prediction purposes the performance of linear models requires further improvements. Care must be taken on the use of regression coefficients outside the range in which they are constructed for, to take into account the dynamic nature of the reservoir bed.

The work is a step forward towards simplifying the complex and computationally demanding task of modeling of long-term sedimentation processes by assimilating dynamic and data modeling techniques.

Zusammenfassung

Sedimentmanagement ist ein wichtiger Bestandteil bei der Planung von Reservoirs, beim Ausbau von Wasserstrassen, sowie bei Fragen der Wasser- und Sedimentqualität. Die Vorhersage von Sedimentationprozessen spielt hierbei eine wesentliche Rolle. Neben der Extrapolation historischer Daten und der Übertragung von Daten von Reservoirs mit ähnlichen Bedingungen können folgende Methoden zur Abschätzung der Sedimentation herangezogen werden: Numerische und empirische Modelle, physikalische Modelle, statistische Modelle oder Kombinationen daraus. In dieser Arbeit wurde die Sedimentation in mittel großen nicht geschichteten Wasserspeichern, wie sie im Bereich der Wasserkraftnutzung und der Hochwasserrückhaltung vorkommen, mit dem Ziel untersucht, vereinfachte Methoden bezüglich der Datenverwertung und der numerischen Langzeitsimulation zu entwickeln.

Trotz der signifikanten Fortschritte, welche im Rahmen der numerischen Modellierung erzielt wurden, stellt die Langzeitmodellierung von Sedimentationsprozessen in Stauhaltung und Speicheranlagen über einen Zeitraum von einigen Dekaden auf Grund der erforderlichen Rechnerressourcen nach wie vor eine Herausforderung dar. Aus diesem Sachverhalt leitet sich die Motivation ab, bestehende Modelle zur Langzeitsimulierung effektiver einzusetzen.

Diese Arbeit widmet sich hauptsächlich der Methodenvereinfachung zur Vorhersage der Sedimentation bezüglich Menge und räumlicher Verteilung. Zwei unterschiedliche Ansätze wurden untersucht: Die vereinfachte numerische Modellierung und die datenbasierte Modellierung. Die Hauptziele dieser Forschungsarbeit sind:

- Systemanalyse zur Beschreibung der Sedimentation in Abhängigkeit von der Form des Speichers und den Zuflussbedingungen.
- Untersuchung verschiedener vereinfachender Modellierungstechniken bezüglich Datenaggregation und quasistationärer Zuflussbedingung zur Anwendung in Langzeitsimulationen.
- Entwicklung eines darauf abgestimmten, datenbasierten Modellierungsansatzes zur Vorhersage von Reservoirsedimentation durch die Assimilation von Daten und Dynamik.

Numerische Modellierung

In dieser Arbeit wurde das zwei-dimensionale, numerische Strömungs- und Sedimentationsmodellsystem TELEMAC verwendet. Im ersten Teil der Arbeit wurden Grundstudien zum Verhalten von Wasserreservoiren auf periodische zuflussschwankungen und quasistationäre Vereinfachungen angestellt. Anschließend wurden Voruntersuchungen zum effizienten Einsatz der erarbeiteten Modellierungstechniken am Fallbeispiel der Stauhaltung Lautrach vollzogen. Das Modell wurde mit den Daten vom Tagesspeicher Lautrach kalibriert und

validiert. Die quasistationäre Annahme wurde getestet und in eine Langzeitvorhersage integriert.

Systemverhalten von Reservoirs

Die Menge der abgelagerten Sedimente sowie deren räumliche Verteilung wird durch Größe und Form des Reservoirs, den Zufluss sowie die Sedimentparameter beeinflusst. Periodische Zuflüsse und Sedimentkonzentrationen mit variierenden Amplituden und Frequenzen wurden auf stark vereinfachte, regelmäßige Beckenformen und typische, unregelmäßig geformte Becken mit Totwasserzonen angewandt. Die Resultate wurden ausgewertet und können wie folgt zusammengefasst werden:

- Aggregierte Parameter wie die theoretische Verweildauer sind sehr nützlich für die Charakterisierung des Antwortverhaltens des Reservoirs.
- Die Übertragungsfunktionen der stationären analytischen Loesungen volldurchmischter Speicher (Continuously Stirred Reactors (CSTR)) und nicht mischungsfähige (Plug Flow Reactors (PFR)) wurden mit numerischen advektions-dispersions Lösungen verglichen. Die Ergebnisse deuten darauf hin, dass sich die regelmäßig geformten Becken durch den PFR-Ansatz und die unregelmäßig geformten Becken durch den CSTR-Ansatz annähernd beschreiben lassen. Die Auswirkungen von Frequenz und Amplitude von Zufluss und Schwebstoffkonzentration, unterschiedlicher Sedimentfraktionen und variierenden Randbedingungen wurden hinsichtlich der Reaktion des Reservoirs ausgewertet.
- Die Untersuchung quasistationärer Näherungslösungen zeigte, dass die Simulation durch Zeitschritte während eines quasistationären Zustandes, die kleiner sind als die theoretische Verweildauer keine nennenswerte Annäherung an das Ergebnis der instationären Berechnung der Sedimentationsmenge gebracht hat. Es wurde gezeigt, dass bei quasistationären Diskontinuitäten die quasistationäre Lösung mit stationärer Modellierung der Strömung und einer instationären Modellierung des Sedimenttransports bessere Ergebnisse erzielt als die rein quasistationären Schritte.

Fallstudie des Lautrach-Reservoirs

Zur Modellierung der Sedimentationsprozesse bedarf es einer großen Datenmenge bezüglich Zufluss, Sediment und der Speichergeometrie. Solche Daten sind selten für lange Zeiträume und in hoher räumlicher Auflösung verfügbar. Der für die Wasserkraftnutzung ausgelegte Tagesspeicher an der Iller, das Lautrach-Reservoir, wurde für die vorgestellten Untersuchungen gewählt, da hier eine relativ gute Datenbasis über angemessen lange Zeiträume verfügbar ist.

Eine Analyse wurde gleichermaßen für die Strömungs- und Sedimentdaten durchgeführt. Mit Hilfe des Netzgenerators MATISSE erfolgte die räumliche Abbildung der natürlichen

Speichergeometrie. Verschiedene Problemfaktoren wurden untersucht, um mögliche Vereinfachungen für die Modellierung zu finden: Einfluss von Datenaggregation (Durchfluss, Wasserstand, Schwebstoff), Auswirkung der Gitternetzverfeinerung, Einfluss der Koppelung von Strömung, Transport, Speichersohle, und Turbulenzmodellierung. Wichtige Erkenntnisse der Untersuchungen sind:

- Die Erfassung von Spitzendurchflüssen erfordert eine sehr hohe Datenauflösung. Die größten Diskrepanzen bezüglich der Sedimentationsmenge resultierend aus der Datenaggregation treten im Bereich der Durchflussspitzen auf. Bei Niedrigwasserperioden kann die Datenaggregation durchaus für Langzeitstudien verwendet werden. Tagesmittelwerte von Zufluss und Schwebstoffgehalt wurden zur Langzeitkalibrierung und-Validierung des Lautrach-Reservoir-Modells herangezogen. Des weiteren wurde der Einfluss multifraktionaler und monofraktionaler Schwebstoffe auf die Berechnung der Sohlevolution analysiert. Hierbei zeigt sich, dass die Annahme eines monofraktionalen Sediments in diesem Rahmen durchaus geeignet ist. Darüber hinaus zeigte eine Analyse der Wasserspiegelschwankungen im Reservoir, dass eine konstante Wasserspiegellage an Absperrbauwerk unabhängig vom Zufluss ohne signifikanten Einfluss auf die Menge sowie die räumliche Verteilung der Sedimente angenommen werden kann.
- Der Grad der räumlichen Diskretisierung ist bezüglich des Rechenaufwandes auf der einen und der nötigen Auflösung der Sohlgeometrie auf der anderen Seite zu optimieren. Die adäquate Darstellung der Sohlgeometrie ist bei Fehlen hochauflösender Daten eine schwierige und unsichere Aufgabe. In dieser Arbeit wurde basierend auf den durchgeführten Voruntersuchungen ein räumlich adaptives Netz verwendet, dessen Maschenweite zwischen 10 und 20 m liegt.
- Weitere Untersuchungen wurden durchgeführt, um die Auswirkung der Kopplungszeiten zwischen Strömungsmodul und Sedimenttransportmodul, der Turbulenzformulierung usw. zu bestimmen. In den Langzeitsimulationen wurden basierend auf den Teststudien das ungekoppelte Verfahren und das $k - \epsilon$ Modell verwendet.

Basierend auf den Modellvereinfachungen wurde die Langzeitkalibrierung mit Daten aus dem Zeitraum von 1988 bis 1992 und die Validierung mit Daten von 1992 bis 1996 vorgenommen. Ungenaue und fehlende Höhenangaben zur Sohle und hieraus resultierende Schwierigkeiten bei der Netzgenerierung, zahlreiche Kalibrierungsparameter, numerische Instabilitäten und lange Rechenzeiten stellten sich als große Herausforderungen heraus.

Die Modellkalibrierung und -validierung erfolgte sowohl für die Strömung als auch den Transport instationär. Obwohl es sich hier um ein kleines Modell mit vereinfachten Modelltechniken handelt, benötigt die Simulation von 4 Jahren Echtzeit 3 Wochen Rechenzeit auf einem Computer mit einem AMD 3400+ Prozessor und 480MB Arbeitsspeicher. Die genaue Bestimmung der räumlichen Sedimentverteilung ist eine große Herausforderung bei der Langzeitmodellierung der Sohlmorphologie. Abweichungen der simulierten Sedimenttiefen von Messdaten bewegen sich größtenteils innerhalb einer Grenze von +/- 0,2 m.

Die Effektivität der quasistationären Vereinfachungen wurde im Weiteren anhand der validierten Entwicklung der Speichersohle untersucht. Grundlegende Kriterien zur quasistationären Vereinfachung wurden herausgearbeitet. Hierbei zeigt sich, dass bei Strömungsverh-

ältnissen unterhalb des erosionskritischen Durchflusses hinreichend genau mit großen quasistationären Zeitschritten gearbeitet werden kann. Daher wurde eine stationäre Behandlung für Durchflüsse unter 200 m^3/s und eine instationäre für höhere Durchflüsse durchgeführt. Dies führte zu guten Übereinstimmungen bei der räumlichen Verteilung und den Sedimentationsmengen.

Aus diesem Grund wurde ein gemischtes quasistationär-instationäres Modell kalibriert und validiert und für die Langzeitvorhersage des Lautrach-Reservoirs verwendet. Das Modell prognostiziert für das Lautrach-Reservoir einen Gleichgewichtszustand im Jahr 2025 bei welchem ein Speichervolumen von 0,92 Mio. m^3, entsprechend einem Verlust von 42% des Volumens, übrig bleibt. Die Form des Reservoirs spielt eine wesentliche Rolle hinsichtlich des Sedimentmanagements. Das Lautrach-Reservoir hat eine komplexe Geometrie, welche für die Sedimentation förderlich ist. Standardisierte Betriebsweisen wie z.B. die Sedimentausspülung sind bei geringer Absenkung des Stauziels wenig effektiv.

Datenbasierte Modellierung

Signifikanter Fortschritt wurde im Bereich der Anwendung von Regressionstechniken zur Modellierung der Sohlmorphologie erzielt. Die Methode wurde unter Verwendung von Daten entwickelt, welche aus der numerischen Simulation gewonnen wurden. Die räumliche Sedimentverteilung wurde mithilfe einfacher linearer Regression und Hauptkomponentenregression ermittelt. Die Hauptkomponentenregression stellte sich dabei als die effektivere Methode zur Beschreibung von räumlich-zeitlichen Sohlevolutionsprozessen heraus. Sedimentmengen wurden mittels multi-linearer Regression berechnet.

Räumliche Verteilung der Sedimentation

Aus der Hauptkomponentenregression der numerisch erzeugten Datensätze für die Stauhaltung Lautrach können bezüglich der Vorhersage der räumlich-zeitlichen Sohlmorphologie folgende Aussagen getroffen werden:

- Die Hauptkomponentenregression erzielte sehr gute Ergebnisse bezüglich der Rekonstruktion der Sohlentwicklung des Lautrach-Reservoirs bei Testperioden von 5 bis10 Jahren.
- Die allein auf dem Zufluss basierende, monovariate Hauptkomponentenregression war nicht ausreichend. Dagegen war es mit der multivarianten Hauptkomponentenregression, basierend auf der Regression der Koeffizienten der ersten vier Hauptkomponenten mit Durchfluss, Zuflussänderung pro Tag und Sedimentkonzentration möglich, die räumlich-zeitliche Entwicklung der Sohlhöhen erfolgreich zu rekonstruieren.
- Die Koeffizienten der Multiregression veränderten sich mit der Zeit. Es zeigte sich, dass die Anfangstopographie, auf der das Modell basiert, signifikanten Einfluss auf

das statistische Ergebnis hat. Die Verwendung von Regressionskoeffizienten des Hauptkomponentenregressionsmodells eines bestimmten Zeitraums mit einer bestimmten Anfangsmorphologie für einen anderen Zeitraum mit einer anderen Anfangsmorphologie erzielte unbefriedigende Vorhersagen. Die Vorhersage zu einer Zeit die sich vom Zeitpunkt der Rekonstruktion unterscheidet, jedoch dieselben Anfangsrandbedingungen verwendet, erzielte gute Ergebnisse.

- Die Vorhersage von Extremereignissen muss separat durchgeführt werden, da hierbei größere Korrelationen auftreten.

Die Sedimentationsmenge

Die Regressionsmodelle wurden ebenso zwischen der täglichen Sedimentationsmenge, und den Tagesmittelwerten von Zufluss und Sedimentinput konstruiert. In der Regression wurden Daten aus den numerischen Simulationen für die Sedimentablagerung verwendet. Die folgenden Aussagen können getroffen werden:

- Die Multi-Linearregression zwischen der täglichen Sedimentationsmenge und Durchfluss, Durchflussänderung sowie Schwebstoffkonzentration erzielte sehr gute Ergebnisse im Hinblick auf die Rekonstruktion verglichen mit der numerischen Vorhersage.
- Für die Vorhersage der Sedimentationsmenge für eine Zeitspanne von 10 bis 20 Jahren wurden gute Ergebnisse erzielt, wenn dieselben Anfangsbedingungen für die Speichertopographie sowie die hydraulischen Parameter zugrunde lagen.

Ausblick

- Die numerische Langzeitmodellierung von Sedimentationsprozessen ist eine komplexe Aufgabe, die eine Menge Unwägbarkeiten enthält. Es bedarf neuer Ansätze für großmaßstäbliche Langzeitsimulationen, welche die Prozesskomplexität der Dynamik über Zeit und Raum in vereinfachter Weise berücksichtigten. Die Anwendung quasistationärer Näherungen für große Speichervorratsbehälter unter Berücksichtigung komplexerer Prozesse wie z. B. Schichtung und Konsolidierung erfordert weitere Untersuchungen.
- Weitere Untersuchungen der numerischen Modellierung von Speicherspülungen sind notwendig. In diesem Zusammenhang stellen insbesondere die auftretenden Nass/ Trocken-Effekte eine Herausforderung dar.
- Weitere Forschung ist nötig, um die Angleichung von Daten und Dynamik in Modellen derart zu gestalten, dass numerische und statistische Modellierungsansätze ergänzend genutzt werden können. Die Anwendung der entwickelten Methoden auf unterschiedlichen Zeitskalen kann untersucht werden.

Chapter 1

Introduction

The annual precipitation on the earth's surface maintains life and also shapes the natural landscape. Sediment transport is associated with land erosion, rivers and coastlines. The process shapes the earth surface and coastlines, effects water quality, wildlife, agriculture, forestry, navigation, flood control, hydro-power, recreation, fishing and bio-diversity. On the global scale, the amount of solids delivered to the sea is estimated to be on the order of 14 billion tons per annum, plus an additional 4 billion tons per annum of dissolved solids. This averages to 100 tons per annum and per km^2 of the earth's surface. Only a fraction of this is directly transported to the sea. Most of it is deposited in intermediate locations, where it may rest for long periods of time, see Raudkivi 1998 [101]. Comprehensive and multi-disciplinary research has been conducted on the physical, chemical, biological, engineering, and socioeconomic dimensions of sediment transport. In order to appreciate the extent of its wide applications, a brief review is provided below.

Integrated reservoir sediment management: Reservoirs are important structural components for water resources management. Major aspects in which water storage is utilized include irrigation, hydropower, domestic and industrial water supply, flood protection, recreational, and ecological protection. Meeting these aims for water storage has regional and climatic implications. In arid and semi-arid regions of the world, the rainfall distribution is limited to few months of a year and suitable reservoirs are found deep underground, often limiting the economic extraction. Water storage is mainly constructed to supply peak demands with reliable supply. On the other hand, in regions of the world where there is abundant availability of water, the use of surface water storage facilities for flood protection may be predominant.

The availability of suitable sites for building new water storage reservoirs is limited because of strict environmental and socioeconomic requirements. It is therefore important to plan sustainable reservoirs for a long service life. Once the reservoirs are constructed, maintaining the original design capacity and operational goals to last long is the ideal strategy. This presents different challenges depending on the specific hydrological, morphological and characteristics of the watershed, as well as on social and economic conditions of the country in which the dams are constructed. In tropical, humid and arid zones, sedimentation is a usually more frequent problem than in temperate zones. On the other hand, in most developing countries in tropical regions, water infrastructure has not yet been well developed. In many industrial countries of temperate zones however, most of the potentially used dam sites have already been utilized. The scientific community at large should work to create solutions for conserving existing water storage facilities in order to enable their functional requirements to provide service, see Silvio 2004 [111].

The mitigation of reservoir sedimentation requires the implementation of a variety of strate-

gies. The reduction of sediment yield from a watershed can be achieved by structural or mechanical measures, vegetative or agronomic measures. Once sediment approaches or enters a reservoir, various sediment mitigation methods can be implemented. Among them are sediment routing, sluicing of turbid density currents, sediment flushing, and dredging techniques. More details can be referred in, Morris 1998 [86], Yang 1996 [146], Lai 1996 [79], Shen 2000 [109], Yalin 1992 [144].

The hydraulic design of reservoirs must take into account the location and site specific conditions of the watershed where the reservoirs are planned, the shape and size of reservoirs, hydraulic structures (dams, bottom outlets, spillways, etc.), and the operation suitability (sediment flushing, routing, etc.).

Navigation, irrigation, and drainage channels: Irrigation, navigation, and drainage channels are among the most important infrastructures. Proper channel design and management plays a critical role with respect to sediment transport processes. Sediment deposition strongly affects a large number open channel irrigation systems fed by sediment laden rivers. The aggradation of channel beds affect the hydraulic functionality of the irrigation distribution systems and may result in poorly controlled water distribution, see Belaud 2002 [11]. Although measures of sediment control can be applied at the system headworks, the design of regime channels, and frequent desilting campaigns can result in a burden of operational and maintenance costs. Furthermore, the maintenance activities unless properly planned may result in interruption of water supplies, thus causing a reduction of agricultural productivity.

Commercial and recreational navigation can be severely impaired by sediment accumulation, especially in delta areas and in the vicinity of ship locks. Human interference in hydraulic systems is often necessary to maintain and extend economic activities related to ports and associated navigation channels. In many situations, engineering structures are required to stabilize shorelines, to reduce sedimentation, to prevent or reduce erosion, or to increase the channel depth to allow large vessels to enter the harbor basins. Sedimentation problems generally occur at locations where the sediment transporting capacity of hydraulic system is reduced due to a decrease in flow velocities and turbulence, see Van Rijn 2004 [124]. Many access channels and harbors suffer from sedimentation and the formation of mud layers. To keep navigation safe and economic, extensive channel dredging is needed, see Delefortrie et al. 2005 [35]. In navigation projects designed by low head dams and locks along rivers, essentially open river conditions will prevail during high discharges, thereby allowing the passage of most sediment through the structures.

Flood protection management: Flood protection works must consider the effect of flow-sediment interaction and take bed morphological changes as well as change in flow patterns into account. Dams built for flood protection may facilitate the formation of deltas on the upstream river reach, creating a flood risk extending several kilometers upstream of the pool. Dykes built along the rivers may no longer serve the intended purpose of flood protection if there exists an aggradation river bed as a result of sedimentation (see for example Li 2004 [83]). The Yellow River (Huanghe) of China is an excellent example. The Sanmenxia Dam built on the middle of this silt laden river has resulted in severe sediment accumulation in the reservoir. Sedimentation did not only threaten the entire desired project benefit but also resulted in raising the bed elevation and flood levels in the Yellow River as far as 260

km upstream of the dam, see Morris 1998 [86].

Sediment quality management: Sediment quality has become a crucial factor in response to growing environmental and health concerns. The interrelation between sediment quantity and quality needs to be properly addressed in integrated sediment management. Contaminants deposited in rivers can be mobilized and released into the water after natural or artificial resuspension of sediments. The effect of flooding on particle transport and its far-reaching effects on chemical changes are issues which need practical attention, see Westrich 2005 [128].

In summary, it is rare to find any area of surface water resources management that is not in some way connected with sediment. Sediment has ecological, social, and economic value. Sediment is one of the key components of the aquatic ecosystem, and sediment serves additionally as an important source of nutrients for organisms. Sediment dynamics and gradients form favorable conditions for biodiversity. Sediment in river systems is utilized in farmlands and as a source of minerals and materials, see Brils 2003 [15]. Therefore it is of crucial importance to take a close look at the methods and the challenges in understanding and quantifying the process of sediment transport in riverine environments. With these broad applications of sediment transport as a motivation, the present work focuses on the problems of quantification of sediment transport processes particularly when estimation of the long-term bed evolution processes is of primary concern in river engineering and sediment management issues.

1.1 Modeling of reservoir sedimentation

The prediction of reservoir sedimentation is very important in order to leave sufficient dead storage, properly design the location of outlet structures, plan operation strategies to extend the life time of reservoirs, etc. Planners use models in order to estimate the amount and spatial distribution of sedimentation. Various modeling approaches are used to quantify the flow and the sediment transport processes in riverine systems, see Figure 1.1. Numerical models, statistical models, physical/scale models, and empirical methods are the most common. Based on the data availability, skill of the planners, cost, level of accuracy required, etc., the methods have their specific advantages and disadvantages. A combination

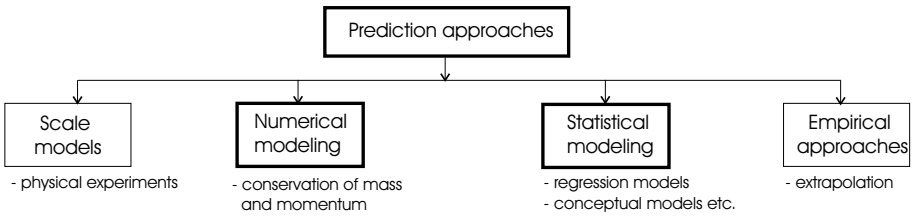

Figure 1.1: Approaches in the prediction of reservoir sedimentation

of these approaches is often necessary. For example; numerical models can be used as a predictive study for physical models, physical models can provide parameter inputs to numerical models, statistical models can supply the numerical models with prediction of flow

scenarios, statistical methods can support estimation of parameters from experiments etc. A brief description is given on the various approaches of modeling in reservoir sedimentation.

1.1.1 Numerical modeling

Sediment transport is a complex phenomenon influenced by physical, chemical and biological interactions of water-sediment mixtures. The necessity of conceptualizing specific aspects of the sediment transport process in a simplified scale model as well as numerical models is the basis in quantifying sediment transport processes.

The governing equations for sediment transport are those expressing the conservation of mass and momentum of flow and the conservation of mass of sediment. The challenge is that the nature is complex and it is often difficult to fully represent transport processes through the implementation of scale or numerical models. Sediment transport models are therefore based on simplifications, assumptions, and approximations.

The basis for developing closed numerical models involve experimental investigation including those of turbulence and sediment transport properties. Numerical models have a number of limitations with regard to computational speed, incomplete sets of equations, turbulence hypotheses, accuracy of assumed relationships, space and time resolution, numerical stability and the convergence of solution schemes.

With the advances in instrumentation and computational science however, the possibility to describe the phenomenon in a sound manner is improving. There is a trend that numerical models are gaining more importance in the quantification of flow and sediment transport processes.

Challenges in long-term simulations

Determination of the long-term sediment transport process in riverine systems is of primary interest in planning water resources infrastructure like reservoirs, navigation channels, irrigation channels and flood protections etc. Simulation of long-term sediment transport processes faces a significant challenge because of the complex dynamic nature of the flow and sediment transport, lack of data, uncertainties relevant to models, parameters, data, and computational demand.

Database: In performing a long-term simulation for predicting morphological processes the demand in data is tremendous. Measurements are rarely available on a continuous long-term basis for most riverine systems. Flow, sediment, and geometric data are subject to both measurement and processing errors. To measure flow parameters like discharge, velocities and stage, see Haeni et al. 2004 [56]; the sediment parameters like critical shear stress for erosion, sediment gradation, settling velocity, see e.g. Shields 1936 [110], Kern et al.1999 [75], Roberts et al. 2003 [103], Xiaqing 2003 [141], Aberle 2006 [1]; bathymetry, Baker and Morlock 1996 [9]. The source of experimental uncertainty and measurement

errors may be seen in Brooks 2005 [17] and Wahlin et al. 2005 [125].

Model uncertainty: The physical processes involved in sediment transport are too complex to be fully represented by a mathematical model. The approximations used in model conceptualization, mathematical formulation, and method of solving are additional sources of various uncertainties.

Parameter uncertainty: The flow and sediment transport models involve a large number of parameters which are used for the calibration of numerical models. The roughness coefficient and the critical shear stress for erosion and deposition are common to many hydraulic engineering problems and known to contain considerable uncertainty. Uncertainty analysis in parameter estimation of flow and sediment transport has been researched by Crissman et al.1993 [34], Johnson 1996 [69], Osidele et al. 2003 [93], Pappenberger et al. 2005 [95] among others.

Computational requirement: Sediment transport models are computationally very expensive. Efficient methods need to be used in overcoming the problem. Efficient numerical methods like using parallel systems may be used when resources allow, see e.g. Hinkelmann 2003 [62]. Another option is to simplify the model concepts, for example through the use of lower dimensional models, simplifying unsteadiness and assumption of quasi-steady approximation, etc., see Bond et al. 1998 [12].

Model simplifications

Simplification of sediment transport models begins from the steps of model conceptualization in which certain aspects of the complex processes are reduced to fewer processes. These in turn can be handled with state-of-the-arts approaches to nearly represent the phenomenon. These may include: selection of mode of transport, consideration of phases of transport, Nguyen and Brbray 2002 [89], the type of coupling between flow and sediment transport, Cao et al. 2002 [22], Soulis 2002 [117], Wang and Wu 2004 [126], simplification on cohesiveness and non-uniformity of sediment, Ziegler and Nisbet [149], Winterwerp 1998 [132], Kessel and Blom 1999 [76], simplification on erosion and deposition phenomenon, Krone 1962 [78], Kandiah 1974 [71], Van Rijn 1984 [122], Wu and Wang 2006 [138], simplification on the dimensions of the model.

A model concept is then converted into a system of partial differential equations expressing the conservation equations of mass, momentum and species transport, see e.g. LeMéhauté 1976 [81], Wu et al. 2000 [140], Donea 2003 [36]. Some of the simplifications involved in numerical modeling may include, simplification of turbulence through statistical turbulence models like Reynolds Average Stress modeling, Rodi 1993 [105], quasi-steady approximations, Bond et al. 1998 [12], Yang 2002 [147], Scott and Jia 2005 [108]. Solution procedures of the partial differential equations based on the simplifications in the model conceptualization are then solved using numerical methods like the finite element, the finite volume, or finite difference methods. The methods of temporal and spatial discretization, solution of algebraic equations, see Press 1992 [98], Reddy and Gartling 1994 [102], etc. are important aspects in model simplifications.

In spite of the complexity and relevant approximations and simplifications involved , numerical modeling of sediment transport is gaining momentum to be a standard tool for the prediction of reservoir sedimentation. A large number of studies have been made using numerical models in reservoir planning. Generally, shallow reservoirs with low water level fluctuation can be modeled using a two-dimensional depth-integrated approach which partly reduces the numerical complexity and computational demand, Chang 1996 [26], Gracía-Martinez [52], Govindaraju et al. 1999 [51], Olsen 1999 [92], Van Wijngaarden 1999 [130], Jacoub and Westrich 2002 [66], Wu et al. 2004 [139]. In order to use the sediment transport model for predictive study, the model needs to be calibrated and validated using standard methods. Quasi-steady approximation is also commonly used in reservoir sedimentation predictions, the advantage being the reduction of computational cost and low demand in data resolution.

There exists no published work available on comparative study on the validity of quasi-steady approximation, effects of data aggregation, and effects of various modeling techniques involved in sediment transport modeling. This work will attempt to reveal the aspects involved in long-term simulation of reservoir sedimentation and presents simplified methodologies in predicting the long-term modeling of reservoir sedimentation.

1.1.2 Data driven modeling

Data driven modeling is an approach of modeling data without getting into details of the physical, chemical, and biological processes. The models are however able to make abstractions and generalization of the processes and often play a complementary role to physically based models. The most common type of the data driven models are the regression models. Solomatine 2002 [115] gave approaches in data driven modeling in water resources management; Sinnakaudan et al. [114] gave a multiple linear regression model for total bed load prediction; principal component regression, e.g. Jolliffe 2002 [70] gave a book-wide review on principal component analysis; Hidalgo 2000 [60] used principal component regression procedures for dendrohydrological reconstructions etc.

The use of data assimilation has shown a growing trend in solving complex dynamic interdisciplinary researches. The estimation of the quantity of interest via data assimilation involves the combination of observational data with the underlying dynamical principles governing the system under observation. The modeling of data and dynamics is a powerful methodology, which makes possible, efficient, accurate, and realistic estimations which might not be otherwise be feasible. Data assimilation can be anticipated both to accelerate research progress in complex, modern multiscale interdisciplinary sciences which otherwise are not possible, Robinson 2000 [104].

A number of studies are made using statistical methods to investigate the interaction among various processes in sediment management issues without going into the details of the processes. Most of the statistical studies are made on the qualitative aspect of sediment. For instance, researches on the biological aspects, e.g. Grizzle 1989 [54]; on chemical parameters, e.g. Thompson 2000 [119]; on physico-chemical aspects e.g. Gerbersdorf 2005 [49], Simeonov 2001 [112], Caeiro et al. 2003 [21]; on ecotoxicological aspect, e.g. Hollert 2004 [63] etc. An

example of a study focusing on the quantitative aspect of sediment can be referred, e.g. Picouet 2001 [97].

Investigation on the amount and spatial distribution of sediment in riverine system demands large amount of spatio-temporal data indicating the dynamics of bed evolution over a long period of time in order to develop reasonable data driven model. Such measurements are often not readily available. Combined modeling of dynamics and data is therefore investigated as a step forward to simulate long-term sediment transport processes in riverine systems. There is no work available to statistically model the flow and sediment transport properties with bed evolution of reservoirs.

This work has attempted to model the bed evolution of the Lautrach reservoir using the spatio-temporal bed evolution data output from numerical model, using of the principal components regression modeling. To the author's knowledge this is the first effort to use principal component regression modeling to attempt to model reservoir sedimentation in a spatio-temporal fashion.

1.1.3 Empirical models

The first attempt to predict sedimentation in reservoirs led to empirical curves relating the reservoir capacity loss with the hydrodynamic parameters, Brune 1953 [19]. The simplest hydraulic model of a reservoir is the zero-dimensional scheme, where the time dependent variables can be expressed in terms of volumes and discharges. For an overall classification of reservoirs, the most relevant variables are the reservoir total capacity, the annual runoff volume, and the annual volumetric sediment transport. A certain amount of sediment is always trapped by the reservoir and the ratio between this amount and the sediment input is called a trapping coefficient. The trapping coefficient depends on the water velocity that generally prevails in the reservoir, on its length and on the material grain size. Large values of trapping efficiency are therefore generally associated with large values of the annual averaged residence time. For this reason, a number of empirical expressions have been proposed for the coefficient basically as theoretical residence time. There is no unique correlation between these quantities, as the trapping depends as well on reservoir morphology, the sorting degree of the transported material, flow, and many other physical parameters, see Silvio 2004 [111].

Sales and Shin 1999 [106], developed an empirical based model and made uncertainty analysis on reservoir sedimentation. Significant advances have been made in understanding the importance of the factors involved in reservoir sedimentation. In estimating reservoir sedimentation, a number of uncertainties arise. These are related to stream flow, sediment load, sediment particle size and specific weight, and reservoir operation. The uncertainty of annual reservoir sedimentation and the effect of each uncertain factor, taken individually and in combinations, on the uncertainty of accumulated reservoir sedimentation through time was examined. The results showed that annual stream flow and sediment load are the important factors determining the variability of annual reservoir sedimentation.

In this work, the approach in which the bulk or aggregate parameters like theoretical residence time, mean discharge and reservoir volume is used as a criteria for reservoir sedimen-

tation prediction, were reevaluated using numerical tools. An attempt were made to conduct a comparative study on system response behaviors with respect to relative sedimentation.

1.1.4 Physical scale models

Scale models are mainly used to model complex local processes using physical experiments in hydraulic laboratories. They are the basis for understanding local processes and theoretical developments, e.g. turbulence models etc. Reservoir problems frequently require the application of combination of various approaches.

1.2 Objectives of the study

The present work is aimed at investigating two complementary approaches to quantify the amount and spatial distribution of sedimentation over a long period of time. The numerical approach and the data-driven principal component regression approach.

The first approach is aimed at investigating the steps towards simplified numerical modeling with specific sub-objectives of:

- investigation of basic system behaviors of reservoir responses to periodic inputs and characterization of reservoirs.
- investigation of modeling techniques to propose a simplified optimal strategy with regard to model quality and computational requirement.
- long-term calibration and validation of bed evolution of the Lautrach reservoir and investigation of a simplified guideline for the applicability of quasisteady approximation in long-term prediction.

The second approach is aimed at using a data-driven regression modeling (principal component and multiple regression), in calibrating and validating the amount and spatial distribution of sedimentation based on the numerical output of the Lautrach reservoir. The specific sub-objectives include:

- calibration and validation of the bed evolution of the statio-temporal outcome from the numerical model results using the principal components regression modeling.
- investigation of the applicability of regression modeling on the rate of sediment mass deposition.

1.3 Structure of the work

In the first part of the work, the simplified numerical modeling procedures were described with the following chapters incorporated.

Chapter 2 gives the details of numerical modeling procedures of the flow and sediment transport. Beginning with the steps of model conceptualization, the chapter goes through the governing equations of flow and sediment transport, turbulence modeling, the finite element formulations, and the method of solution of discrete system of equations for flow and sediment transport processes. It describes the model used for the study, the TELEMAC modeling system. It also briefly touches the procedures in numerical model application, the pre-processing, the processing, and the post-processing aspects.

Chapter 3 is devoted to the investigation of fundamental system behavior of reservoirs of distinct shapes and sizes. The responses to discharge and sediment inputs of various amplitudes and frequencies were investigated with respect to unsteady and steady calculations using numerical simulations. Investigation of quasisteady approximations revealed that the regular reservoir is more favorable for ranges of quasisteady approximation as compared to the irregular reservoir. Investigations made on the use of aggregate paraments like theoretical residence time and mean flow indicated a methods of characterizing the steady approximations. A non-dimensional analysis using the analytical solution of ideal reactors, PFR and CSTR, were compared with the result of the two dimensional numerical modeling (advection-dispersion model) with respect to the concentration and mass of sediment deposition. The comparisons indicated that the ideal PFR and CSTR are useful as first hand-tool in characterizing reservoir sedimentation behaviors.

Chapter 4 starts with describing the challenges of data acquisition for modeling reservoir sedimentation. Some methods in data acquisition are briefly presented. The database available for the Lautrach reservoir is analyzed from the data of gauging station of the Kempten and the Lautrach. The data consists of the inflow discharge, the head, the suspended sediment concentration, the bed evolution data and the sediment parameters. A supplementary field data collection and estimation of the critical erosion shear stress in hydraulic laboratory of IWS, in the course of the research shows similarity with the past measurements.

Chapter 5 of the work focuses on the investigation of modeling techniques through using sensitivity analysis on the effect of data aggregation (discharge, suspended sediment concentration, head, sediment gradation), grid refinement, temporal descretization, coupling methods etc. in order to have an optimum model with reasonable computational demand without significant loss of model quality. The chapter further proposes various simplification on the basis of which long-term model calibration and validation of the Lautrach reservoir was performed.

Chapter 6 of the work begins with long-term calibration and validation of bed evolution of the Lautrach reservoir. Sensitivity analysis were made on the erosion and deposition parameters with respect to their effects on the rate of sediment mass deposition. The chapter continues with the investigation on quasisteady approximation using typical daily events, monthly events, and long-term events over a period of years. The application of a mixed-

quasisteady-unsteady simulation was validated and used for the long-term prediction of bed evolution of the Lautrach reservoir.

The second part of the work describes an attempt made to develop a complementary statistical approach for long term simulation of bed evolution processes, based on the outcome of the numerical simulations.

Chapter 7 gives a short review on data driven modeling approach. The simple and multiple regression methods, the principal component analysis, and the principal component regression are presented briefly. The structure of the data used in the regression modeling are also presented.

Chapter 8 presents the investigation resulting from the use of principal components regression modeling as a complementary approach for long-term simulation of bed evolution of the Lautrach reservoir. The reconstruction is well in agreement with the numerical results on the use of multivariate principal components regression between the eigenvectors of the first four principal components and the discharge, differential discharge, and suspended sediment concentration. Furthermore, a regression model on the amount of sediment mass deposition was analyzed with very good agreement in the reconstruction step. For the steps of prediction, the regression modeling showed satisfactory results with a room for further improvement.

Chapter 9 of the work presents the conclusion by integrating the works done on both numerical and regression approaches. It closes by giving an outlook on further studies that can be made with respect to developing further techniques towards improving long-term simulation, and for the use in reservoir planning.

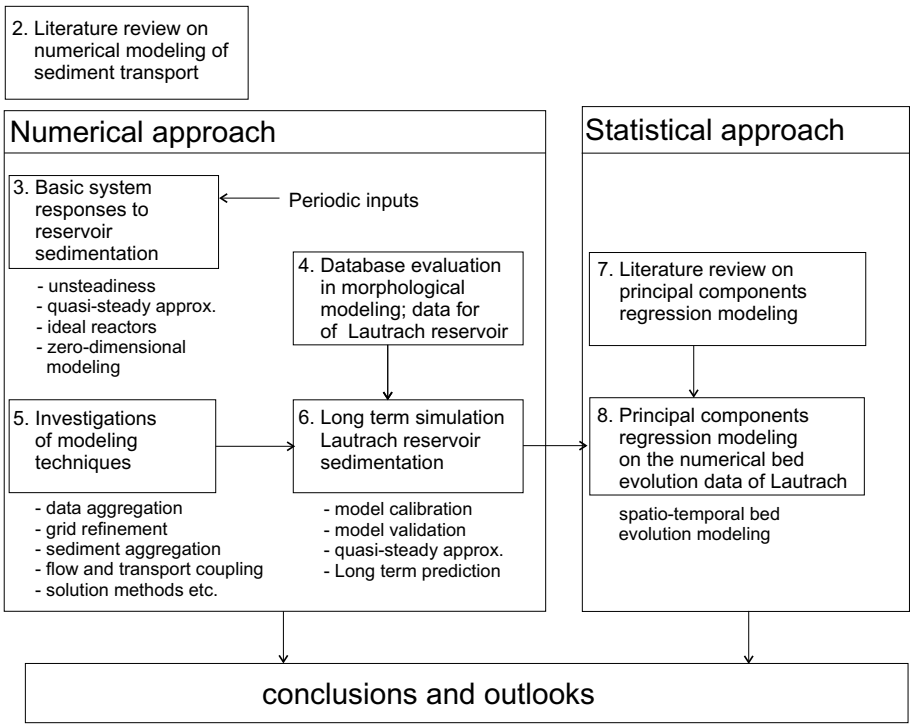

Figure 1.2: Schematic of this work

Part I

Physically-Based Modeling Approach

Chapter 2

Modeling of Flow and Sediment Transport

A model is defined as the result of an abstraction which, based on certain criteria, reduces the system into fewer single aspects. A conceptual model is description of a system, subsystem, or process which is able to represent those aspects of the system behavior that are relevant to model application. A mathematical model transfers concepts to a mathematical formulation, which includes the balance equations for mass, momentum and species as well as system dependent equations of states, see Helmig (1997) [58].

A physically-based model approach describes the physical processes involved in flow and transport by solving conservation laws of mass, momentum, and species transport such as in the case of sediment. It is necessary to simplify the model concepts based on state-of-the-art knowledge in the field for particular aspects of applications. The mathematical formulation of sediment transport equations are solved using numerical models involving a series of simplifications. Simplifications and approximations are then further developed using experimental results. An example of such simplifications are Boussinesq's approximation, turbulence closure models, etc. In this section a brief review on state-of-the-art mathematical modeling and numerical methods to solve flow and sediment transport are presented.

2.1 Mathematical models of flow

2.1.1 Continuity and Navier-Stokes equations

The governing equations of fluid dynamics are expressed in the conservation of mass, energy and momentum. The continuity equation formulates the conservation of mass of flow as:

$$\frac{\partial \rho}{\partial t} + \rho \boldsymbol{\nabla} \cdot \mathbf{u} + \mathbf{u} \cdot \boldsymbol{\nabla} \rho = 0, \tag{2.1}$$

where ρ is the density of a fluid and $\mathbf{u} = [u_1 \quad u_2 \quad u_3]^T$ is the instantaneous velocity vector. For incompressible fluids, the variation in density is neglected in space and time resulting in a simplified continuity equation, known as the condition of incompressibility

$$\boldsymbol{\nabla} \cdot \mathbf{u} = 0. \tag{2.2}$$

The Navier-Stokes equations for momentum conservation are given as:

$$\underbrace{\mathbf{u}_t}_{local\ inertia} + \underbrace{\mathbf{u}\cdot\boldsymbol{\nabla}\mathbf{u}}_{convective\ inertia} = \underbrace{-\frac{1}{\rho}\boldsymbol{\nabla}(p+\rho g z)}_{pressure\ \&\ gravity\ force} + \underbrace{\nu\boldsymbol{\nabla}^2\mathbf{u}}_{viscous\ force} + \underbrace{\mathbf{b}}_{external\ forces} \tag{2.3}$$

where $\mathbf{u}_t$ is the local change of the velocity vector with time, $\mathbf{b}$ is the external forces like the friction, the wind, and the Coriolis, ν is the kinematic viscosity in the friction term, p is the instantaneous pressure, g is the acceleration of gravity, and z is the free surface elevation. More details may can referred in the books by LeMéhauté 1976 [81] and Donea 2003 [36]. Rodi 1993 [105] gave an alternative expression in the tensorial notation based on the Boussinesq approximation in which the density is neglected everywhere except in the buoyancy term.

The continuity, the momentum, and the species transport equations in tensorial form are respectively:

$$\begin{aligned} \frac{\partial u_i}{\partial x_i} &= 0, \\ \frac{\partial u_i}{\partial t} + u_j\frac{\partial u_i}{\partial x_j} &= -\frac{1}{\rho}\frac{\partial(p+\rho g z)}{\partial x_i} + \nu\frac{\partial^2 u_i}{\partial x_j \partial x_j} + b_i, \\ \frac{\partial c}{\partial t} + u_i\frac{\partial c}{\partial x_i} &= \lambda\frac{\partial^2 c}{\partial x_j \partial x_j} + s, \end{aligned} \tag{2.4}$$

where u_i is the instantaneous velocity component in the direction x_i, p is the instantaneous static pressure, b_i surface forces in the i direction, s is the volumetric source term in species transport, and λ is the diffusivity of the energy or the suspended sediment concentration c in this work. The subscript i is the free index indicating the component considered, and the component j is the dummy index indicating the repeated operation.

2.1.2 Turbulence closure assumptions

Turbulence can be modeled using various techniques. A direct numerical simulation (DNS) is a method that attempts to solve the Navier-Stokes equation numerically without simplified turbulence model. The whole range of spatial and temporal scale of turbulence need to be resolved. The computational cost of DNS is very high. However, direct numerical simulation is a useful tool in fundamental research in turbulence. Using DNS it is possible to perform "numerical experiments", and extract from them information difficult or impossible to obtain in the laboratory, allowing a better understanding of the physics of turbulence. In addition, direct numerical simulations are useful in the development of turbulence models for practical applications, such as sub-grid scale models for Large eddy simulation (LES) and models for methods that solve the Reynolds-averaged Navier-Stokes equations (RANS).

LES requires less computational effort than direct numerical simulation (DNS) but more effort than those methods that solve the Reynolds-averaged Navier-Stokes equations (RANS).

The computational demands also increase significantly in the vicinity of walls, and simulating such flows usually exceeds the limits of modern supercomputers today. For this reason, zonal approaches are often adopted, with RANS or other empirically-based models replacing LES in the wall region. The main advantage of LES over computationally cheaper RANS approaches is the increased level of detail it can deliver. While RANS methods provide "averaged" results, LES is able to predict instantaneous flow characteristics and resolve turbulent flow structures, see eg Wissink 1996 [133] etc.

Present day computers are not powerful enough to solve the small-scale turbulent motion in a numerical solution of exact time dependent equations above. For flows of practical relevance a statistical approach as suggested by Reynolds by separating the instantaneous variable in the mean and the fluctuating quantities are used, see (Rodi, 1993) [105].

The instantaneous terms of continuity and Navier-Stokes equations are transformed based on the Reynolds approach into the mean and random fluctuating terms, $u_i = \overline{u}_i + u_i^{'}$, $p = \overline{p} + p^{'}$, $c = \overline{c} + c^{'}$. The mean values of the parameters are averaged over time as

$$\overline{u}_i = \frac{1}{t_2 - t_1}\int_{t1}^{t2} u_i \; dt, \qquad \overline{p} = \frac{1}{t_2 - t_1}\int_{t1}^{t2} p \; dt, \qquad \overline{c} = \frac{1}{t_2 - t_1}\int_{t1}^{t2} c \; dt. \tag{2.5}$$

The Reynolds equations which are closed and exact are

$$\begin{aligned}
\frac{\partial \overline{u}_i}{\partial x_i} &= 0, \\
\frac{\partial \overline{u}_i}{\partial t} + \overline{u}_j\frac{\partial \overline{u}_i}{\partial x_j} &= -\frac{1}{\rho}\frac{\partial(\overline{p} + \rho g z)}{\partial x_i} + \frac{\partial}{\partial x_j}\left(\nu\frac{\partial \overline{u}_i}{\partial x_j} - \overline{u_i^{'}u_j^{'}}\right) + b_i, \\
\frac{\partial \overline{c}}{\partial t} + \overline{u}_i\frac{\partial \overline{c}}{\partial x_i} &= \frac{\partial}{\partial x_i}\left(\lambda\frac{\partial \overline{c}}{\partial x_i} - \overline{u_i^{'}c^{'}}\right) + s.
\end{aligned} \tag{2.6}$$

The term $-\overline{u_i^{'}u_j^{'}}$ is a correlation between fluctuating velocities while $-\overline{u_i^{'}c^{'}}$ is that between the velocity and the concentration. When multiplied with the density ρ the correlations $-\rho\overline{u_i^{'}u_j^{'}}$ and $-\overline{u_i^{'}c^{'}}$ represent the transport of momentum and mass (energy) respectively. $-\rho\overline{u_i^{'}u_j^{'}}$ is the transport of x_i-momentum in the direction x_j, acts as a stress on the fluid and is therefore called turbulent or Reynolds stress. $-\overline{u_i^{'}c^{'}}$ is the transport of the scalar quantity c in the direction x_i and is therefore a turbulent mass flux. The introduction of turbulence models is necessary to approximate lower order correlations and mean flow quantities. Turbulence models simulate the average character of real turbulence. These laws are expressed in differential and algebraic equations together with the mean flow equations. The Boussinesq eddy viscosity concept, which assumes the turbulent stresses proportional to the mean velocity gradient, is the basis of most turbulence models and is given as

$$-\overline{u_i^{'}u_j^{'}} = \nu_t\left(\frac{\partial \overline{u}_i}{\partial x_j} + \frac{\partial \overline{u}_j}{\partial x_i}\right) - \frac{2}{3}k\delta_{ij}, \tag{2.7}$$

where ν_t is the turbulence viscosity or the eddy viscosity which indicates the state of turbulence, δ_{ij} is the Kronecker delta, which is equal to 1 when $i = j$. The first part of the Equation 2.7 involving the velocity gradients yields the normal stresses:

$$\overline{u_1^{'2}} = -2\nu_t\frac{\partial \overline{u}_1}{\partial t}, \qquad \overline{u_2^{'2}} = -2\nu_t\frac{\partial \overline{u}_2}{\partial t}, \qquad \overline{u_3^{'2}} = -2\nu_t\frac{\partial \overline{u}_3}{\partial t}. \tag{2.8}$$

The sum of all normal stresses is two times kinetic energy of fluctuation motion

$$k = \frac{1}{2}\left(\overline{u_1'^2} + \overline{u_2'^2} + \overline{u_3'^2}\right). \tag{2.9}$$

The second term of the is integrated into the pressure term as an unknown $p + \frac{2}{3}k$.

Similarly the turbulent mass transport is expressed as:

$$\overline{u_i' c'} = \Gamma \frac{\partial c}{\partial x_i}, \tag{2.10}$$

where Γ is the turbulent or the eddy diffusivity which is approximated as

$$\Gamma = \frac{\nu_t}{\sigma_t}, \tag{2.11}$$

where σ_t is the turbulent Prandtl or Schmid number expressing the turbulence diffusivity of mass. Usually it is assumed that $\Gamma \approx \nu_t$ taking $\sigma_t = 1$.

A large number of turbulence models have been developed. The most common ones are mentioned here in order to bring in to review the complexities behind and the approximations made in modeling turbulence. Zero-equation models like constant eddy viscosity/diffusivity, Prandtl mixing-length model, Prandtl's Free-shear-layer-model; one-equation models like Kolmogorov-Prandtl model; two-equation models like $k-\epsilon$ model are some to mention, see Rodi, 1993 [105].

The $k-\epsilon$ model is the most widely used approach. For high Reynolds number where local isotropy prevails, the rate of dissipation ϵ is equal to the molecular kinematic viscosity times the fluctuating vorticity $(\frac{\partial u_i'}{\partial x_j})^2$. The equation contains terms representing rate of change, convection, diffusion, generation of vorticity due to vortex stretching connected with the energy cascade, and the viscous destruction of vorticity. The diffusion, generation, and destruction terms require further model assumptions. The difference of the generation and the destruction terms are modeled. The ϵ-equation, together with the k-equation and Kolmogorov-Prandtl expression forms the basis of $k-\epsilon$ model. The Kolmogorov-Prandtl expression for the eddy viscosity is

$$\nu_t = c_\mu \frac{k^2}{\epsilon}, \tag{2.12}$$

where c_μ is an empirical constant, k is the turbulent kinetic energy and ϵ is the dissipation of turbulent kinetic energy. The k and ϵ equations respectively are

$$\begin{aligned}
\frac{\partial k}{\partial t} + \overline{u}_i \frac{\partial k}{\partial x_i} &= \frac{\partial}{\partial x_i}\left(\frac{\nu_t}{\sigma_k}\frac{\partial k}{\partial x_i}\right) + \underbrace{\nu_t\left(\frac{\partial \overline{u}_i}{\partial x_j} + \frac{\partial \overline{u}_j}{\partial x_i}\right)\frac{\partial \overline{u}_i}{\partial x_j}}_{\mathrm{P}} + \underbrace{\beta g_i \frac{\nu_t}{\sigma x_i}}_{\mathrm{G}} - \epsilon, \\
\underbrace{\frac{\partial \epsilon}{\partial t}}_{\text{rate of change}} + \underbrace{\overline{u}_i \frac{\partial \epsilon}{\partial x_i}}_{\text{convection}} &= \underbrace{\frac{\partial}{\partial x_i}\left(\frac{\nu_t}{\sigma_\epsilon}\frac{\partial \epsilon}{\partial x_i}\right)}_{\text{diffusion}} + \underbrace{c_{1\epsilon}\frac{\epsilon}{k}(P+G)\left(1 + c_{3\epsilon}R_f\right) - c_{2\epsilon}\frac{\epsilon^2}{k}}_{\text{generation - destruction}}.
\end{aligned} \tag{2.13}$$

The constants in the $k-\epsilon$ model are c_μ=0.09; $c_{1\epsilon}$=1.44; $c_{2\epsilon}$=1.92; σ_k=1.0 and σ_ϵ=1.3. $c_{3\epsilon}$ is constant a for the buoyant condition and R_f is the Richardson number for buoyancy correction.

The kinematic viscosity and diffusivity terms are replaced by turbulence viscosity and diffusivity in simplifying the turbulence processes in flow and transport phenomenon. Equation 2.3 becomes

$$\bar{\mathbf{u}}_t + \bar{\mathbf{u}} \cdot \boldsymbol{\nabla} \bar{\mathbf{u}} - \boldsymbol{\nabla} \cdot (\nu_t \boldsymbol{\nabla} \bar{\mathbf{u}}) + \frac{1}{\rho} \boldsymbol{\nabla} (\bar{p} + \rho g z) = \mathbf{b}, \tag{2.14}$$

where $\bar{\mathbf{u}}$ represents mean portion of the instantaneous velocities, i.e. $\bar{\mathbf{u}} = [\overline{u_1} \quad \overline{u_2} \quad \overline{u_3}]^T$, and $\bar{p}$ the mean part of instantaneous pressure.

Turbulence models for depth integrated flow are developed on a similar basis by integrating all the variables over depth. Suppose the flow and transport variables are integrated over depth from the bottom z_b to the water surface z, and the depth averaged values of the variables velocity U and concentration C are:

$$U_i = \frac{1}{h} \int_{z_b}^{z} u_i \, dh; \qquad C = \frac{1}{h} \int_{z_b}^{z} c \, dh \tag{2.15}$$

which is resolved into mean and fluctuating terms for the depth averaged flow variables U_i and C to develop a depth averaged turbulence model,

$$-\overline{U_i' U_j'} = \tilde{\nu}_t \left(\frac{\partial \overline{U}_i}{\partial x_j} + \frac{\partial \overline{U}_j}{\partial x_i} \right) - \frac{2}{3} \tilde{k} \delta_{ij}; \qquad \overline{U_i' C'} = \tilde{\Gamma} \frac{\partial \overline{C}}{\partial x_i} \tag{2.16}$$

where $\bar{U}_i^{'}$ and $\bar{U}_j^{'}$ are the mean part of the instantaneous depth averaged velocities in the direction i and j; $U_i^{'}$ and $U_j^{'}$ are the fluctuating part of the depth averaged velocities in the i and j directions; $\bar{C}$ and $C^{'}$ are the mean and fluctuating part of the concentration; $\tilde{\nu}_t$ is turbulent viscosity for depth averaged flow; $\tilde{k}$ is depth averaged turbulence kinetic energy; $\tilde{\Gamma}$ is the depth averaged eddy viscosity. Details in modeling the turbulence may be referred in Rodi 1993 [105] and Clifford 1993 [31].

From this review on turbulence modeling, it can be observed that the mathematical model to describe flow and transport involves various approximations without which solutions are complex to present day's state-of-the art. The next level of approximation used in mathematical modeling of hydrodynamics and transport is an approximation related to model dimensions.

2.1.3 Shallow water equations

Shallow flows are bounded, layered turbulent flows in a domain for which the flows in the direction of flow as well as one transverse dimension highly exceeds the third dimension. This is a kinematic condition for shallow flows. The dynamic requirement is that the nature of the bounding surface in which at least one boundary have to be a shear supporting,

e.g a solid bottom in channels or a density interface. The other interface may largely be shear-free, e.g. air, see Jirka and Uijttewall 2003 [68].

For shallow flows in rivers and reservoirs, depth integrated flow and transport models are commonly used. The three-dimensional continuity and momentum equations are integrated over depth to obtain the Saint-Venant equations. The assumptions included are the fluid is Newtonian, incompressible, the pressure distribution is hydrostatic, and a Reynolds decomposition and stochastic averaging is applied in order to model turbulence. The complete set of equations under these assumptions yield a non-conservative (depth-velocity) formulation for continuity and momentum:

$$\begin{aligned} \frac{\partial h}{\partial t} + \boldsymbol{\nabla} \cdot (h\mathbf{U}) &= q, \\ \frac{\partial \mathbf{U}}{\partial t} + \mathbf{U} \cdot \boldsymbol{\nabla}(\mathbf{U}) - \boldsymbol{\nabla} \cdot (\tilde{\nu}_t \boldsymbol{\nabla}\mathbf{U}) + g\boldsymbol{\nabla} z &= \mathbf{b}, \end{aligned} \tag{2.17}$$

where, h is the depth of flow, $\mathbf{U} = [U \quad V]^T$ is the depth averaged mean velocities in the longitudinal and lateral directions, q is the source/sink term of the continuity equation, $\tilde{\nu}_t$ is the depth averaged turbulent viscosity, $\mathbf{b}$ is the external force vector in the longitudinal and lateral directions, and z is the free surface elevation.

2.2 Mathematical model for sediment transport

2.2.1 Basics of model conceptualization

The conceptual formulation of the mathematical model for sediment transport processes is very complex. The interaction between water and sediment, erosion and deposition processes, and sediment properties are of major importance. Sediment transport is very challenging when non-equilibrium sediment transport problems are to be assessed. It is always necessary to focus on a dominant processes in developing sediment transport model concepts. Mathematical formulation of sediment transport can be approached on the basis of mode of transport, phase of transport, properties of sediment, model conceptualization, etc. Before giving a formulation for suspended sediment transport a review is given on relevant parameters and processes.

Mode of transport: Generally two modes of sediment transport are identified. Bed load transport is a type of sediment transport in which the solid particles glide, roll or jump but stay very close to the bed. A large number of empirical relations are developed to model the bed load. A summary on the bed relations by Schoklitsch, Einstein, Toffaleti, Madden, Yang, DuBoy, Ackers-White, Colby, Meyer-Peter and Müller, Madden, Copeland can be referred to HEC-6 documentation [121], Raudkivi 1998 [101], Graf 1998 [53], Yalin 1972 [143] etc. Suspended load transport is the mode of transport where solid particles displace themselves by making big jumps and are transported by diffusion, convection and dispersion. Works done by Einstein, Krone and Partheniades relevant to suspended sediment

relation are summarized in the book by Raudkivi 1998 [101]. Total sediment transport is the sum of bed load and suspended load. The work by Einstein and Laursen can be seen in the Raudkivi 1998 [101].

Model phases: Mono-phase models are formulated based on the hypothesis that solid and fluid particles move at the same velocity. In such models, flow fields should be first determined by resolving the hydrodynamic equations. The convection, diffusion, and generation of suspended sediment are then modeled by the transport equation. The advantage of the mono-phase models are that they demand lower computational time and present results that are acceptable for engineering problems. An interaction between fluid and solid particles and between the particles is not taken into consideration. The exchange between fluid and bed is evaluated through deposition and erosion fluxes crossing the fictive-bed surface by many empirical formulas, in which many parameters must be given by user. These parameters depend on the flow and geological conditions such as bed material and degree of consolidation; information which is often insufficient. Indeed, mono-phase models can be calibrated and verified by tuning the parameters. The calibrated model could still be correct only for conditions which approach the simulation. In two-phase models, all interaction such as fluid-particle, particle-particle, particles-walls are taken into computation. Since the consolidation of solid particles could be taken into computation, no fictive bed definition is necessary. The approach is however at its infancy and has no practical application so far. Nguyen 2002 [89].

Cohesiveness: Non-cohesive sediment is sediment in which the inter particular forces are negligible. Each fraction is assumed to act independently. They do not exhibit consolidation as well as flocculation. Determination of settling velocity and critical shear stress for deposition is relatively simple especially when the sediment is uniform.

Cohesive sediments on the other hand form a coherent mass rather than a collection of individual particles in contact to each other. They contain significant amount of clay minerals which control the behavior of the sediment. Cohesive properties arise from electro-chemical forces in the clay-water medium. The transport and fate of fine-grained cohesive sediment is influenced by settling velocity of the sediment, which in turn is affected by flocculation effects. The flocculation process depend on strong physico-chemical properties of sediment and the water, and on several physical mechanisms, of which turbulence is a major one.

The depositional processes of cohesive sediment involve aggregation and disaggregation of flocks governed by turbulence and sediment concentration. The dynamics of settling velocity of flocks is quite distinct from that of a single non-cohesive particles acting independently. Interested reader may refer to the references by Ziegler 1995 [149] and Winterwerp 1998 [132]. The settling velocity is influenced by the degree of flocculation which depends on particle size, density of particles, sediment concentration, viscosity and turbulence.

Concentrated cohesive sediment suspension exhibits strongly non-Newtonian and time dependent characteristics caused by particle interactions, which complicates the prediction of their strain or shear rate response to applied forces, see Kessel 1999 [76]

Erosion and deposition processes: In a non-equilibrium transport condition, the shear boundary of flows are changing under acting forces. The governing parameters in determin-

ing the erosion and sedimentation are critical shear stress for erosion and deposition.

The initiation of particles motion from bed is investigated through physical experiments. One of the earliest work was carried out by Shields 1936 [110]. It was represented by the relationship between the dimensionless shear parameter (Reynold's number) and dimensionless particle diameter (Froude's number). Similar works on the beginning of suspension of sediment were done by Bagnold 1966 [7], Bridge 1981 [14], Engelund 1967 [43] and Van Rijn 1984 [122]. Generally, the critical shear stress for initiation of motion is lower than that for suspension. The works show large variation for defining ranges of critical stresses for suspension. Xu 1998 [142] summarized the works in more detail.

Compared to non-cohesive sediment dynamics, cohesive sediment dynamics are much more complicated as a result of the relevant physical, chemical and biological processes. The parameters may not be adequately evaluated in the laboratory conditions, and their application for field assessments, computer modeling, and/or theoretical developments may often be insufficient. To overcome this problem, various field methods have been developed for direct measurement of cohesive sediment properties and dynamics. The most common tools are the benthic in-situ flumes. Although several such devices are actively used, there is still little agreement on the methods for data interpretation and analysis, see Aberle 2006 [1].

Sandia National Laboratories has developed an Adjustable Shear Stress Erosion and Transport (ASSET) Flume that quantifies in situ erosion of a sediment core with depth while affording simultaneous examination of transport modes (bed load versus suspended load) of the eroded material, see Roberts 2003 [103].

The SETEG (Ein Strömungskanal zu Ermittlung der tiefenabhängige Erosionsstabilität von Gewässersedimneten) System is a flume developed by Institut für Wasserbau an der Universität Stuttgart to measure the erosion of cohesive aquatic sediment as a function of depth. See Kern et. al 1999 [75]. Witt and Westrich 2003 [135] developed a method called SEDICA, based on SETEG system, which is used to measure depth and time dependent erosion rate of cohesive undistributed sediment core, using digital image processing. The erosion rate (flux) E_b is approximated using various, but similar empirical formulations. Witt 2004 [134] has summarized the works by Krone 1962 [78], Kandiah 1974 [71], Arulanandan 1975 [6], Parchure 1985 [96], Christensen 1973 [29] and Lambermont 1978 [80] etc.

The relationships for determining the erosion flux, $E_b[kg/(m^2 s)]$, generally involve the difference of bottom shear stress τ_o and critical shear stress for erosion τ_{ce} with various factors in use. Erosion will take place for $\tau_o > \tau_{ce}$. Some of the relations are given below.

$$E_b = M\left(\frac{\tau_o}{\tau_{ce}} - 1\right), \tag{2.18}$$

$$E_b = M'(\tau_o - \tau_{ce}), \tag{2.19}$$

$$E_b = \varepsilon_f e^{\left[\alpha(\tau_o - \tau_{ce})^{\frac{1}{2}}\right]}, \tag{2.20}$$

where Equation 2.18 is the most widely used and was proposed by Kandiah 1974 [71], in which M is the erosion coefficient in $kg/m^2 s$ determined from experiment; in Equation 2.19

M' is in s/m and is also determined from experiment; Equation 2.20 is used for fresh deposits of cohesive sediments with sediment specific coefficients ε_f between 0.67 and 88 g/m^2s and α between 7.9 and 18.4 $(N/m^2)^{0.5}$.

The critical shear stress for the erosion of cohesive sediment is generally considered as having a measured value common to all of the particle gradation. Because of the inter-particular attraction of cohesive consolidated sediment, the different fractions of aggregate will resuspend together and selective resuspension theories have not yet been investigated. The total amount of sediment is not resuspended instantaneously. The erosion rate is variable in time, with a high rate at the initiation of erosion followed by a decreasing resuspension flux until the bed becomes armored and the rate goes zero. Hence, as a first approximation it is commonly assumed that the resuspension rate is constant and equal to its initial value until all available sediment is resuspended. E is then set to zero until further sediment is deposited and available for resuspension, or until the shear stress increases. Gailani et. al 1991 [46] conducted a study based on this assumption, achieving a good agreement between the predicted and measured sediment concentrations in riverine system during flood conditions. The results indicated that the assumption of constant erosion until bed armoring occurs is valid for the spatial and temporal scales typically considered in modeling studies of aquatic systems. The resuspension rate of class n is then given by $E_n = f_n E$, where f_n=fraction of class n sediment in the surficial layer of cohesive bed. The initial distribution of f_1 and f_2 in the cohesive sediment bed, i.e., fractions of class 1 and 2 sediment, was assumed to be horizontally constant.

The deposition flux is given by the probability formulation of Ariathuri 1976 [5],

$$D_{bn} = p_n v_{sn} c_n, \tag{2.21}$$

with $p_n = 1 - \frac{\tau_o}{\tau_{cdn}}$ for $p_n = \tau_o \leq \tau_{cdn}$ and 0 for $\tau_o > \tau_{cdn}$. Where p_n is the probability of deposition of the sediment class n, v_{sn} is the settling velocity of for a particle class n, τ_o is the bottom shear stress given by ρu_o^2, τ_{cdn} is the critical shear stress for deposition given as $\tau_{cdn} = \rho u_{cdn}^2$ and u_{cdn} is the critical shear velocity for deposition for particle class n.

Wu and Wang 2006 [138] gave a review on methods for determining settling velocities and porosity. The terminal settling velocity of sediment particle can be determined by equating the effective weight force to the drag resistance as

$$v_s^2 = \frac{4}{3C_d}\frac{\rho_s - \rho}{\rho} gd. \tag{2.22}$$

In 1851 Stokes solved the Navier-Stokes equation with the aid of a shear function and neglecting the inertial terms, and theoretically derived the drag coefficient for a spherical particle in the streamline settling region. For $R < 0.5$, $C_d = 24/R$, where the Reynolds number $R = v_s d/\nu$, with ν the kinematic viscosity of water. For higher R, C_d has to be determined experimentally. Cheng 1997 [28] approximated the drag coefficient by:

$$C_d = \left[\left(\frac{M}{R}\right)^{1/n} + N^{1/n}\right]. \tag{2.23}$$

Values of M, N, and n for 7 various relations are shown in the work. For Cheng's approach, the parameters are approximated to be, $M = 32$, $N = 1$ and $n = 1.5$.

Wu and Wang 2006 [138] proposed a relation which they argue to be superior over all previous relations:

$$v_s = \frac{M\nu}{Nd}\left[\sqrt{\frac{1}{4}+\left(\frac{4N}{3M^2}D_*^3\right)^{1/n}}-\frac{1}{2}\right]^n, \tag{2.24}$$

where $D_* = d[(\rho_s/\rho - 1)g/\upsilon^2]^{1/3}$, $M = 53.5e^{-0.655S_f}$, $N = 5.65e^{-2.5S_f}$, and $n = 0.7 + 0.9S_f$ where S_f is a Corey shape factor. Other relations that are mentioned for settling velocities of fine suspended sediment include those by Westrich 1988 [127], Käser 1980 [72]. For cohesive sediment forming flocks, a review on relations of settling velocities are reviewed by Nikora et al. 2004 [90]. More details on various empirical relations developed to approximate settling velocities can be found in Krone 1962 [78], Stringham 1965 [118], Van Rijin 1984 [122] and in Simons 1992 [113].

The presence of a large number of relations proposed by various researchers shows that it can be quite difficult to fix which equations to choose in determining critical shear stress for deposition, settling velocities, porosity, etc. in modeling sediment transport. It must be carefully approached by choosing the methods under which each relation is developed. Furthermore, experimental investigations and practical experience may better guide the way to provide the greatest utility when deciding on the crucial parameters. Generally, there is still a gap of formulating universal equations for erosion and deposition processes as a result of the complex physical, chemical, and biological phenomenon involved in sediment transport.

2.2.2 Governing equations of suspended sediment transport

Overall sediment transport in open channel is governed by the following equation:

$$\frac{\partial c}{\partial t} + \frac{\partial}{\partial x_i}[(u_i - v_s\delta_{i3})c] = \frac{\partial}{\partial x_i}\left(\frac{\upsilon_t}{\sigma_c}\frac{\partial c}{\partial x_i}\right); \qquad i = 1,2,3, \tag{2.25}$$

where c is local sediment concentration, v_s is settling velocity of sediment, δ_{i3} is Kronecker delta with $i = 3$ indicating the vertical direction; σ_c is turbulent Schmidt number representing turbulent diffusivity of the sediment to the eddy viscosity ν_t, see Wu 2000 et al. [140], Fang 2003 [44]. The sediment equation is solved with the following boundary conditions: At the free surface, the vertical sediment flux is zero and hence the condition applied is:

$$\frac{\nu_t}{\sigma_c}\frac{\partial c}{\partial z} + v_s c = 0. \tag{2.26}$$

At the lower boundary of the suspended sediment layer, the net flux across the interface is considered. The net flux across the boundary between the two layers is the difference of deposition flux and erosion flux, $D_b - E_b$. The deposition rate at the interface is $D_b = v_s c_b$ while for the entrainment rate E_b, various erosion model have to be introduced. Following Van Rijn 1987 [123] and Celik 1988 [25] it is assumed that the entrainment rate is equal to the deposition rate at equilibrium concentration, $E_b = D_b$.

$$E_b = v_s c_{b*}, \tag{2.27}$$

where c_{b*} is the equilibrium concentration just above the saltation layer $z^{'} = \delta_b$. The sediment flux at the lower boundary of the suspended-load layer to be prescribed is thus:

$$D_b - E_b = v_s(c_b - c_{b*}) \tag{2.28}$$

where c_b is the bottom concentration.

The 2D depth averaged non-equilibrium and uniform suspended sediment transport in the non-conservative form is:

$$\frac{\partial(hC)}{\partial t} + \frac{\partial(UhC)}{\partial x} + \frac{\partial(VhC)}{\partial y} - \frac{\partial}{\partial x}\left(\varepsilon_s h\frac{\partial C}{\partial x}\right) - \frac{\partial}{\partial y}\left(\varepsilon_s h\frac{\partial C}{\partial y}\right) = -\alpha v_s(C - C^*), \tag{2.29}$$

where C is the depth averaged sediment concentration, α is the adjustment coefficient, v_s is the settling velocity, C^* is the sediment carrying capacity, U and V are depth averaged velocities in the longitudinal and lateral directions and ε_s is the sediment turbulent diffusion coefficient given as $\varepsilon_s = \tilde{\nu}_t/\sigma_t$. The bed evolution is thus given by the expression:

$$\rho_s(1 - \rho^{'})\frac{\partial z_b}{\partial t} + \frac{\partial(hC)}{\partial t} + \frac{\partial(q_{Tx})}{\partial x} + \frac{\partial(q_{Ty})}{\partial y} = 0, \tag{2.30}$$

where z_b is the local bed level above datum, $\rho^{'}$ is the porosity of the bed material, ρ_s is the sediment concentration, C is the depth averaged concentration, and q_{Tx} and q_{Ty} are the components of the total-load sediment transport in the x and y directions respectively. The second term is the storage term and can be neglected for the steady flow conditions e.g. Van Rijn 1987 [123], Wu 2000 [140]. For purely suspended sediment transport, Fang and Rodi 2003 [44] gave the mass-balanced equations for river bed material as:

$$\rho_s(1 - \rho^{'})\frac{\partial z_b}{\partial t} + D_b - E_b = 0. \tag{2.31}$$

Guo 2002 [55] proposed a slightly modified formulation by considering the non-uniformity of the whole sediment mixture into several size groups in which the sediment is considered to be uniform by introducing an adjustment coefficient. The concentration in the convective and dispersive terms are the total concentration of the mixture. While the term dealing with entrainment and deposition is reformulated as follows:

$$\alpha v_s(C - C^*) \equiv \sum_{n=1}^{N} \alpha_n v_{sn}(C_n - C_n^*), \tag{2.32}$$

where α_n, v_{sn}, C_n, and C_n^* denote the non-uniformity adjustment coefficient, the fall velocity, the concentration, and the carrying capacity of sediment class n respectively. For nonuniform, non-equilibrium fine sediment transport, Ziegler and Nisbet 1995 [149] formulated an approach based on considering an individual sediment fraction being transported independently. The sediment concentration for each sample was taken rather than the averaged sediment concentration resulting in;

$$\frac{\partial(hC_n)}{\partial t} + \frac{\partial(UhC_n)}{\partial x} + \frac{\partial(VhC_n)}{\partial y} - \frac{\partial}{\partial x}\left(\varepsilon_s h\frac{\partial C_n}{\partial x}\right) - \frac{\partial}{\partial y}\left(\varepsilon_s h\frac{\partial C_n}{\partial y}\right) = E_{bn} - D_{bn}, \tag{2.33}$$

where C_n is the mean concentration of the suspended sediment of particle class n, E_{bn} is the resuspension flux of class n, and D_{bn} is the deposition flux of class n. Similarly the mass balance equation for bed-load based on the Van Rijn 1987 [123] may be given by:

$$\rho_s(1-\rho^{'})\frac{\partial z_b}{\partial t}+\frac{\partial(\delta\bar{c}_{bn})}{\partial t}+\frac{\partial(\alpha_{bx}q_{bxn})}{\partial x}+\frac{\partial(\alpha_{by}q_{byn})}{\partial y}=-\alpha v_{sn}(C_n-C_n^*), \tag{2.34}$$

where $\bar{c}_{bn}$ the concentration in the bed-load layer averaged over the layer thickness for the class n, and q_{bxn} and q_{byn} are the bed-load transport in the x and y directions for the class n. Neglecting the bed load, and the storage term it simplifies to:

$$\rho_s(1-\rho^{'})\frac{\partial z_b}{\partial t}=\alpha_n v_{sn}(C_n-C_n^*)=E_{bn}-D_{bn}. \tag{2.35}$$

2.3 Coupling flow and suspended sediment transport

Models of flow and suspended sediment transport can be formulated as uncoupled/decoupled, semi-coupled and fully-coupled. For uncoupled flow and sediment transport models, flow and sediment transport models are solved separately for the whole computational period. The flow models generate simulated flow field for the entire model period which is used by sediment transport models to solve sediment transport equations. The flow field and morphological change may be updated at a critical intervals of changes in bed evolution determined by a modeler. The transport model is then run with the updated flow field. The method is more effective for cases where the change in profiles is negligible or under condition of equilibrium transport.

For semi-coupled flow and sediment transport models, flow and sediment transport fields are updated for each computational time step. The flow model first solves the flow field for the current time step. The predicted flow field is then used to calculate the sediment transport. Next the flow field calculation takes into account the predicted change due to erosion and deposition processes, see Hayter et al. [57].

In a strong (full) coupling between flow and sediment transport, flow and sediment transport equations are completely coupled and solved simultaneously. The continuity equation, the momentum equations of flow and the continuity equation, and sediment distribution equations of sediments are solved simultaneously for each computational time step. This method may provide the best accuracy but demands a higher computational cost and involves more numerical complexity. The works by Murillo et al. 2006 [88], Murillo et al. 2005 [87], Cao et al. 2002 [22], and Soulis 2002 [117] should be mentioned. A simplified 2D formulation of fully coupled flow and non-equilibrium transport can be expressed as:

$$\frac{\partial \mathbf{F}}{\partial t}+\frac{\partial \mathbf{G}}{\partial x}+\frac{\partial \mathbf{H}}{\partial y}=\mathbf{B}, \tag{2.36}$$

where the **F**, **G**, **H**, and **B** are given by:

$$\mathbf{F} = \begin{bmatrix} h \\ hU \\ hV \\ hC \\ \rho_s(1-\rho^{'})z_b \end{bmatrix}, \qquad \mathbf{G} = \begin{bmatrix} hU \\ hU^2 + gh^2/2 - \tilde{\nu}_t \left[2\frac{\partial(hU)}{\partial x}\right] \\ hUV - \tilde{\nu}_t \left[\frac{\partial(hU)}{\partial y} + \frac{\partial(hV)}{\partial x}\right] \\ UhC - \varepsilon_s \left[\frac{\partial(hC)}{\partial x}\right] \\ q_{bx} \end{bmatrix},$$

$$\mathbf{H} = \begin{bmatrix} hV \\ hUV - \nu_t \left[\frac{\partial(hU)}{\partial y} + \frac{\partial(hV)}{\partial x}\right] \\ hV^2 + gh^2/2 - \nu_t \left[2\frac{\partial(hV)}{\partial y}\right] \\ hVC - \varepsilon_s \left[\frac{\partial(hC)}{\partial y}\right] \\ q_{by} \end{bmatrix}, \qquad \mathbf{B} = \begin{bmatrix} q \\ gh(S_{ox} - S_{fx}) \\ gh(S_{oy} - S_{fy}) \\ D_b - E_b \\ D_b - E_b \end{bmatrix}, \tag{2.37}$$

where $S_{ox} = \frac{\partial z}{\partial x}$, and $S_{oy} = \frac{\partial z}{\partial y}$ are the channel slopes in x and y directions. S_{fx} and S_{fy} are friction slopes determined from Manning-Strickler or similar equations, and q_{bx} and q_{by} are the sediment discharge per unit width in the x and the y directions.

Most sediment transport models adopt the assumptions that the sediment concentration is so low that the interaction between flow and sediment movement can be neglected and bed change is much slower than flow movement such that at each time step, the flow can be calculated by assuming a fixed bed. Furthermore, the hiding and exposure mechanism in the bed load material is considered through the introduction of correction factors in the non-uniform sediment transport capacity formulas. Wang and Wu 2004 [126]. Fully-coupled models are not in common use as the standard for flow and sediment transport modeling of the aqueous environment.

2.4 Finite element method in flow and suspended sediment transport

The mathematical models of flow and sediment transport processes, expressed as partial differential equations, are solved by numerical models. Numerical models describe the transfer of mathematical models to numerical algorithms. Numerical model must guarantee the solution of the constitutive equations for different geometries, initial and boundary conditions with respect to known system state variables. The result is a simulation program which can be used for the computation of a specific process. Hinkelmann 2003 [62] gave a review on efficient numerical method for problems in environment water.

The finite element method is a powerful computational technique for the solution of differential and integral equations that arise in various fields of engineering and applied science. The method is a generalization of the classical variational (i.e. Rayleigh-Ritz) and weighted-residual (e.g. Galerkin, least squares, collocation, etc.) methods. The traditional variational and weighted residual method suffers from the shortcoming of construction of the approximation functions that satisfy the boundary conditions of the problem to be solved. Most real world problems are to be defined on an extremely complex geometry. It is therefore difficult to generate approximation functions satisfying different types of boundary conditions on different portion of the boundary of complex domain.

The approximation functions are constructed from interpolation theory, and hence are called interpolation functions. The major steps in the finite element method analysis of a typical problem are: discretization of the domain into a set of finite elements (mesh generation), weighted integral or weak formulation of the differential equation to be analyzed, development of the finite element model of the problem using its weighted integral or weak form, assembly of finite elements to obtain the global system of algebraic equations, imposition of boundary conditions, solution of equations, post-computation of solutions and quantities of interest, see Reddy 1994 [102].

In order that a discretization technique be effectively used, they need to fulfil certain criteria. The methods must be consistent, meaning the discretization error must approach zero up on spatial and temporal refinement. Stability, ensures that perturbations are continuously damped out in the course of simulation and do not lead to increasing oscillation. In addition, a discretization method must be convergent, that is the numerical solution of the discretized equation converges towards the exact solution as space and time steps tend to zero. If a system is consistent and stable, convergence is mathematically proven, see e.g. Hinkelmann 2003 [62], Helmig 1997 [58], Donea 2003 [36].

A classical method in finite element discretization is the semi-discrete method in which the time discretization is made using finite difference method and the spatial discretization with finite element method.

The partial differential equation of the flow and/or transport problem can be expressed as:

$$\mathbf{f}_t + \mathbf{A}\mathbf{f} - \mathbf{s} = 0, \tag{2.38}$$

where $\mathbf{f}_t = \frac{\partial \mathbf{f}}{\partial t} = -\mathbf{A}\mathbf{f} + \mathbf{s}$, $\mathbf{A}$ is a partial derivative of any form representing the fluid dynamic problem, $\mathbf{f}$ is any of the fluid dynamic parameters (e.g. for the depth averaged case, $\mathbf{f} = [h\ U\ V\ C]^T$), and $\mathbf{s}$ is the source/sink term.

2.4.1 Time discretization

Temporal discretization can take various form depending on the degree of accuracy required and computational cost involved. The most common method is the θ family method. It is a single step method in which values of $\mathbf{f}^{n+1}$ at time $t^{n+1} = t^n + \triangle t$ is calculated from the

known $\mathbf{f}^n$ at time t^n.

$$\frac{\mathbf{f}^{n+1} - \mathbf{f}^n}{\triangle t} = \theta \mathbf{f}_t^{n+1} + (1-\theta)\mathbf{f}_t^n, \tag{2.39}$$

θ is a parameter taken to be in the interval $[0, 1]$. For $\theta = 0$ the method is explicit forward Euler method, for $\theta = 1$ the method is implicit backward Euler method. For $\theta = 1/2$ the method is called Crank-Nicolson which is second order accurate method, for $\theta = 2/3$ the method is called Galerkin. For $\theta \geq 1/2$, the scheme is stable. Usually, the Crank-Nicolson scheme is used for true transient problems where time accuracy is important. For explicit schemes the Courant stability criteria must be fulfilled. See 2003 [36].

Mixed hyperbolic and parabolic equations are difficult to handle. Techniques to simplify the equations by splitting into simpler parts are often necessary. Operator splitting (fractional step) method is a method widely used in time integration of unsteady problems. They can differ based on the nature of splitting from case to case. See e.g. Yanenko 1971 [145], Malcherek 2000 [84], Ames 1992 [4], Mitchell 1980 [85], Quarteroni 1997 [99] for details on splitting techniques.

2.4.2 Spatial discretization

The classical method uses the Galerkin formulation that is also known as a method of weighted residual. The spatial discretization is based on interpolation functions, usually polynomials, that interpolate the values over the elements. Thus the values $f(\mathbf{x})$ any where in the domain are interpolated from the nodal values $\hat{f}(\mathbf{x})$. The interpolation functions are not time dependent but dependent on the shape of the elements. That is why the term shape function is used. They take various form depending on whether the elements are triangular, quadrilateral, hexagonal etc. The finite element approximation for each element is

$$f(\mathbf{x}) \approx f^e(\mathbf{x}) = \sum_{i=1}^{n^e} N_i \hat{f}_i(\mathbf{x}), \tag{2.40}$$

where N_i is the interpolation function and n^e is the number of nodes per element. The finite element approximation $f^e(\mathbf{x})$ of $f(\mathbf{x})$ over an element must be continuous, i.e. all terms in the weak form are represented as non-zero values. That is, all interpolation polynomials should be included and all polynomials should be linearly independent. For details on interpolation functions of finite elements one may refer to Connor 1976 [33], Rao 1989 [100], Reddy 1994 [102].

The finite element approximation deviates from analytic solution by residual error ε. Considering Equation 2.38, the finite element approximation results in:

$$\mathbf{f}_t + \mathbf{A}\mathbf{f}^e - s^e = \boldsymbol{\varepsilon}. \tag{2.41}$$

Using the method of weighted residuals, the residual $\boldsymbol{\varepsilon}$ is multiplied by weighting function $\mathbf{w}$ and is forced to zero through integration over the spatial domain Ω.

$$\int_\Omega \mathbf{w}\boldsymbol{\varepsilon}\ d\Omega = 0. \tag{2.42}$$

For the standard Galerkin formulation, the weighting function w is assumed to be the same as the interpolation function N_i. This assumption has significant deficiencies in convective dominated problems. These deficiencies are overcome by Petrov-Galerkin techniques. The key idea practically in all the proposed finite element formulations of upwind type has been to replace the Standard Galerkin formulation with the Petrov-Galerkin weighted residual formulation in which the weighting function to be selected on different classes of functions than the approximate solution. Modified weighting functions, such that elements upstream of a node are weighted more heavily than the elements downstream of the node are considered. The concept of adding diffusion along the streamlines in consistent manner has been successfully exploited in the Streamline-Upwind Petrov-Galerkin (SUPG) method. An example of modified interpolation function for stabilization is given by Brooks and Hughes 1982 [16] in which elements upstream of the nodes are weighted more.

$$\mathbf{w}_s = \mathbf{w} + k\frac{\mathbf{u}}{|\mathbf{u}|} \cdot \boldsymbol{\nabla}\mathbf{w}, \tag{2.43}$$

where $\mathbf{w}_s$ is the stabilized weighting function, k is a coefficient, and $\mathbf{u}$ is the velocity at nodes and $\mathbf{w}$ is the standard weighting function (test function). Other stabilization techniques can be looked through in Christie 1976 [30], Hughes 1978 [64], Kelly 1980 [74], Brooks 1982 [16], Codina 1998 [32].

The distribution of the differentiation among $\mathbf{f}$ and $\mathbf{w}$ so that $\mathbf{f}$ and $\mathbf{w}$ are only differentiable once is achieved by the Green-Gauss divergence theorem that produce the weak form and produce a natural Neumann boundary condition.

The assembled form of the flow and transport process in a compact assembled algebraic equation can be given as:

$$\mathbf{M}\dot{\mathbf{f}} + (\mathbf{C} + \mathbf{K})\mathbf{f} = \mathbf{r} \tag{2.44}$$

where $\dot{\mathbf{f}}$ is ordinary time derivative of the unknown flow and transport vectors $\mathbf{f}$, and $\mathbf{r}$ is the contribution of source/sink terms. By topological assembly of element contributions with the assumption of standard Galerkin method,

$$\mathbf{M} = \int_{\Omega_e} N_i N_j \, d\Omega, \qquad \mathbf{C} = \int_{\Omega_e} N_i(\mathbf{u} \cdot \boldsymbol{\nabla} N_j) \, d\Omega, \qquad \mathbf{K} = \int_{\Omega_e} \boldsymbol{\nabla} N_i \cdot (\nu_t \boldsymbol{\nabla} N_j) \, d\Omega, \tag{2.45}$$

where $\mathbf{M}$ is the mass matrix, $\mathbf{C}$ is the convection matrix and $\mathbf{K}$ is the viscosity/dispersion matrix, $\mathbf{u}$ is the velocity vector, N_i is the interpolation function, and N_j is the weighting function over the spatial element domain Ω_e. Details may be referred in Donea 2003 [36], Jacoub 2004 [65], and Hinkelmann 2003 [62].

2.5 Aspects in application of numerical models

An ideal sediment transport model should have the following capabilities: 1) provide fully-unsteady and steady or quasisteady simulation capability, 2) provide analysis of varying flow regimes from subcritical to supercritical flow, 3) provide a layered bed with bed sorting capability, 4) provide multiple grain size analysis capability for both non-cohesive and

cohesive sediments, 5) provide a selection of sediment transport relationships for both bed, suspended, and total load transport, 6) provide a selection of turbulence modeling schemes for enhanced hydrodynamic simulation, 7) provide a method for computing the effects of bend on hydrodynamics and sediment transport, and 8) provide a suitable interface for mesh generation and visualization of results, Scott and Jia 2005 [108].

Generally models dealing with all relevant flow and transport processes are rarely available. Developing a modeling system sharing the basic computational methods on which various modules can be built is commonly practiced. Modules for bed load transport, suspended load transport, water quality, temperature etc. can be treated independently.

2.5.1 Selection of appropriate model

Dominant process: A model describing the predominant mode of transport sufficiently can be assumed to represent the whole process. For example, for most reservoirs, the major mode of transport is suspended transport. Therefore, for reservoir studies suspended load transport models can be applied to simulate bed evolutions.

Model dimension: Three-dimensional models are applied for studying local processes that can not be sufficiently described by 2D model approximations. The works by Sanjou and Nazu 2004 [107], Fang and Rodi 2003 [44], Cesare and Hermann 2001 [24], Lin and Falconer 1997 [82] are among the important works on 3D numerical modeling studies on sedimentation. Two-dimensional models are the most predominantly used models in reservoir and riverine sedimentation studies to describe the quantity and spatial distribution of sedimentation. Examples on two-dimensional suspended sediment transport studies may be referred in Wu et al. 2004 [139], Gracía-Martinez [52], Jacoub and Westrich 2002 [66], Govindaraju et al. 1999 [51], Olsen 1999 [92], Van Wijngaarden 1999 [130], Chang 1996 [26]. One-dimensional models are also widely used for modeling rivers that are nearly straight where longitudinal flows are predominant. See eg. Zhou 1998 [148], Bahadori et al. 2006 [8].

Coupling method: The coupling method between the flow, the transport, and the bed evolution is an important criteria. In most models the flow, the transport, and the bed evolution are coupled loosely because of the simplifications attained in solving the loose coupling. The updating of the bed morphology for the calculation of flow for each numerical step may not be necessary in a slow changing reservoir beds. The coupling can be assumed at a step causing significant change in flow fields. The coupling methods is therefore an important criteria in model simplifications.

Unsteady, quasisteady, steady: In quasisteady approximation, a continuous flow record is partitioned into a series of steady flows of variable discharges and durations. For each flow, a potential sediment transport rate is computed and the geometry is updated. The computation then proceeds to the next flow in a sequence of cycle. Such a method is considered as a quasisteady approximation, see HEC6 documentation [120]. HSCTM-2D, CCHE2D are examples of models that were developed to simulate both unsteady and quasisteady sediment transports in unsteady as well as series of steady or quasisteady simulations. MIKE2D is another example.

The variety of computational techniques are also a point worth considering. Some models are built to run on a single computer. When resources are available, for handling computationally expensive problems, models built using parallel systems are chosen. Models having options for various techniques of solution are preferable to those having a single solution methods for various algorithms involved. Details on efficient computational methods can be referred in Hinkelmann 2003 [62].

The selection of appropriate numerical method is another criteria in choosing modeling procedures. The major methods are FD, FV, and FE methods which follow particular solution procedures and formulations. Furthermore, a variety of discretization techniques, and solution methods of algebraic equations are considered. For complex geometries, it is advisable to use models using FE or FV methods. When local as well as global mass conservation, has to be guaranteed the FV method should be used. Clarity, adaptability and transferability, quality, and cost are other important criteria to consider.

A large number of flow and sediment transport models are available for use. Some are developed for research purposes in research centers and universities. Others are developed for commercial purposes. Commonly used models for example include models developed by EDF (TELEMAC-System); models developed by Hydraulic Engineering Center US Army Corps of Engineers (HEC2, HEC-RAS, HEC6); models by Danish Hydraulic Institute (MIKE family); models by National Center for Computational Hydro-science and Engineering (CCHE family); models developed by TUDelft and Delft Hydraulics (DELFT); models by USGS (FESWMS-2DH), and models developed by the Hydraulic Laboratory of the University of Stuttgart, IWS (COSMOS).

For this study the TELEMAC Modeling System was chosen. The tool was well-validated by various users all over Europe and North America in its capability to model flow, suspended sediment transport as well as water quality. For example Hervouet et al. 2000 [59] edited a collection of major application of the TELEMAC modeling system in a special issue of hydrological processes. In addition, the system offers several subroutines that can be used to deal with particular flow and sediment issues to be involved. For example Jacoub 2004 [65] developed a 2D particulate contaminant transport module using TELEMAC Modeling System.

2.5.2 TELEMAC modeling system

TELEMAC is a finite element modeling system designed for free surface hydrodynamics, sedimentology, water quality, waves and underground flows. It is developed by the National Hydraulics and Environmental Laboratory (Labouratoire National d'Hydraulique et Environment- LNHE) of the Research and Development Directorate of France Electricity Board (EDF-DRD). It consists of three-and two-dimensional modules for the study of currents, sedimentation, waves and water quality. The hydrodynamic model TELEMAC-2D and the suspended sediment transport model SUBIEF-2D are chosen in this work. The preprocessor called MATISSE is used for mesh generation. A post processor called RUBENS is used. Other preprocessors like JANET and postprocess like TECPLOT can also be used.

The model is coded with FORTRAN 90. A finite element library, Bibliothèque d'Elements Finis (BIEF) is organized and solved for all sorts of terms like advective, diffusive, various types of sources and boundary conditions systematically. This makes the improvement of codes suitable for users without getting into the basic steps of finite element algorithms. Details may be referred to Programming with BIEF 2004 [42].

TELEMAC-2D flow module

The assumptions used in TELEMAC-2D include that the fluid is Newtonian, incompressible, the pressure distribution is hydrostatic, and that the three-dimensional set of equations can be depth-averaged. Reynolds decomposition and stochastic averaging is applied in order to model turbulence. TELEMAC-2D solves the depth averaged continuity, momentum and conservative species transport equations and $k-\varepsilon$ equations simultaneously. The equations solved by the module are Equations 2.17 (the first three raws of the Equation 2.39) and a simplified form of the $k-\epsilon$ Equations 2.13. The model has a large number of options for treating the terms involved. For more details see TELEMAC users manual [41] and TELEMAC reference manual [40].

Similarly different solution strategies are integrated in the module. In this work, the method of fractional steps were used in which the advection steps are solved by the method of characteristics for the velocities U and V, and $k-\epsilon$. The semi-implicit method with the θ=0.55 was used for the time discretization. Propagation, diffusion, and source/sink terms were solved by SUPG method with the upwinding set equal to the Courant number. The results at each node of the computational mesh are the depth of water h, the horizontal components of depth averaged velocities U and V, and the turbulent viscosity. For more details see TELEMAC users manual [41] and TELEMAC reference manual [40].

SUBIEF-2D sediment transport module

SUBIEF-2D simulates the unsteady advection-dispersion equation for suspended sediment transport, with a source/sink term describing erosion and deposition. The equations solved by the module are Equation 2.33 and Equation 2.35. The erosion flux is solved using Equation 2.18 and the deposition flux using the Equation 2.21. The variables U, V and h are imported from the hydrodynamic model result. If $k-\varepsilon$ is used the turbulent viscosity is exported from the flow module TELEMAC-2D. Elder model is also integrated for use.

Several solution options are integrated in the module. In this work the advective term was treated using the method of characteristics. The dispersion and the source terms were treated using the SUPG in which the upwinding was assumed as the Courant number.

When simplification of the use of quasisteady approximation is to be used in the decoupled flow and sediment transport modules TELEMAC-2D - SUBIEF-2D:

- TELEMAC-2D is an unsteady flow algorithm. A steady simulation is based on the

steady flow input in which a criteria for the flow fields (U, V, and h) is set to be assumed steady after the change in each time step of the flow variables can be neglected.

- the transport module SUBIEF-2D then uses the last step of the hydrodynamic calculation to simulate the suspended sediment transport. SUBIEF-2D solves the unsteady advection dispersion equation.

- this type of coupling has deficiencies, especially in quickly changing morphological conditions. A criteria to stop the computation uses the critical evolution ratio (ratio of change in bottom to water depth) as a requirement for updating morphology.

Figure 2.1 below shows a schematic in quasisteady approximation used in quasisteady morphological modeling. Details of the basic equations used and the solution methods can be

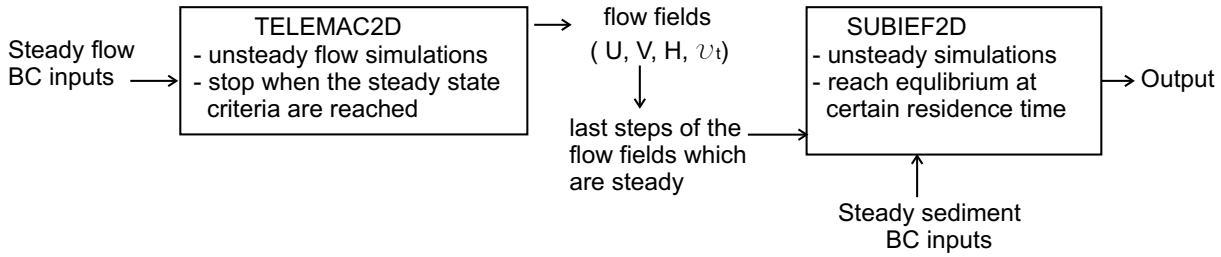

Figure 2.1: Algorithm of steady transport simulations in the TELEMAC-SUBIEF

found in the TELEMAC-2D principal notes 2001 [39], the TELEMAC-2D User's Model 2002 [41], and the SUBIEF-2D Manuel De L'utilisateur 2000 [38].

2.5.3 Steps in morphological simulation

The finite element analysis in engineering applications comprises three phases: domain discretization, equation solving, and error analysis. The domain discretization or mesh generation is the pre-processing phase which plays an important role with regard to the accuracy of the solutions, see Bui 1990 [20]. Preprocessing is concerned with all the tasks which must be carried out before a numerical simulation, i.e. all valuable data must be processed to determine model setups. Necessary steps consists of geometry approximation, assignment of physical parameters to geometric units, mesh generation and determination of initial and boundary conditions, see Hinkelmann 2003 [62]. The mesh should represent the geometry of the computational domain and the boundary flux representation accurately. The mesh should adequately capture large gradients of flows. In addition, the mesh should avoid elements with very high aspect ratios. For theory behind mesh generation and mesh adaptivity, the reader is referred to George et al. 2004 [48]. The grid refinement technique is a discrete iterative procedure which generates sequences of approximate solutions to two-point variational problems defined on continuous field. The approximate solutions are obtained by calculating the optimal path through discrete grids constructed throughout the continuous field, see Braddock 1971 [13].

The preprocessor used for this work was MATISSE. It is designed based on criteria based refinement in which the user defines areas of high refinement. A preprocessor JANET offers more options and transparency on the algorithm used in grid generation. The quality of grid generated is very important in morphological studies, see JANET documentation [50] and MATISSE documentation [37].

A model need first to pass through a verification of the numerical results by comparing them to analytical solutions which are available for simple systems. It can be done by plausibility tests like checking the global mass conservation. Then model calibration in which numerical results are compared to the field or experimental results. In calibration step parameters are tuned so that the numerical model agrees with the field measurement within reasonable range of accuracy. The model need to be validated to proof that it can be used under general conditions under which the model is calibrated, by applying sets of data different from that used in calibration. Hinkelmann 2003 [62]. For long-term simulation, the computational costs, numerical instability, and data availability are often a big challenge.

The results of interest from flow and transport analysis generally include fluid velocities, sediment concentrations, bed profile changes etc. Many of these items are directly available from the finite element results in terms as nodal values; other variables must be derived from the primary quantities. The spatial derivatives of the interpolation functions can be converted to derivatives involving the local element coordinates through use of the co-ordinate transformation. The quality of displayed information in a form of graphics and animation are useful for interpretation and publication purposes. In this work RUBENS and TECPLOT were alternatively used.

Summary

The chapter provided an insight into the flow and sediment transport modeling. The details behind the concepts of sediment transport are reviewed showing the major simplifications and assumptions considered. The complexity and uncertainties behind numerical models for both flow and sediment transport processes were briefly reviewed. Details on mathematical modeling of flow and sediment transport, numerical methods, and solution algorithms is too vast to get covered. Complete book reviews are usually given on various related topics such as turbulence, hydrodynamics, fluvial hydraulics, sediment transport, computational fluid dynamics, numerical methods etc.

Chapter 3

Reservoir Response and Unsteadiness Simplifications

Reservoirs are one of the most important facilities in water resources engineering. Reservoirs may be classified on the basis of purpose (flood control, water supply, hydropower, multipurpose, water treatment, storage tanks etc.); size (large, small); shapes (regular, irregular, long, wide, deep, shallow); operation (run-off-the river, storage) etc., see eg. Kobus et al. [77], Gebrewubet [47]. Reservoirs can also be classified depending on their hydrodynamic characteristics, which are affected by the inflow and outflow design, geometry, the degree of density stratification, and bottom boundary conditions. Relatively small reservoirs having the maximum residence times in the order of days were investigated. As a result, stratification, density currents, and wind effects were neglected.

In spite of the variability in flow and sediment properties, boundary conditions, and reservoir geometries, simplified hypothetical reservoirs were used in attempting to answer questions relevant to reservoir responses and their characterization. A systematic study were performed on the impact of unsteady inputs and possible steady approximation with respect to reservoir sedimentation. The studies were conducted using hypothetical reservoirs of various shapes and sizes, and scenarios of simplified ideal inputs accommodating various amplitudes and frequencies. The results of the analysis were aggregated using bulk parameters like the mean residence time and simplified analytical solutions available for ideal mixing reactors. The study also gives comparisons between the numerical solution of the advection-dispersion processes with the simplified analytical solution of the mixing reactors, which revealed reasonably comparable results.

3.1 Ideal reactors and their application

Simplified models are commonly used in dealing with sediment transport behaviors. Among them are the concepts of the mixing and plug flow reactors. The concepts are developed based on spatial and temporal scale analysis of the advection, diffusion, reaction, and settling processes. One important parameter is the Peclet number, $P_e = \frac{UL}{D}$, which is the ratio of advection to diffusion, where U is the velocity, L is the characteristic length and D is the diffusivity. The other important criteria is the residence time.

Continuously stirred reactor (CSTR): This model assumes that as each fluid parcel enters the reactor it is instantaneously mixed throughout the volume. Effectively, $D \to \infty$ so that the $P_e \to 0$.

A systematic study was made to compare the results of simulations on hypothetical reservoirs based on the FE advection dispersion model with simplified zero dimensional modeling concepts of steady-state solutions based on the CSTRs. This aids in giving an insight into reservoir characteristics.

Plug flow reactor (PFR): This model assumes that the fluid particles pass through and leave the system in the same order as they enter. It assumes perfect mixing in the lateral and vertical directions, but no mixing occurs in the longitudinal direction. This creates a slab of fluids which do not communicate with one another as they pass through the system. The Peclet number, $P_e \to \infty$ or the diffusion coefficient $D \to 0$, indicating the transport through the systems is advection-dominated. For this model to be reasonable, the lateral length scale must be sufficiently small (or the lateral diffusion sufficiently large). Before going further into the analysis made, a brief review is made on zero dimensional modeling concept of species transport in basins/reservoirs.

Mass balance

The mass balance for a well mixed reservoir in a zero dimensional way can be given by

$$\underbrace{V\frac{dc}{dt}}_{Accumulation} = \underbrace{Qc_i}_{loading} - \underbrace{Qc}_{outflow} - \underbrace{kVc}_{reaction} - \underbrace{v_s A_s c}_{settling}, \tag{3.1}$$

where V is volume of the system, Q is the volumetric flow rate, c_i is the inflow concentration, $c = c_o$ is the reservoir concentration for a well mixed domain, k is a first order reaction coefficient, v_s is the settling velocity of sediment, and A_s is the surface area of a reservoir.

The formulation is based on the assumption that the reservoir volume and flows are relatively constant. In spite of the simplicity of the assumption, important studies has been made on using ideal CSTRs, see e.g. Chapra 1997 [27]. If the system is subjected to constant loading for a sufficient long time, a dynamic equilibrium state called steady-state will be reached in which the reservoir concentration can simply be given as

$$c = c_o = \frac{Qc_i}{Q + kV + v_s A_s} \Rightarrow \frac{c}{c_i} = \beta = \frac{1}{1 + kt_{th} + v_s \frac{A_s}{V} t_{th}} = \frac{1}{1 + kt_{th} + v_s \frac{t_{th}}{H}}, \tag{3.2}$$

where β is known as a transfer function, and $H = V/A_s$ is the average water depth of a reservoir.

The transfer function, β, is a useful first hand tool in characterizing reservoirs assimilation capacity of pollutants. For reservoirs with high settling and reaction ($\beta << 1$), the reservoir species concentration will be low whereas for reservoirs with low reaction and settling ($\beta \to 1$), the reservoir species concentration will be high showing low assimilation capability.

Equation 3.1 can be expressed as $\frac{dc}{dt} + \lambda c = \frac{W(t)}{V}$; where $\lambda = \frac{Q}{V} + k + v_s A_s$ and $W(t) = Qc_i$ is the loading. For certain type of simple ideal loadings analytical solutions are available for the unsteady pollutant transport, see Chapra 1997 [27]. Equation 3.3 below summarizes

the analytical solution for simple inputs using the mixing reactor concept for pulse, step, linear, exponential, and sinusoidal loadings respectively:

$$\begin{aligned} c &= c_i e^{-\lambda t}, \rightarrow pulse \\ c &= \frac{W}{\lambda V}\left(1 - e^{-\lambda t}\right), \rightarrow step \\ c &= \pm\frac{\beta_l}{\lambda^2 V}\left(\lambda t - 1 + e^{-\lambda t}\right), \rightarrow linear \\ c &= \frac{W_e}{V(\lambda \pm \beta_e)}\left(e^{\pm\beta_e t} - e^{-\lambda t}\right), \rightarrow exponential, and \\ c &= \frac{\overline{W}}{\lambda V}\left(1 - e^{-\lambda t}\right) + \frac{W_a}{V\sqrt{\lambda^2 + w^2}}\left[sin(wt - \theta - \phi(w)) - (sin(-\theta - \phi(w))e^{-\lambda t}\right] \\ &\rightarrow periodic \end{aligned} \tag{3.3}$$

where β_l is the rate of change for linear input; β_e is the rate of growth or decay for exponential load; $\overline{W}, W_a, \theta, w$, and $\phi(w)$ respectively are the mean loading, the amplitude of the loading, the phase shift, the angular frequency of oscillation for sinusoidal input and an additional phase shift that is a function of frequency. Note that as time $t \rightarrow \infty$, a steady-state solution is reached with simpler expressions replacing the terms $e^{-\lambda t}$ by unity. Theoretically speaking it takes an infinite time to reach a purely steady concentration in reservoirs.

The transfer function for the PFR can be derived from the first order reaction/sedimentation

$$\frac{\partial c}{\partial t} = -U\frac{dc}{dx} - kc \tag{3.4}$$

Assuming steady state condition and $c = c_i$ at x=0, the solution is $\frac{c_o}{c_i} = e^{-\frac{k}{U}x}$. At the time $t = t_{th}$, and settling velocity v_s, the relative concentration can be given by:

$$\beta_{sp} = \frac{c}{c_i} = e^{-v_s\frac{A_s t_{th}}{V}} \tag{3.5}$$

more can be referred in Chapra 1997 [27] and Westrich 2002 [129].

Residence time distribution (RTD)

Although basins and reservoirs are of different size and serve different purposes, they all have a common characteristics that they have one or several inflows separated by a retention volume. They can be categorized to a first approximation, by the theoretical residence time. The theoretical residence time is given as

$$t_{th} = \frac{V}{Q} \tag{3.6}$$

where t_{th} is the theoretical residence time, V is the volume of the reservoir, and Q is the outflow discharge.

Olivet et. al [91] used residence time distribution techniques to study the hydrodynamic behavior of a full-scale wastewater plug-flow bioreactor, using physical experiments. The conclusion of the experiment was that the determination of unique global RTD may not provide enough information to accurately describe local mixing regime conditions in complex systems such as full-scale bioreactors in which at least three phases are involved (namely biomass, air and liquid phases).

Real systems are complicated and do not fit the Plug-Flow or Stirred Reactor models perfectly. The residence time distribution function, describes the time spent in the system by different fractions of fluids. The probability density function of residence time is given by

$$RTD(t) = -\frac{1}{m_o}\frac{dm}{dt} = \frac{Qc}{\int_0^\infty Qc\ dt}, \tag{3.7}$$

where, m_o is the initial mass comprising the whole mass of a conservative tracer in the water body and c is the concentration at the outlet of the system. Note that $\int_0^\infty RTD(t)\ dt = 1$.

By definition, the mean residence time $\bar{t}$ is the first moment of the residence time distribution. Considering a steady flow, the mean residence time is given by

$$\bar{t} = \int_0^\infty RTD(t)t\ dt = \frac{1}{m_o}\int_0^\infty m(t)\ dt = \frac{\int_0^\infty ct\ dt}{\int_0^\infty c\ dt}, \tag{3.8}$$

where $m(t)$ is the time-varying tracer mass remaining in the water body. The mean residence time is also known as the effective residence time or the detention time.

A natural system may have regions that are linked to the main flow by turbulence interaction only, e.g. regions of dense vegetation and stagnant water. If excluded zones exists, then the theoretical residence time is less than the mean residence time. This comes from the excluded zones available if the effective volume is reduced, and the effective residence time is similarly reduced. If no zones are excluded from the flow, the mean residence time is equal to the theoretical residence time, $\bar{t} = t_{th}$. The second moment of the RTD is the variance, σ^2 and the spread of observed residence times around the mean residence time. The variance of the RTD results from the mixing or from the distribution flow paths and flow speeds through the system, and is given as

$$\sigma^2 = \int_0^\infty (t-\bar{t})^2 RTD(t)\ dt = \frac{\int_0^\infty c(t-\bar{t})^2\ dt}{\int_0^\infty c\ dt}. \tag{3.9}$$

$\sigma = 0$ for the plug flow systems, $0 \leq \frac{\sigma}{\bar{t}} \leq 1$ for real flow systems and $\sigma = 1$ for mixing (stirred) flow systems. The theoretical residence time is however the same as the mean residence time for all the three systems. For more details one may refer in Westrich 2002 [129], Hilton et. al 1998 [61].

So far on the basics, the coming sections discuss the numerical experiments based on advection-dispersion solutions (TELEMAC-2D - SUBIEF-2D) as compared with the simplified CSTR and PFR solutions for a steady-state condition, as in Equation 3.2.

3.2 Periodic system inputs

Hypothetical shapes and size of reservoirs as well as flows and sediment properties were assumed based on possible realizations. The following sections present the data used in a simplified qualitative description.

Shape and size

Figure 3.1 below present some of the investigated domains. The reservoirs on the left are regular reservoirs having volume of $\approx$ 0.3 million m^3 at the water level of 105 m.a.s.l. The irregular reservoirs on the right are having volumes ranging from 6 to 10 million m^3 depending on the water level fluctuating between 101.5 and 108 m.a.s.l. Irregular 1 is relatively shallow while irregular 2 and 3 have a deepened flushing channel and over-bank channel on both sides of the main channel. The bottom elevation of the reservoirs are shown in the Figure 3.1. The regular shaped reservoirs have the highest depth at the outlet. The condition is similar for irregular reservoirs. Irregular reservoir 1 has a shallower depth of the main channel. Irregular reservoir 2 has a deeper main channel. Irregular reservoir type 3 has a narrowed and deeper bottom topography.

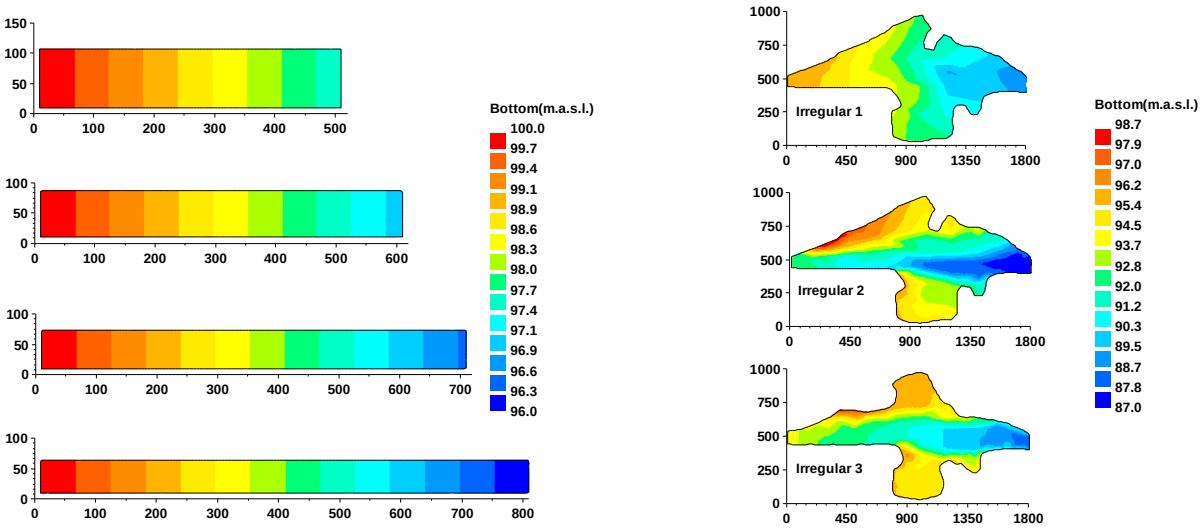

a) Regular shaped reservoirs b) Irregular shaped reservoirs

Figure 3.1: Various hypothetical reservoir shapes investigated, distances are in meters

Periodic discharge and sediment inputs

Flow fields and transport in reservoirs show a great variability as a result of input fluctuation, reservoir shape and size, and operations. For natural rivers the variability may be

challenging to generalize in a given simplified shape of input hydrographs. The discharge and sediment input were chosen time dependent and described by a periodic function with triangular shape as shown in Figure 3.2 below. Basic properties of the response of the

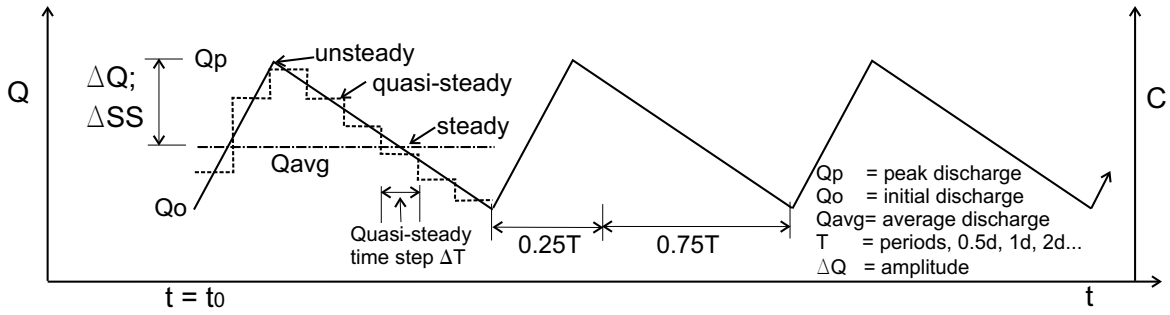

Figure 3.2: Definition for basic investigation on response to periodic inputs

reservoirs to unsteady input were analyzed using periodic input functions of discharge and suspended sediment with different amplitudes and frequencies. Discharges of various magnitudes reaching the peak Q_p from their initial Q_o in a period T were assumed. The discharges were assumed to oscillate to suffice the targeted treatment that focuses on the stable oscillations of output concentrations and sediment mass depositions. The mean flow over the period T were considered for the steady-state calculations. For the quasisteady-state assumptions, the inputs were averaged over a time assuming quasisteady step $\triangle T$.

The suspended sediment concentrations were idealized to be a linear function of discharge given by, $SS = 0.0012Q + 0.001$, which were obtained form long-term flow and sediment data of the Lautrach reservoir. Non-uniform sediment gradations were assumed with 50 % of the sediment as SS1 having coarser grain size and the remaining 50% as having SS2 of finer grain size. The erosion constant M of 0.0005 kg/m^2s was used for both grain sizes. The sediment parameters used are given in Table 3.1.

Sediment	$u_{ce}(m/s)$	$u_{cd}(m/s)$	$v_s(m/s)$
SS1	0.063	0.0100	0.000090
SS2	0.050	0.0077	0.000035

Table 3.1: Erosion and depostion parameters used in the hypotetical study

Assuming each periodic discharge as $Q(n)$ and sediment concentration as $SS(n)$, where n is representing each numerical run, three types of downstream boundary conditions were assumed in the analysis.

- **Discharge controlled cases (QC)** in which the outflow discharges were kept as an average of the inflow discharge over the whole period T.
- **Head controlled cases (HC)** in which discharge dependent on head calculated from the discharge controlled cases (QC) were considered, $\overline{H(n)} = f(\overline{H(Q(n))})$.
- **Head controlled cases (HCC)** in which the downstream head were kept constant irrespective of inflow discharges.

Table 3.2 below gives the summary of the boundary conditions assumed for unsteady and steady simulations.

BC assumed	QC		HC		HCC	
BC type	Unsteady	Steady	Unsteady	Steady	Unsteady	Steady
Upstream	Q(n)	$\overline{Q(n)}$	Q(n)	$\overline{Q(n)}$	Q(n)	$\overline{Q(n)}$
Downstream	$\overline{Q(n)}$	$\overline{Q(n)}$	$\overline{H(n)}$	$\overline{H(n)}$	H_o	H_o
Initial conditions	H_o	$\overline{H(n)}$	$\overline{H(n)}$	$\overline{H(n)}$	H_o	H_o
SS inflow	SS(n)	$\overline{SS(n)}$	SS(n)	$\overline{SS(n)}$	SS(n)	$\overline{SS(n)}$

Table 3.2: Boundary condition types used in the hypothetical study

3.3 Aggregate response of reservoirs to inputs

The outcome of the numerical simulations performed on the hypothetical reservoirs was analyzed in an aggregate manner using non-dimensional parameters. The relation of sediment input to output in reservoirs can be given in a general non-dimensional form as:

$$\frac{m_i - m_o}{m_i} \propto \frac{c_o}{c_i} = f\left(\underbrace{geometry}_{reservoir}; \underbrace{\frac{\triangle Q}{\bar{Q}}, \frac{t_{th}}{T}}_{hydrology}; \underbrace{\frac{\triangle H}{H_o}, \frac{Q_o}{Q}}_{operation}; \underbrace{\frac{u_{cd}}{u_o}, \frac{u_{ce}}{u_o}, \frac{v_s t_{th}}{H}}_{sediment}; \underbrace{\frac{\triangle T}{T}}_{numerics}\right) \tag{3.10}$$

where m_i is the mass of sediment input, m_o is the mass of output sediment or mass in suspension, $m_i - m_o$ is the mass of sediment deposition; $\triangle H$ is water level fluctuation and H_o is initial water level in a reservoir; Q is discharge into and Q_o is discharge out of a reservoir; u_o is the bottom shear velocity , u_{ce} is the critical shear velocity for erosion, u_{cd} is the critical shear velocity for deposition, v_s is the settling velocity, and H is average reservoir water depth. The term $\frac{\triangle T}{T}$ indicates the dependence of the numerical results on the quasisteady approximations, where T is the period and $\triangle T$ is the quasisteady time step. The non-dimensional terms in the equation were numerically investigated and compared with the analytical solutions. Comparisons between the unsteady and steady simulations based on reservoir shapes and inputs were also evaluated.

Effects of reservoir shapes

Four rectangular-shaped reservoirs of equal volume but varying depth, width and length were considered, see Figure 3.1 a). The same initial and boundary conditions, numerical and physical parameters were assumed. The models were run for various durations for each shape. It was concluded that the narrower the cross sections the better the possibility to overcome sedimentation. This is in line with the reservoir sedimentation mitigation strategy suggested by various authors, see e.g. Morris 1998 [86]. It was also found out that dead water zones of the reservoirs are subjected to deposition irrespective of the inflow discharge peaks. Figure 3.3 below shows the eddies that forms zones of pure sedimentation.

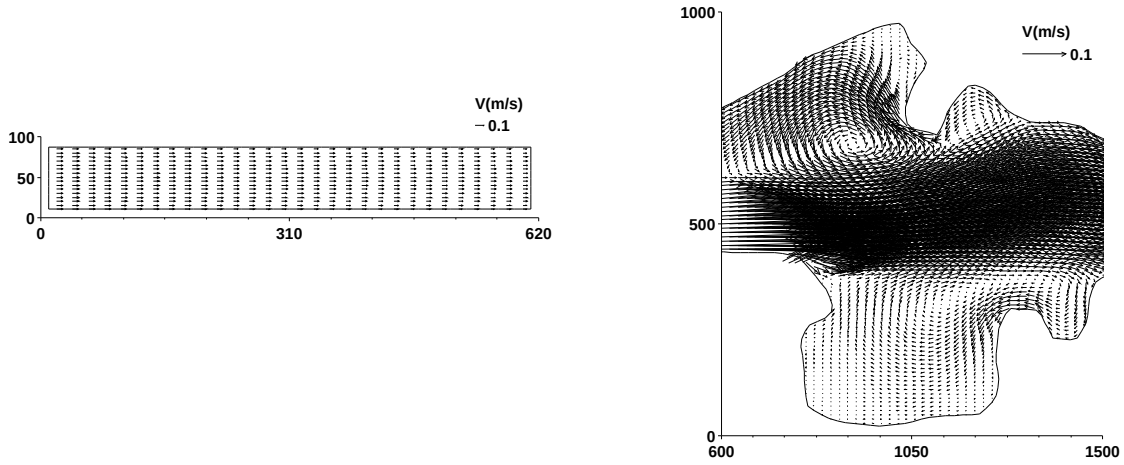

Figure 3.3: Comparison of typical velocity fields for regular and irregular reservoirs

Aggregated results with respect to sediment concentration

All the numerical runs were made on one regular reservoir and two irregular reservoirs (1 and 2) under unsteady and steady conditions; with boundary conditions QC, HC, and HCC; with sediment gradations $SS1$ and $SS2$. The results are aggregated in a non dimensional form and are shown in Figure 3.4. In the graph, c_o/c_i indicates the ratio of reservoir (outflow) concentration to inflow concentration and the transfer function β is given as $\beta = [1 + (v_s A_s/V)t_{th}]^{-1}$. For the periodic cases, the peak values of input and output concentrations were taken. For the steady case the output concentrations c_o were taken after reaching a steady-state condition. Only part of the simulations before net erosion was reached were integrated into the graphs. After the erosion was reached, the ratio c_o/c_i were found to have values higher than unity whereas the β values were close to unity as a result of reduction of the residence time. In the Figure R stands for regular and IR stands for irregular reservoir.

From this analysis the following points can be concluded:

- at longer residence time (lower β), the assimilative (pollutant removal $\rightarrow$ in this work sedimentation) capacity of regular reservoir is higher than that of the irregular reservoirs. As the residence time reduces the assimilative capacity of the irregular reservoir overtakes the regular reservoirs. This can be concluded as the influence of dead water zone for irregular shaped reservoirs showing sedimentation irrespective of high inflow boundary conditions. At low flows, the regular reservoir showed higher relative sedimentation to the input sediment mass. The irregular reservoir responded with lower sedimentation because of the flushing effect of the mid channel which transport the sediment at higher velocities.
- the trend is clearer for the steady case. The regular reservoir showed only minor scattering from the straight line as compared to the irregular reservoirs, irrespective of input variabilities.
- strong scattering is the result of sediment grades, unsteadiness, and reservoir shapes.

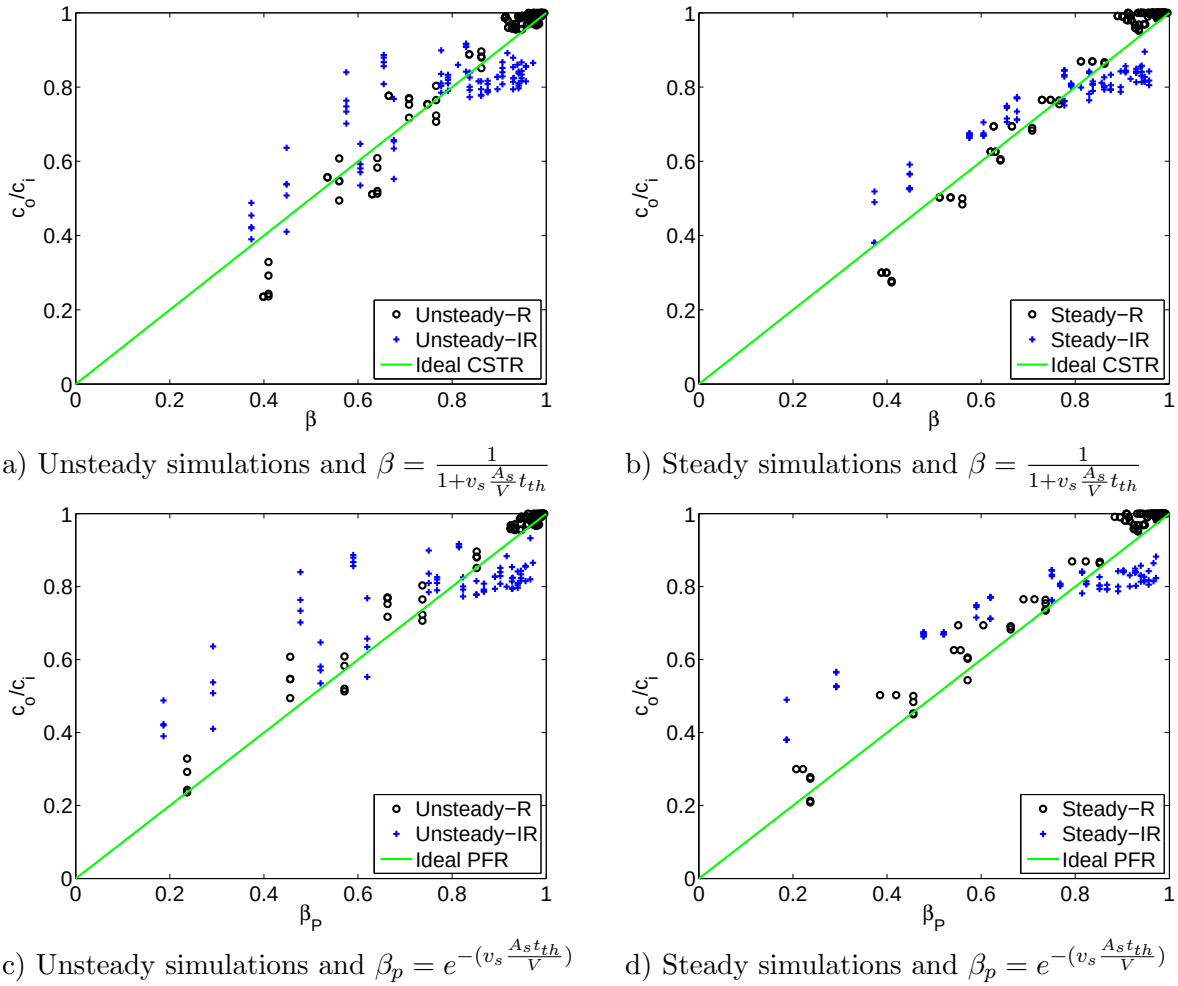

a) Unsteady simulations and $\beta = \frac{1}{1+v_s \frac{A_s}{V} t_{th}}$

b) Steady simulations and $\beta = \frac{1}{1+v_s \frac{A_s}{V} t_{th}}$

c) Unsteady simulations and $\beta_p = e^{-(v_s \frac{A_s t_{th}}{V})}$

d) Steady simulations and $\beta_p = e^{-(v_s \frac{A_s t_{th}}{V})}$

Figure 3.4: Aggregate reservoir assimilation capacity (c_o/c_i) for regular (R) and irregular (IR) reservoirs (1 and 2) with sediment fractions (SS1 and SS2), downstream boundary conditions (QC, HC, and HCC), and amplitude $\triangle Q$, and period T of inputs

The numerical solutions of the concentration scattered around the simplified ideal steady analytical solutions of the CSTRs. This indicates the importance of simplified solutions as a first-hand tool in answering engineering problems sufficiently. The steady-state simulations of the regular reservoir are much closer to the ideal line, particularly for the $0.65 < \beta < 0.85$, see Figure 3.4 b). For β close to 1, the integrated scatters involved effect erosion, which is not included in the β, and for lower β, the reservoir responds differently from the CSTR solution.

- for regular reservoir at low flows the relative concentration is closer to the ideal line of the PFR than the ideal line of CSTR, Figure 3.4 c) and d). For the irregular reservoir the ideal CSTR is more representative than the PFR. At high discharges the performance of CSTR and PFR is similar.

It can be more interesting to look at the results by disaggregating the whole picture into specific aspects. Figure 3.5 shows the influence of sediment grain and period for regular and irregular reservoir 2 under steady and unsteady simulations at ranges of inputs. The following remarks can be made form the results:

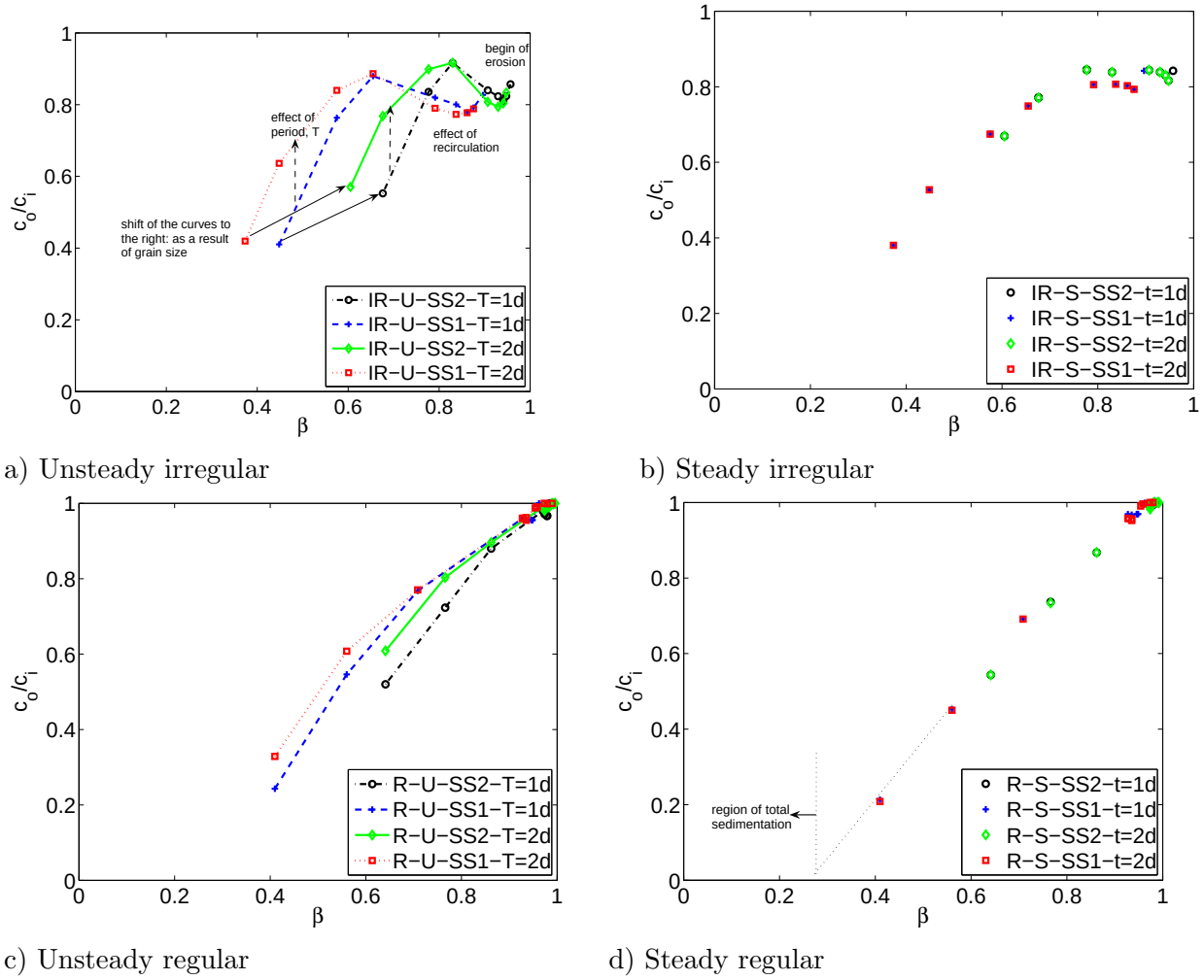

a) Unsteady irregular

b) Steady irregular

c) Unsteady regular

d) Steady regular

Figure 3.5: Comparison of assimilation capacity of the regular (R) and irregular (IR) reservoir 2 for various sediment fractions (SS1 and SS2), and periods T: $\beta = [1+(v_s A_s/V)t_{th}]^{-1}$

- the assimilative capacity of the reservoirs is lower (less sedimentation) for fine-grained particles $SS2$ compared to the coarse-grained particles $SS1$ as can be seen by a shift to the right and slightly higher concentration ratio for the finer particle. This is an indication of higher sedimentation for the coarser grained material and is more clearly shown in the steady-state cases in Figure 3.5 b) and d).

- for the irregular reservoirs with lower β (longer t_{th}), the effect of recirculation zones is insignificant and the reservoir acts as a full sedimentation basin. As β increases the recirculation effect becomes more important, see Figure 3.5 a).

- increase of periods T of the inputs for the same amplitude and mean inputs, increased the relative concentration of output. For shorter residence times, the shift of this assumption was observed as can be seen in Figure 3.5 a).

- after the net erosion was reached, the relative concentration of outflow increased more than unity.

Constant volume and varying sediment input test cases

Another study was made focussing on the regular reservoir and irregular reservoir 3. The reservoir volumes were kept constant and various steady flows were applied. A fluctuating suspended sediment input with period T of 1 day for the first four days and 0.3 hours for the next four days were used. For irregular reservoirs a mean theoretical residence time ranging from 0.39 hours to 24 hours were imposed by varying inflow discharges. Similarly for the regular reservoir, mean theoretical residence times varying from 0.83 hours to 42 hours were imposed. Figure 3.6 shows the input and output concentrations. The following can be concluded from the results:

- input concentration of higher frequency and longer residence time can be replaced by mean inputs with respect to its response.
- for the same residence time, the regular reservoir reaches higher relative peak concentration as compared to the irregular reservoir. The reason is that the irregular reservoir is characterized by mixing that has damping effect, see O-24h for the regular and irregular reservoir; O-1.52h for the regular and O-1.55h for the irregular reservoir.

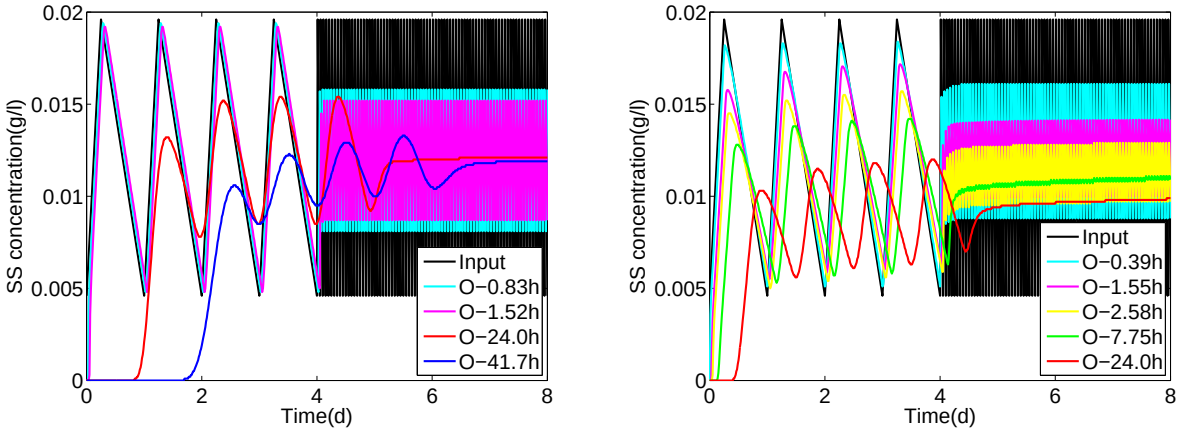

a) Regular b) Irregular

Figure 3.6: Reservoir damping effect: output concentration depending on sediment inflow frequency and reservoir residence time

The Figure clearly indicates that for flows of long residence time and higher frequency of oscillations of inputs, the output approaches the mean concentration of inputs. This behavior is indeed in line with the sinusoidal analytical solution of inputs to ideal mixing reactors, and may have importance in quasisteady approximation with respect to sediment concentration.

Aggregate results with respect to sediment mass deposition

Numerical results were evaluated with regard to sediment mass deposition in the reservoirs. Figure 3.7 below gives comparisons of typical mass deposition behavior under various input

amplitudes for irregular and regular shaped reservoirs. The input periods were 2 days and the boundary conditions were of the type head controlled (HC). In the Figure, the rate of sediment mass deposition for each unsteady case and its corresponding steady case are shown as the same line type and/or color. For simplicity, the theoretical residence time t_{th}, for each unsteady calculations and its corresponding steady calculations were assumed to be the same. The mean discharge $\bar{Q}$ and amplitude $\triangle Q$ corresponding to each t_{th} on the

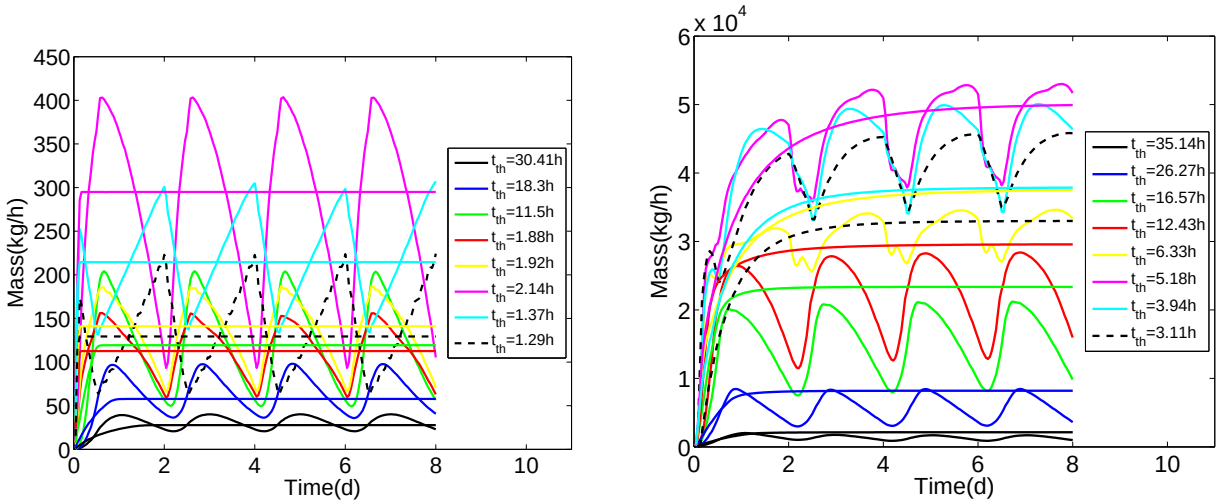

a) Rate of deposition in the Regular reservoir b) Rate of deposition in Irregular reservoir

Figure 3.7: Responses of the reservoirs for periodic and the corresponding steady inputs having the same theoretical residence time t_{th}, period T of 2 days, and the head controlled (HC) boundary conditions (in same color)

figures can be referred in Table 3.3. The following points can be noted from the results:

- for the regular reservoir, the rate of mass deposition for the steady-state calculations generally passed midway of that of the unsteady calculation, see Figure 3.7 a). This was not necessarily the case for the irregular shaped reservoir in which there is an overestimation of mass deposition by steady calculation at higher residence times and vice-versa, see cases for t_{th} lower than 5.18 hours in Figure 3.7 b). For the condition of net erosion the gap between the unsteady calculation and steady calculation were found to be more significant.

- for the same theoretical residence time, the irregular reservoir required a longer time to reach steady-state in terms of sediment deposition.

- the amount of deposited sediment increased gradually with decreasing residence time, until it reached a point where a further decrease in residence time resulted in lower mass deposition. This is a result of initiation of erosion and higher turbulence that keeps the sediment in suspension allowing to pass through the reservoirs without deposition.

For comparative analysis on the influence of frequencies on sediment deposition behavior between the unsteady and the steady simulations, few samples of the results after the rate of deposited sediment mass reached a constant for steady simulations and stable periodic

oscillation for the unsteady simulation were considered. Few samples with boundary conditions HC were selected and depicted in Figure 3.8. In the Figure, the red colors results from the lowest amplitudes and means of inputs having three different periods T (0.5d, 1d and 2d) and the green lines resulted from the highest amplitudes and means of inputs having periods T (0.5d, 1d and 2d). The horizontal lines correspond to the steady-state rate of mass deposition. From the Figures 3.7 and 3.8 and the results of similar numerical runs,

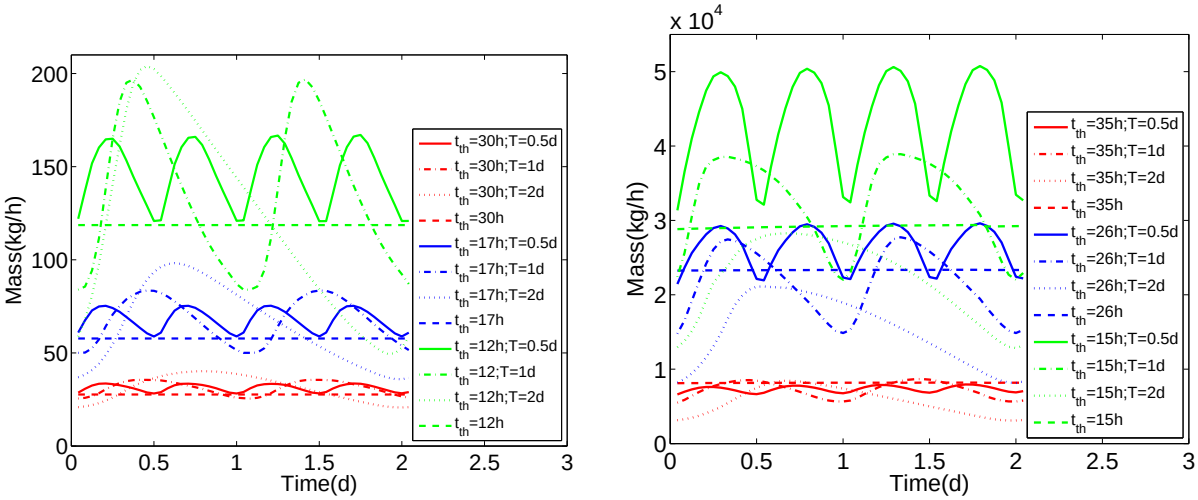

a) Regular with head controlled (HC) BC b) Irregular with head controlled (HC) BC

Figure 3.8: Effect of frequencies of input on the sediment deposition rate for different theoretical residence time t_{th}

the following remarks can be made:

- for the regular reservoirs, as shown in Figure 3.8, increasing periods from $0.5d \rightarrow 1d \rightarrow 2d$, the same amplitude $\triangle Q$ and mean input discharges $\bar{Q}$ resulted in a closer amount of sediment deposition rate between the fully-unsteady and the steady simulations. This follows the fact that as $\frac{\partial Q}{\partial t} \rightarrow 0$ and $\frac{\partial c}{\partial t} \rightarrow 0$ a steady assumption becomes more reasonable. This was not necessarily true for the case of irregular reservoir which have a strong shaped-induced mixing characteristics.

- input periods shorter than the theoretical residence time resulted in higher discrepancies in the amount of sedimentation over the whole period T.

Similar runs were performed for a wide a range of inputs with various amplitudes and frequencies and boundary conditions QC, HC, and HCC. Formulation of empirical relations between the amount of deposited mass and $\triangle Q$, $\bar{Q}$, t_{th}, $\frac{\triangle Q}{\bar{Q}}$, $\frac{\triangle Q}{\bar{Q}}\frac{t_{th}}{T}$ were investigated, showing trends describing the relative mass deposition between unsteady and steady simulations. Among them, t_{th} was found to show simplified trends characterizing the relative discrepancies on the amount of sedimentation, as shown in Figure 3.9. Note that the sediment mass depositions were taken after stable state were reached, though no major differences were observed on consideration of the total mass all through the duration of simulations. For convenience, the aggregated presentation of the percentage mass differences between sediment mass deposition of the steady simulation and from the corresponding unsteady simulation are presented in Figure 3.9. In the Figure, the cases are ordered from the longest

to the shortest residence times; SS1, SS2, and T indicate the mass of sediment deposition for grain sizes SS1 and SS2, and total respectively. l indicates the period of 2 days.

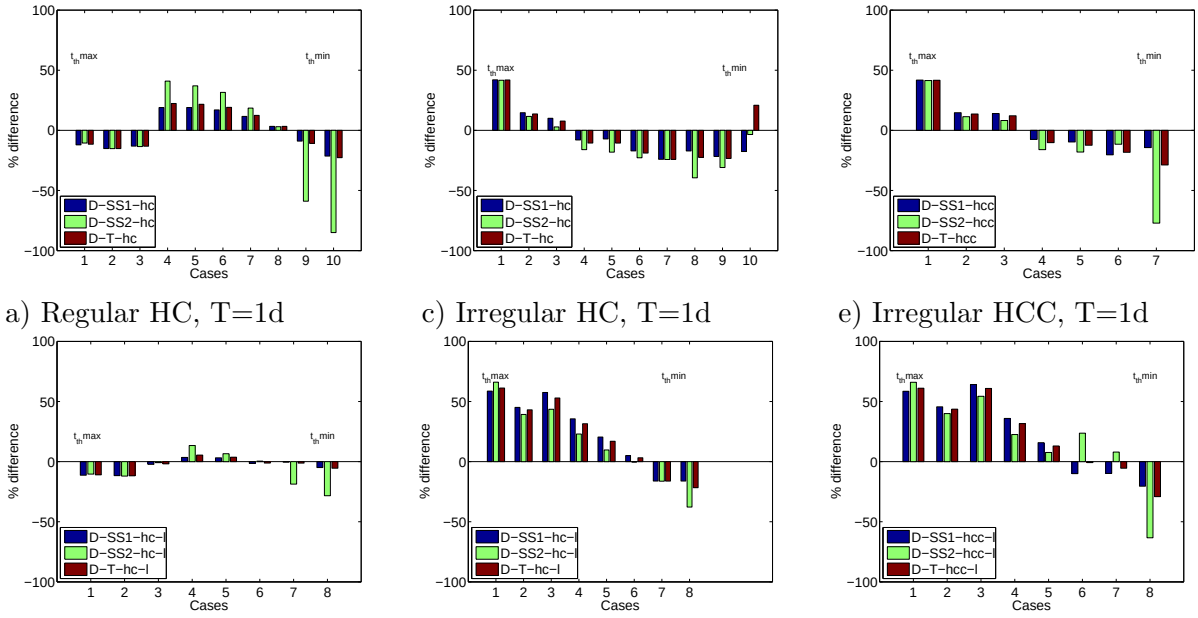

a) Regular HC, T=1d c) Irregular HC, T=1d e) Irregular HCC, T=1d

b) Regular HC-l, T=2d d) Irregular HC-l, T=2d f) Irregular HCC-l,T=2d

Figure 3.9: Percentage difference of mass deposition between unsteady and steady simulations: cases described in Table 3.3

In Table 3.3, the mean theoretical residence time, and the mean and amplitudes of discharges are given for each case 1 to 10 in Figure 3.9. Multiple views of the trends in percentage difference of sediment mass deposition are given. Only those cases with net sedimentation are integrated in the table.

Type	Cases	1	2	3	4	5	6	7	8	9	10
a	t_{th}	29.96	17.25	11.83	1.91	1.89	1.87	1.79	1.74	1.26	1.14
	$\bar{Q}$	3	5.5	10.5	80	77.5	75	62.5	55	100	110
	$\triangle Q$	2	4.5	9.5	30	27.5	25	12.5	5	20	20
b	t_{th}	30.41	18.43	11.50	2.13	1.92	1.88	1.37	1.23		
	$\bar{Q}$	3	5.5	10.5	62.5	56.25	55	90	100		
	$\triangle Q$	2	4.5	9.5	12.5	6.25	5	10	10		
c	t_{th}	35.14	26.27	16.57	12.43	6.33	5.18	3.94	3.11	2.89	2.67
	$\bar{Q}$	55	75	125	175	350	475	575	650	800	1050
	$\triangle Q$	5	25	75	125	150	275	175	50	200	450
d	t_{th}	35.14	26.27	16.57	12.43	6.33	5.18	3.94	3.11		
	$\bar{Q}$	55	75	125	175	350	475	575	650		
	$\triangle Q$	5	25	75	125	150	275	175	50		
e	t_{th}	34.94	25.63	15.38	10.98	5.49	3.34	2.96			
	$\bar{Q}$	55	75	125	175	350	575	650			
	$\triangle Q$	5	25	75	125	150	175	50			
f	t_{th}	34.95	25.62	15.38	10.98	5.49	4.05	3.34	2.95		
	$\bar{Q}$	55	75	125	175	350	475	575	650		
	$\triangle Q$	5	25	75	125	150	275	175	50		

Table 3.3: Mean residence times, mean discharges, and amplitudes for cases in Figure 3.9

The following can be concluded from the results of the analysis:

- from the boundary conditions QC, HC, and HCC studied for the regular and irregular reservoirs, it can be concluded that reservoir operation plays a key role in reservoir sedimentation characterization. The discrepancy of deposited sediment were found to be the highest for discharge controlled conditions QC where the water level fluctuations ($\frac{\triangle H}{H_o}$) were the highest.
- percentage difference may not be a real indication for validity of steady assumption in a sense of long-term simulations since the weight of the specific temporal contribution can be more important in its contribution to total balance. An aggregate of fluctuations with an over- and underestimation, resulting in favorable steady approximation should be investigated with respect to duration and the weights of specific patterns of sedimentaion/erosion, e.g. in the case of heavy erosion.
- for the regular reservoir, at lower flows for which the residence time is longer than half a day, the steady-state approximation underestimated the mass deposition. As discharge increased, the steady simulation overestimated the sedimentation which again were reversed after net erosion was reached, see e.g. Figure 3.9 a). For the irregular reservoir as shown on Figure 3.9 c), d), e) and f), an opposite condition were observed. For longer residence times the steady approximation overestimated the amount of mass deposition ($t_{th} > 0.5d$). For residence times shorter than half a day, the steady approximation underestimated the amount of sediment mass deposition.
- mid-way between pure sedimentation and the beginning of erosion steps were reached were the discrepancy in sediment deposition were low. This can be considered as predominance of pure transport.
- once the erosion starts, it begins with unsteady simulations since the peak is not dampened by averaging. As the discharge increased sufficiently, conditions were reached where the steady assumptions results in higher erosion than the unsteady assumptions. Such conditions are however generally not frequent in nature.
- the gap between the sediment mass depositions over a period T, showed higher variability for the fine grained material SS2 as compared to the coarser-grained SS1 revealing the importance of sediment properties in steady approximation.
- the validity of steady approximation were found to be more suitable for the regular reservoir as compared to the irregular reservoir.

In order to aggregate mass deposition in a non-dimensional form, an analogous expression as in Equation 3.1 for mass instead of concentration was used. A simplified zero-dimensional expression for suspended sediment mass balance referring to well mixed reservoir may be given as,

$$V\frac{dm}{dt} = Qm_i - Qm - v_s A_s m, \tag{3.11}$$

where m_i is inflowing sediment mass and m is the mass of sediment in the reservoir. For a steady-state condition, the ratio of mass input to the mass of sediment in the reservoir simplifies to the form

$$\frac{m_d}{m_i} \propto \frac{m}{m_i} = \beta_s = \frac{Q}{Q + v_s A_s} = \frac{1}{1 + v_s \frac{A_s}{V} t_{th}}, \tag{3.12}$$

where m_d is the sediment mass deposition, see, Chapra 1997 [27]. From the numerical simulations performed on the regular reservoir and the Irregular reservoir 2, the sediment mass input and deposition per period T, for the BCs HC and HCC, steady and unsteady simulations with sediment grain size SS1 and SS2, were integrated in a non-dimensional form as shown in Figure 3.10. Only cases with net sediment deposition were considered.

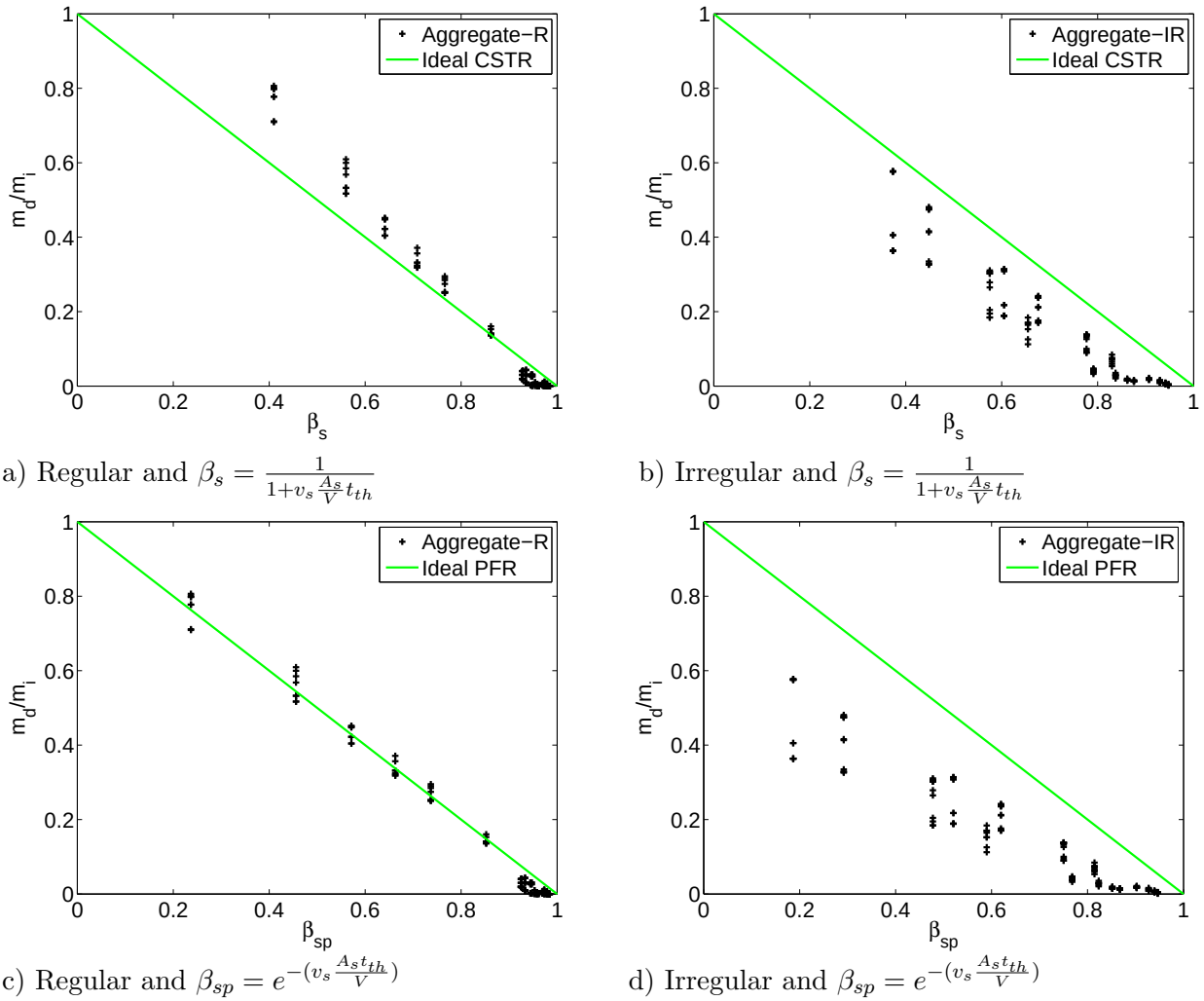

a) Regular and $\beta_s = \frac{1}{1+v_s \frac{A_s}{V} t_{th}}$

b) Irregular and $\beta_s = \frac{1}{1+v_s \frac{A_s}{V} t_{th}}$

c) Regular and $\beta_{sp} = e^{-(v_s \frac{A_s t_{th}}{V})}$

d) Irregular and $\beta_{sp} = e^{-(v_s \frac{A_s t_{th}}{V})}$

Figure 3.10: Comparison of relative sediment mass deposition between the numerical and the analytical solutions: Aggregated data include: multiple fraction, head and discharge controlled boundary conditions as well as steady and unsteady simulations

In the Figure the value m_d in the ratio $\frac{m_d}{m_i}$ was calculated from the numerical model, whereas the abscissa β_s shows the ratio of mass in suspension (outflow) to the mass input and was calculated based on Equation 3.12. The following remarks can be made from the analysis:

- similar to the results on suspended sediment concentration as in Figure 3.4, regular reservoir showed minor scattering irrespective of the unsteadiness, the sediment gradation, the period and the amplitudes of input, and the BCs. The irregular reservoir responses showed stronger scattering as compared to the regular reservoir, and the scattering is lower as compared to that of sediment concentration.

- an increase of mass in the water body compared with the sediment mass input ($\frac{m}{m_i}$) resulted in lower relative sedimentation. This is the effect of transport capacity at higher discharges that lowers the sedimentation rate.
- for the same relative sediment mass in a water body, the analysis indicated, a higher relative mass deposition in the regular reservoir as compared to the irregular reservoir.
- at shorter theoretical residence times, the numerical solutions both for the regular and irregular reservoir approached the analytical solution of the CSTR and PFR.
- the regular reservoir responded more like the ideal PFR, see Figure 3.10 c). The irregular reservoirs however responded neither as a PFR nor as the CSTR; their response however, is generally closer to the CSTR, see Figure 3.10 b).

3.4 Quasisteady approximations

In this section, the results of refining the inputs by quasisteady steps of various $\triangle T$, investigated with respect to the improvement they showed in approaching the unsteady solutions are presented. The context of quasisteady considered in this section may be classified as:

Quasisteady based on the TELEMAC algorithm: TELEMAC algorithm solves an unsteady flow equation and transport equation in decoupled way. When steady-state simulations are to be considered in the sediment transport module, the flow is run under an unsteady algorithm and steady boundary conditions and criteria are set to obtain a steady condition in the flow fields. The last time step of the flow field (which is steady) is then used for the steady case simulation in SUBIEF-2D, in which the boundary conditions are steady but the solution algorithms are still unsteady.

Pure quasisteady steps: the pure quasisteady steps are also solved with the same algorithm above. However, the suspended sediment concentration or mass deposited is considered for each quasisteady step after the steady-state concentration or rate of sediment mass deposition were achieved.

The computational time reduction, therefore, mainly comes from flow simulations and the fact that longer time step can be used without interpolation of the flow field in the transport module. It is within this context that the validity of quasisteady approximation were studied for suspended sediment concentration as well as the rate of sediment mass deposition.

Quasisteady approximation with respect to sediment concentration

Figure 3.11 shows various approximation levels on the regular reservoir and the irregular reservoir 3. Two cases were chosen from the Figures 3.5, O-55 for regular reservoir and O-1000 for irregular reservoir for which the two reservoirs have a theoretical residence time of about 2 hours. The selection is from the region of β where the relative concentration of irregular reservoir is lower than that of the regular reservoir as the result of strong

recirculation. The volume of the reservoirs and the input discharges were kept constant. The input sediment concentration Unsteady U-in, Steady S-in, and Quasisteady QS-in were used in the runs under equilibrium transport assumptions (no erosion and sedimentation). The outcome of the outflow sediment concentration were shown by U-o for unsteady, S-o for the steady, QS-o for the quasisteady and QS-o-S for quasisteady steps considered after the concentration approached a steady-state for each step $\triangle$T. In the figure, the concentration attained at the end of 1 day simulation, were considered as a steady-state for each quasisteady steps. The first step of the periodic output were considered as the unsteady output concentrations. For the regular reservoir stable oscillation were reached within the first period, while for the irregular reservoirs stable oscillation is slightly higher than the first periodic output, see Figure 3.5.

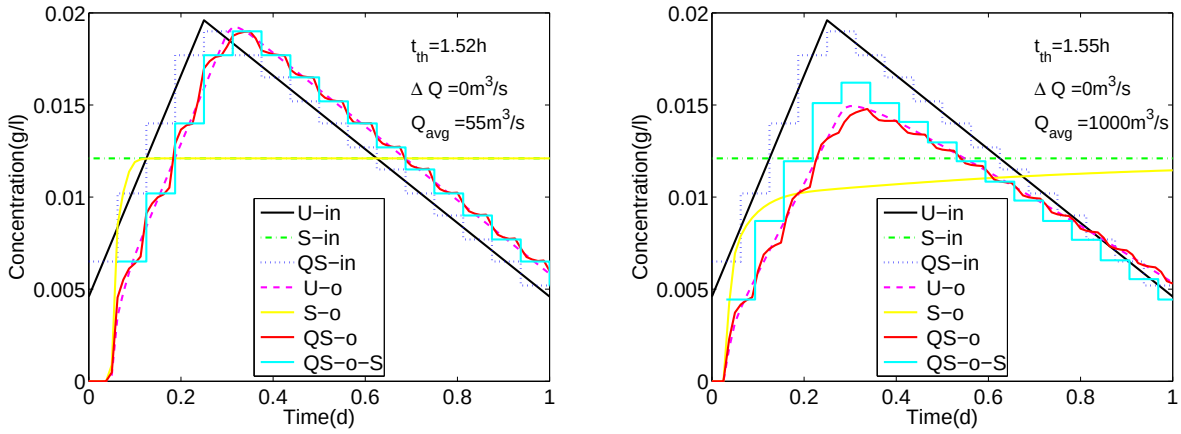

a) Regular b) Irregular

Figure 3.11: Suspended sediment concentration inputs and responses with various refinements of quasisteady steps for two reservoirs with the same residence time

The following remarks can be made from the outcome:

- quasisteady simulation QS-o-S better approximated the output concentration as compared to the fully steady simulations.
- for the regular reservoir, a time of response corresponding to the theoretical residence time were needed until a steady concentration were reached. For the irregular reservoir a time much longer than the theoretical residence time is required to reach steady concentration, see e.g. S-in and S-o that were attained at the end of 1 day. This is the result of strong recirculation in the dead water zone.
- the quasisteady simulations, in which each steady-state step were considered at the end of 1 day simulation were quite close to the complete unsteady simulation for the regular reservoir. For the irregular reservoir however, this showed discrepancies. U-o and QS-o are however in a good agreement, as the QS-o were solved with an unsteady solution for each quasisteady step.
- for the irregular reservoir, the output concentration approaches the input concentration asymptotically and took about 8 days for complete periodic response, while for regular reservoir complete recovery were attained within few hours, see S-in and S-o.

These are indications of the effect of reservoir shape and size as an important criteria in quasisteady approximation.

Quasisteady approximation with respect to rate of sediment mass deposition

Investigations made on the improvement that refining quasisteady steps brings with respect to mass deposition is shown in Figure 3.12. QS-NE-0.25T is quasisteady simulations following TELEMAC algorithm with the quasisteady time step of 0.25T; QS-0.25T is for pure steady steps of 0.25T, and QS-0.125T is for pure steady steps of 0.125T. For regular reservoir, steady-state rate of mass deposition were reached after 0.5 days of real flow time, while for the irregular reservoir more than 3 days were required.

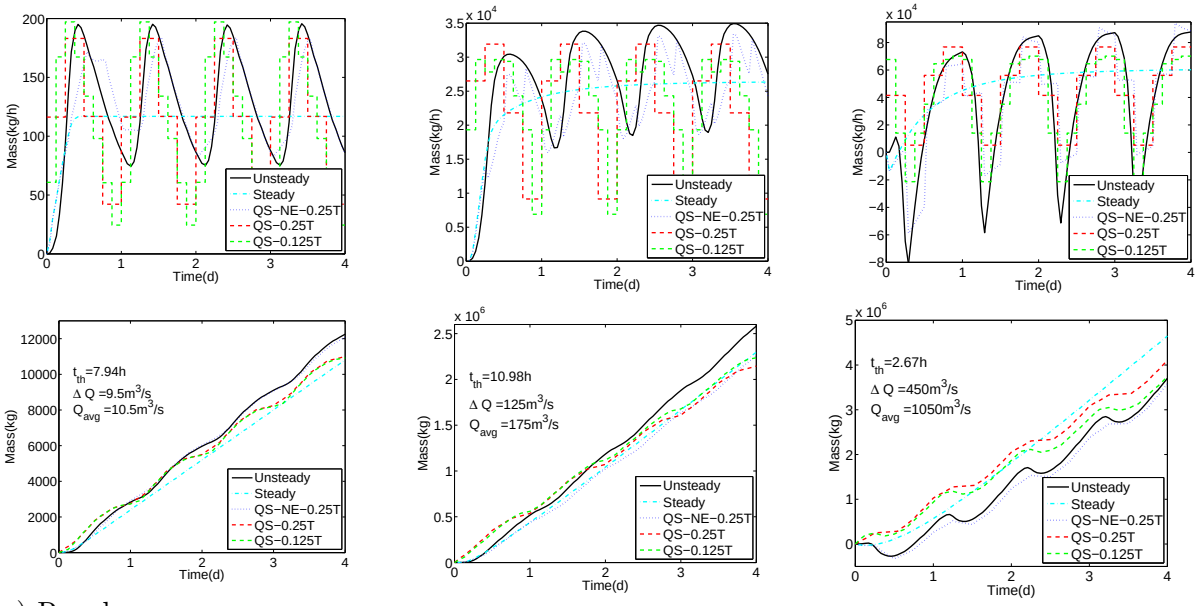

a) Regular b) Irregular c) Irregular* involving erosion

Figure 3.12: Effect of the refinement of the quasisteady steps $\triangle T$ in approaching the fully-unsteady solution: upper diagram showing rate and lower diagram cumulative deposition; period T=24h

Considering a single period T, after stable oscillation of mass deposition were reached for unsteady simulations, a constant rate of mass deposit were reached for the steady, and a constant rate of mass deposit were reached for each steps of quasisteady simulations, a clearer picture on the rate of sediment mass deposition are shown in the Figure 3.13 for the regular a) and irregular b) cases of the Figure 3.12. The discrepancy in the amount of sediment mass deposition were reduced on refining the quasisteady steps in comparison to the fully steady simulations.

The following remarks can be made from the analysis made:

- the quasisteady approximations, QS-NE-0.25T, performed using the unsteady algorithm and consideration of the effect of previous quasisteady steps for the new qua-

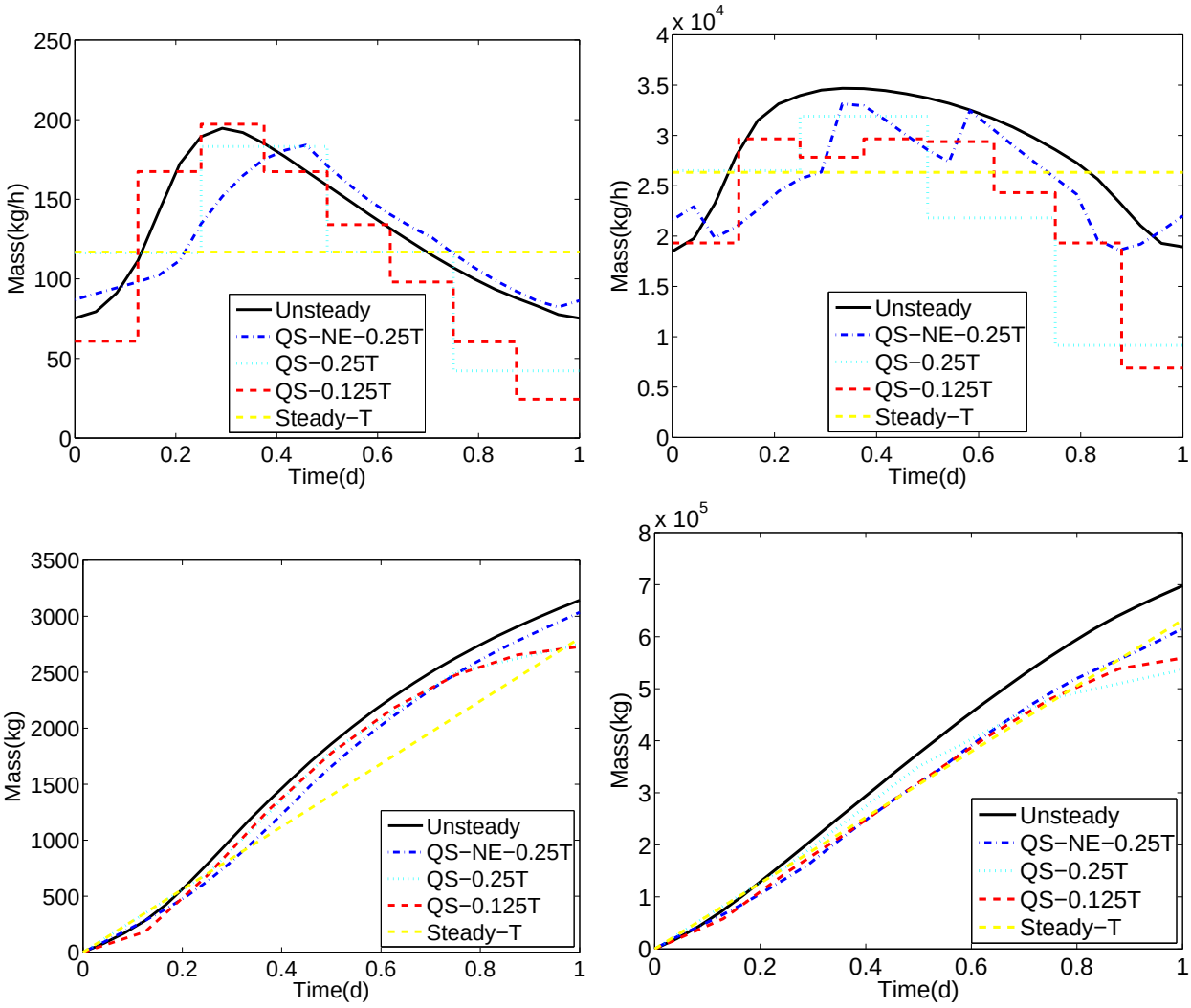

a) Regular; T=24h, t_{th}=7.95h b) Irregular; T=24h, t_{th}=10.98h

Figure 3.13: Focus on part of the Figure 3.12 after stable oscillation/steady rate of mass deposition were reached: upper diagram hourly and lower cumulative mass deposition

sisteady steps, led to a better approximation. Quasisteady steps shorter than the residence time showed no significant improvements in approaching a complete unsteady simulation.

- refining the QS-steps $\triangle$T generally led to better approximation. Uncertainties are however involved in the numerical and data aggregation aspects. For the case a) and c) in Figure 3.12 there is an indication that reducing $\triangle$T improved the approximation. Whereas in b) a clear trend was not observed. The time scale for simulation of the pure quasisteady steps, were not the same as that of the unsteady and quasisteady simulation following the TELEMAC algorithm, which can be one source of uncertainty.

- reservoir shape and geometry has a significant influence on the limits of validity of QS-approximations. Regular reservoirs can have a wider range of valid QS approximations.

It is challenging to give a universal guidelines over the validity of quasisteady approximation

as a result of the various uncertainties and non-linearities involved. Based on the study made in this chapter, case-dependent simplification strategies need to be investigated. The following general statements can be used towards application of quasisteady simulation towards long-term simulation:

- quasisteady approximations must be carefully performed in the range of shift from net sedimentation to net erosion and vice-versa. In long-term morphological simulations, the part of the flow behavior in which there exists no sedimentation and erosion can be taken out of the model.
- the quasisteady simulation based on the unsteady algorithm is superior to the pure quasisteady solutions, and is the way considered in investigating the validity of quasisteady approximations, in long-term simulations of the Lautrach reservoir.
- theoretical residence time can be used as an important criteria in classification of sedimentation pattern in implementing quasisteady approximation.
- case-specific investigation is necessary in characterizing reservoir responses, to the patterns of inputs. It can be more useful to base the investigation over longer time steps, say a year to come up with clearer picture on the condition for the validity of the quasisteady approximations.
- the boundary conditions investigated QC, HCC and HC revealed that reservoirs with relatively low water level fluctuation are favorable in the validity of quasisteady approximations.

Summary

Two extremely different reservoir types have been presented using simplified periodic discharge and sediment inputs as test functions for studying reservoir sedimentation processes. The 2D-numerical results were compared with the steady-state analytical solution of CSTRs and PFR, revealing the validity of such systems as a first-hand tool. The regular reservoir response is closer to the PFR while the irregular reservoir acted neither as PFR nor CSTR, but closer to the CSTR. The influence of residence times, amplitudes, and frequency of inputs on sediment deposition were analyzed aiming to find criteria to facilitate/imporve long-term simulation.

From the studies made on the unsteadiness, it was concluded that reservoir shapes, residence times, mean flows, amplitude of flows play a crucial role in quasisteady approximations. Although the universal relations were not obtained, useful conclusions were made on the trends that the aggregate parameters had indicated.

Nature shows more variability with respect to flow and sediment data and other relevant parameters. The studies made in this chapter extend to the case of the Lautrach with further investigation on numerical aspect of modeling morphology. The next chapter continues with data organization and management in morphological modeling with a focus on the Lautrach reservoir.

Chapter 4

Data Evaluation in Morphological Modeling

Long-term morphological simulation demands a large amount of data on topography, hydraulic and sediment parameters. Organizing appropriate and sufficient data is one of the challenging aspects in simulation of river morphology. Data requirements depend fundamentally on the engineering objective. Modeling a small reservoir might demand more data resolution compared to modeling at river basin scale. Similarly modeling flood events may need more resolved data than mean flows. In this chapter, description of state of the art of data acquisition techniques, the data available for this study, as well as new measurements conducted in the scope of this work are presented.

4.1 Data acquisition and management

Obtaining flow and sediment data at dense spatial and temporal resolution is ideal. Expense, technical difficulties, and safety concerns often hinders the quantity and quality of data acquisition. It is essential to device optimal strategies in data management and quality. Focus must be given on the most important data demands. For example, it is impossible to measure critical shear stress for erosion at within 1 m^2 grid for an entire area of a large reservoir in one day time interval and only depths of a few centimeters. It might be sufficient to have measurements before and after the flood event at locations determined by knowledge of basic hydraulics. A strategy must be devised based on the state of the art knowledge and experience.

Advances in instrumentation, experimental science, and data management is making the process of data acquisition more feasible. It should, however be noted that advanced systems are available for only those who can afford and manage the systems appropriately. In many parts of the world, even flow measurements are not available at the required density, not to speak of complete data for morphological modeling.

The International Association of Hydrological Science (IAHS) has for example recently launched an initiative called Prediction in Ungaged Basins (PUB). The problems related to uncertainty in prediction methods in ungauged or poorly gauged basins, performance of the methods, the use of new data sources like remote sensing, experimental field research or transfer of information from gauged surrogate basins to ungauged basins, are the primary issues. Utilizing readily available geo-hydrological observations, predictions are made on flows and suspended sediment behavior at river basin scale. Implementing techniques such as data assimilation, data aggregation and disaggregation, scaling, uncertainty analysis,

interpolation techniques, and various statistical techniques are often necessary in tackling the problem of data deficiencies. The data requirement in morphological modeling may be classified as:

Topographic data

Topographic data include longitudinal profiles, cross sectional profiles, hydraulic structures, etc. available in a domain to be modeled. The density and accuracy of topographic data needed are influenced by a model's purpose. For large scale models, coarser cross sectional profiles may be sufficient. For complex geometries very fine measurement are generally required. The use of Global Positioning System (GPS) and Acoustic Doppler Current Profiler (ADCP) in measuring lake bathymetric has replaced the traditional systems of profile surveying along selected cross sections, see Baker 1996 [9].

Hydraulic data

Water depths, stages and velocities from which discharges are evaluated are the main types of hydraulic data needed to construct flow models. Discharges are measured using various techniques. ADCP, calibrated rating curves on hydraulic structures (e.g. weir) where stage measurements are used to calculate flows, tracer concentration etc. When there is technical difficulty in working closely to water surface, ground penetrating radar (GPR) methods can be used, e.g. Haeni et al. 2004 [56].

Sediment data

Suspended sediment concentration, gradation, settling velocities, critical shear stresses for erosion and deposition are some of the observations required for suspended sediment transport models. Samples for measuring of suspended sediment concentration has to be well-distributed along a river cross sections and depth. Point measurements which represent the whole cross section may be insufficient. Procedures for determining the suspended sediment concentration can be fixed depending on the purpose of observation, sediment properties, costs and technical difficulty.

Depth sampling utilize two methods. Sampling by points in which samples are taken at 0.0, 0.2, 0.6, 0.8 and 1.0 of the water depth. Depth-integrated sampling, taking samples continuously along the depth with a sampler moving at constant speed. Along cross sections; selection of verticals based on the transverse distribution of concentration, equal discharges between verticals, equally spaced verticals, simplified index-sampling methods are commonly practiced. For more details, see the manual by Xiaqing 2003 [141].

The frequency and sampling time is another important issue. Suspended sediment should be more frequently sampled during flood events than during low flows. Hourly data may be reasonable during flood events. During the rest of the year, the sampling frequency can

be taken daily, weekly or even monthly. For watersheds with a wide variety of soils and geological conditions, frequent uncontrolled human intervention like flushing or agricultural practices, and an uneven distribution of precipitation, no definite sediment sampling schedule may be designed.

In addition to velocity and channel shape etc., sediment size is a major factor influencing the non-uniform distribution of sediment concentration across a section. If coarse particles, greater than 0.0062 mm are predominant, non-uniform sediment concentration is more likely to occur. Generally the variation of sediment gradation with time is less important compared with the variation of concentration with time.

Sediment gradation can also be determined from samples of sediment deposits. Laboratory procedures to estimate sediment concentration may include evaporation, filtration and displacement methods.

For conditions where the bed load plays a significant role of the transport, bed load transport measurements are conducted using bed load samplers. In practice it is more difficult to measure bed load discharge accurately compared to suspended sediment load. Details may be referred in Xiaqing 2003 [141].

There are many methods available for size analysis. The size distribution of a sediment sample may spread over a wide range. Two or more methods may be necessary to analyse the whole sample. For instance, the sieve method may be used for small fraction of coarse particles while the visual accumulation (VA) method or its equivalent size-analyzer method is used for particles greater than 0.0062 mm, and the pipette or photo-sedimentation method is used for particles smaller than 0.0062 mm.

Procedures for obtaining critical shear stresses for erosion and deposition were reviewed in Section 2.2. These parameters are of central importance in morphological models and are challenging to fix them for long-term simulations as a result of their spatial and temporal variability. The parameters can also be be calibrated using numerical models.

4.2 Database of the Lautrach reservoir

In this section, a summary of the database available for this study is given. Examining the theoretical and practical background in modeling and data acquisition aspects discussed in Chapter 2 and Section 4.1, it is necessary to choose a case where an objectively good database on topographic, hydraulic and sediment properties was possible to obtain. The Lautrach reservoir, on the river Iller in Germany was considered to investigate the proposed scientific research objectives. The database were obtained from various sources:

- a previous study done by Institut für Wasserbau together with Lahmeyer International had a collection of data on topography, sediment properties measured and processed in the hydraulic laboratory of IWS.

- Bayerisches Amt für Wasserwirtschaft provided this research with supplementary data on flow and suspended sediment concentration.
- Lahmeyer International supported the research by providing flow, suspended sediment, and topographic information.
- Lech Elektrizitätswerk (LEW), the company owning and operating the reservoir, had also given data on flow and head at an interval of 15 minutes for the year 2004.
- sediment samples were taken during the field visit to the Lautrach reservoir, from which critical shear stress for erosion were determined in the hydraulic laboratory of IWS using the SETEG system. Supplementary data on reservoir operation were also obtained during the field visit.

4.2.1 Description of the Lautrach reservoir

Lautrach reservoir is a small reservoir located close to the village of the Lautrach on River Iller, a tributary of River Danube. It came into operation in 1959. The reservoir was designed to regulate head and daily discharge fluctuation for reliable water supply during peak power demand. The reservoir is operated and owned by Lech Elektrizitätswerk (LEW). LEW operates four other small reservoirs; Maria-Steinbach, Legau, Fluehmüle and Altusried between the city of Lautrach and Kempten. A gauging station for flow and suspended sediment concentration measurement is located at Kempten. Figure 4.1 below shows the location of the study area.

Figure 4.1: Location of the study area

The aerial photo of the reservoir under partly emptied condition is shown in Figure 4.2. The reservoir has a very complex geometry. The depth of the reservoir is higher along the

Figure 4.2: Aerial view of the Lautrach reservoir

main canal compared to the wide area on the left bank. In this work, the deficiencies in the database were supplemented by standard analysis. In the following section, summary of the available database is given. Furthermore, the data used throughout the work are described. For efficient presentation, only the database used for major works and typical data are presented rather than forwarding all available data in its integrity.

4.2.2 Topographical data analysis of the reservoir

Measurement of bed profile changes were conducted along defined cross sections at a distance of 200 meters for the years 1957, 1962, 1965, 1972, 1978, 1983, 1988, 1992, 1996, 1999 and 2002. To correctly approximate the topography of such a complex geometry, it is necessary to have a large amount of measurements of the bottom elevations. A systematic linear interpolation was run between adjacent cross sections. The interpolation base was developed by use of the previous study by Al-Zoubi and Westrich 1997 [2]. In Figure 4.3 a), bold lines show measuring cross sections while the light lines show the interpolated points. Profile measurements were also made at dashed darker lines, mid-way between the sections in 200 m intervals for the year 1999. Figure 4.3 b), shows a typical cross sectional change over 17 years at section 60.6.

The profile changes at the cross section 60.6 in Figure 4.3 b) indicates a gradual deposition of sediments over a long period of time. Even after the peak flood event of the year 1999 erosion did not take place at this cross section. Sections upstream of 61.1 show a stabilized bed. The most important change in bed evolution occurred in the central part of the reservoir, where the reservoir has its maximum width.

Systematic interpolation is necessary between measuring cross sections for sufficient representation of topography because the density of measurements is too coarse. For river reaches with very complex geometry the interpolation lines should be carefully chosen. For the Lautrach reservoir the interpolation lines were chosen as shown in Figure 4.3 a). It was tried to follow the general topography and curvature of the reservoir. Elevation values

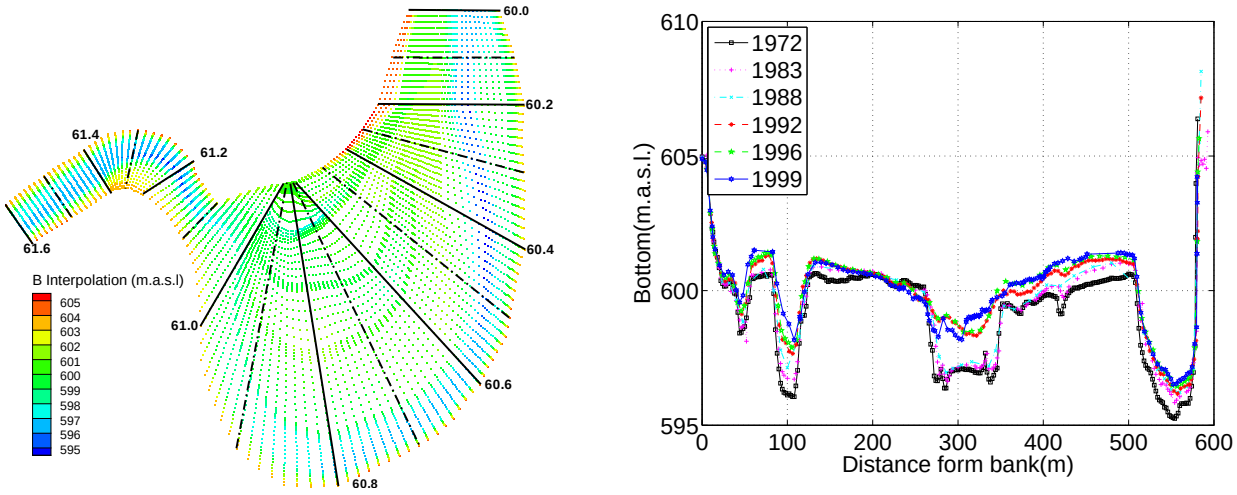

a) Measurement cross sections

b) Profile change at cross section 60.6

Figure 4.3: Location of cross section measurements and typical cross section change over years

were then linearly interpolated to generate elevations of series of points that supports in the generation of meshs. For the generation of intermediate points between measuring cross sections, linear interpolation programmed in FORTRAN was used.

The reservoir was affected by gradual sedimentation and has lost 30% of its volume to sedimentation Al-Zoubi and Westrich 1997 [2]. There was no net erosion over a long period of time as can be seen in Figure 4.4. Note that the volume of reservoir in the figure were for the water volume between cross sections 60.0 and 62.0.

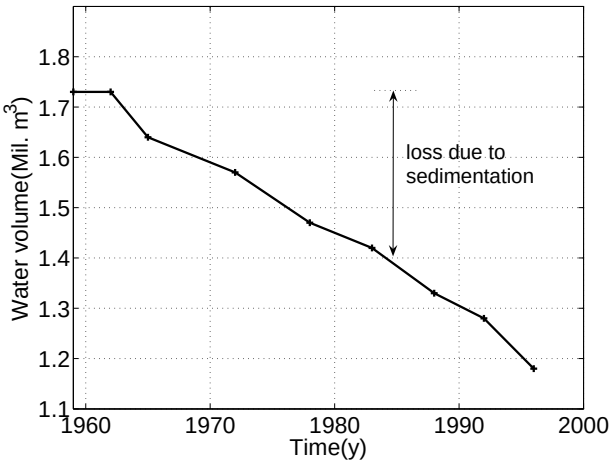

Figure 4.4: Change of the reservoir water volume over years, Al-Zoubi and Westrich 1997 [2]

4.2.3 Flow and suspended sediment data analysis

Long-term daily flow and suspended sediment concentration data were available from measurements at Kempten. There were also some hourly data available during peak flows at

this station. Since long-term flow data for the Lautrach reservoir was not available, a linear regression between daily flow at Lautach and Kempten was used to adjust the flow at Lautrach. At the Lautrach reservoir, the discharge and head measurements for the year 2004 available at an interval of 15 minutes were used for the regression. The relation has a correlation coefficient of 0.9782 and was used to adjust the discharge at the Lautrach.

$$Q_{Lautarch} = 1.2197 Q_{Kempten} + 1.8 \tag{4.1}$$

Suspended sediment concentration measurement were not conducted at Lautrach. The nearest station where long-term suspended sediment measurements were available is at the Kempten gauging station located some 25 km upstream. In a previous study by Al-zoubi and Westrich 1996 [3] and 1997 [2], it was concluded that the four reservoirs upstream of the Lautrach and the gauging station had not shown significant morphological change. It was determined that the river reach between the Lautrach and Kempten was stable, and that the catchment area was assumed not to substantially contribute to change in suspended sediment concentration. Based on similar arguments, the suspended sediment concentration at Kempten was taken directly for the work. The daily averaged suspended sediment concentration from the gauging station at Kempten was used in this research.

Daily averaged flow and concentration

Averaged daily discharge data from 1970-2005 were available. There are gaps in suspended sediment concentrations data for some years in the period. The period for which both daily discharge and suspended sediment data are available were used for model calibration and validation. Figure 4.5 below shows the daily averaged discharge and suspended sediment concentration data used in the calibration step 1988-1992, validation steps 1992-1996 and 1996-2001 and the data for the phase of prediction from the year 1996-2032. The discharge and suspended sediment data of the years 1992 to 2005 were assumed to repeat themselves for the prediction steps of the years 2005-2032.

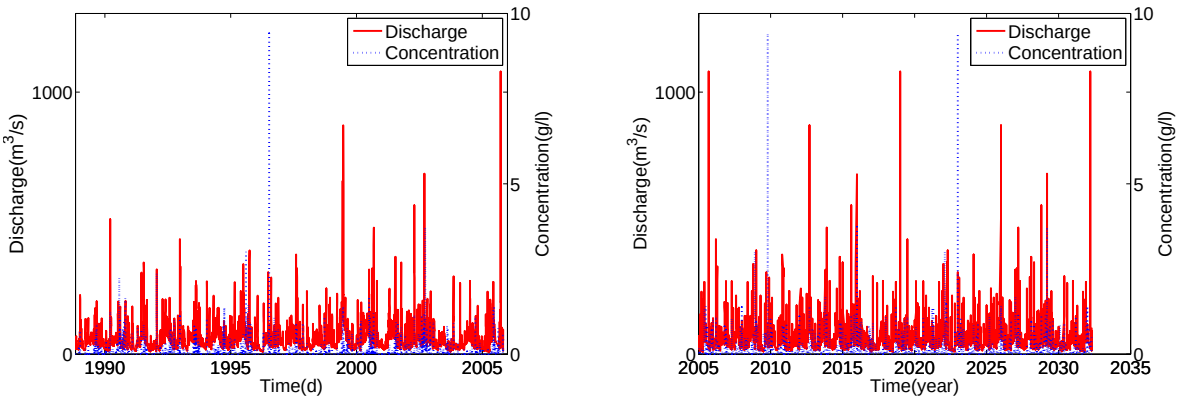

a) Oct. 1988 - Jun. 2005 b) Jul. 2005 - Aug. 2032

Figure 4.5: Discharge and suspended sediment concentration

Analysis was made to find out a deterministic relation between discharge and suspended sediment concentration. Correlation analysis was undertaken using various methods: shifting

the data by days, sorting the data by season, and by the rank correlation. The maximum correlation was that obtained by sorting data by month, showing maximum r^2 of 0.50. Seasonal influence, change in the patterns of discharge-concentration relation from year to year and data quality can determine the extent of correlation.

Refined flow and head data

Flow observations at Lautarch were available for this study on hourly basis including the following periods: 17.12. - 26.12. 1993, 12.04 - 20.04. 1994, 05.08. - 10.08. 2000. For the periods 11.05. - 17.05. 1999, 21.05. - 25.05. 1999 and 05.08. - 10.08. 2000 flow at an interval of 15 minutes was obtained for the study. In addition, for the whole year 2004, discharge and water level measurements at the Lautrach at an interval of 15 minutes were provided. Figure 4.6 a) shows discharge at an interval of 15 minutes and its daily average and b) shows the water level (head) measurements at an interval of 15 minutes and its average on daily and annual basis.

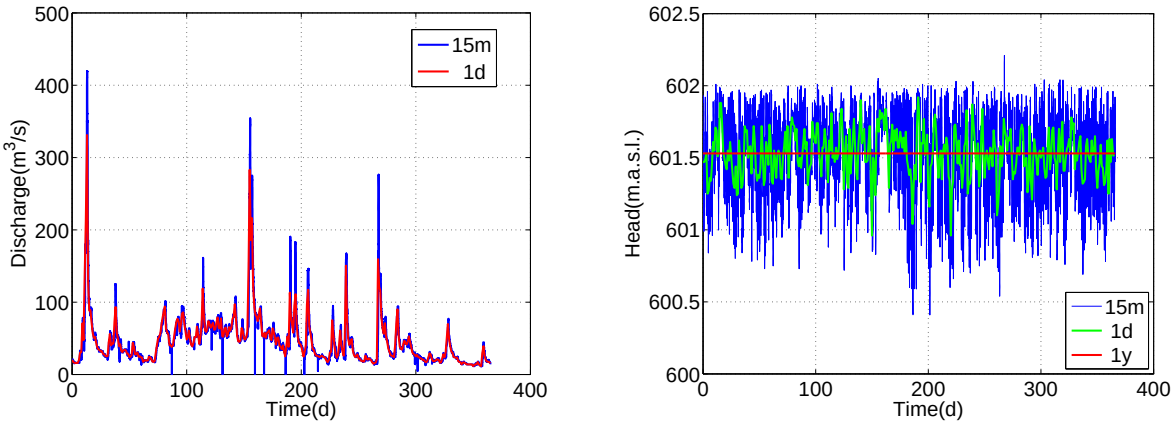

a) 15 minutes and daily averaged discharge b) 15 minutes, daily and annual averaged head

Figure 4.6: Discharge and head measurements at the Lautrach for the year 2004

The uncertainty as a result of data aggregation needs to be carefully assessed in data use of the numerical simulations. Sensitivity analysis can be made on the limit of the aggregation with acceptable uncertainty. In Chapter 5 more details are given on the study made on the effect of data aggregation on the sediment mass deposition.

Reservoir operation

Reservoir operation is one of the most important mechanisms in controlling reservoir sedimentation. The operational method employed is particularly sensitive for reservoirs storing water for long period of time. The operation of the Lautrach reservoir has no defined patterns. Reservoir emptying and filling is dependent on energy demand from the power grid system. The reservoir does not tend to store water for a long period of time. The reservoir is operated to fill the gap in daily power demand fluctuation.

The scheme has four turbines each with an installed discharge capacity of 25 m^3/s. The crest level of the weir is 602.00 m.a.s.l. The reservoir is mostly operated at 50 cm below the pool level. On average, the water level in the reservoir is kept at 601.53 m.a.s.l. See the water fluctuation in Figure 4.6 b). The average reservoir water level fluctuations in the reservoir is of the order of 1 m.

4.2.4 Experimental investigations on sediment parameters

Sediment gradation and critical shear stress for erosion were the major sediment parameters investigated. Two studies were available for the work. An early study conducted by Al-Zoubi and Westrich 1996 [2] and a study made during this research. Figure 4.7 shows the locations of samples investigated. Small circles along cross sections 60.2, 60.4, 60.8 and 61.0 were done by previous study, and samples marked with star marks from 1 to 7 were investigated in the present study.

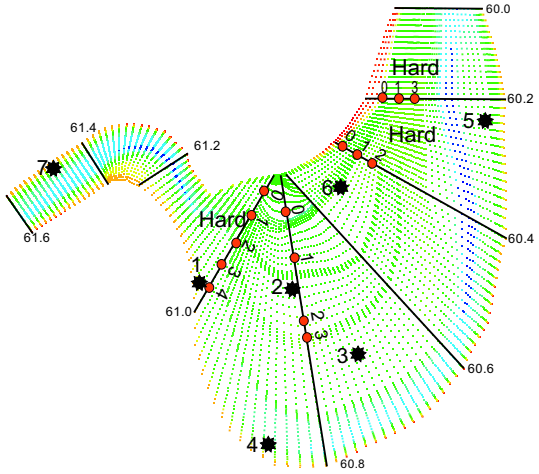

Figure 4.7: Sediment sampling points of 1996 •, and 2006 ∗

Table 4.1 shows experimental result of sediment gradation conducted in 1996. The relation

Sampling points	$d_{10}(\mu m)$	$d_{50}(\mu m)$	$d_{60}(\mu m)$	$d_{84}(\mu m)$
60.2.0	1.8	12	17	34
60.2.2	2.1	14	20	41
60.4.0	1.7	9	11	27
60.4.1	3.3	21	31	50
60.4.2	3	19	23	41
60.4.4	2.2	27	39	63
60.4.6	3.3	37	47	105
60.8.0	10	51	60	160
60.8.3	-	53	61	160
61.0	2	14	21	38
61.1	2.3	40	46	105
61.4	4.3	44	54	130
61.5	2.1	16	21	44

Table 4.1: Sediment gradation measurement, Al-Zoubi and Westrich 1996 [2]

of bottom shear stress τ_o to erosion rate E$(g/m^2 s)$ studied by Al-Zoubi and Westrich 1997 [2]

is given in Table 4.2. The measurement were made on samples at two points, one at 60.8.3 and the other at 60.4.2, see Figure 4.7. In Table 4.2 the notations U 60.8.3a and U 60.8.3b indicate undisturbed samples of 15 cm and 23 cm depth respectively, at location 60.8.3 and D 60.4.2a, and D 60.4.2b are two disturbed samples at location 60.4.2.

U 60.8.3a		U 60.8.3b		D 60.4.2a		D 60.4.2b	
τ_o (Pa)	E (g/m^2s)	τ_o (Pa)	E (g/m^2s)	τ_o (Pa)	E (g/m^2s)	τ_o (Pa)	E (g/m^2s)
0.55	0.01	0.58	0.05	0.843	0.020	1.19	0.005
0.64	0.02	0.64	0.08	1.00	0.035	1.36	0.000
0.71	0.11	0.73	0.05	1.19	0.070	2.30	0.110
0.80	0.20	0.81	0.07	1.36	0.035	-	-
0.93	0.37	1.15	0.30	1.60	0.071	-	-
1.10	0.45	1.42	0.40	-	-	-	-

Table 4.2: Relation of the bottom shear stress to erosion rate, Al-Zoubi and Westrich 1997 [2]

In June of 2006, four samples were chosen among 7 samples and experimental investigation on depth dependent critical shear stress for erosion were conducted using SETEG-System, see in Figure 4.7). The results are shown in Table 4.3.

Depth (cm)	τ_{ce}(Pa) at sampling points			
	1∗	2∗	3∗	5∗
0.00	0.46	0.47	0.40	0.42
3.00	0.78	0.91	0.61	1.03
6.00	2.09	0.50	0.61	1.69
9.00	2.66	1.42	0.62	0.81
12.00	2.85	2.95	0.58	0.95
15.00	-	2.79	0.55	0.80
18.00	-	4.05	0.58	1.26
21.00	-	-	0.61	0.99
24.00	-	-	0.59	1.72
27.00	-	-	0.55	4.64
30.00	-	-	0.55	3.39
33.00	-	-	-	6.79

Table 4.3: Experimental results of the critical shear stress for erosion using SETEG system

Summary

In this chapter, the data required for morphological modeling of the Lautrach reservoir is briefly organized and presented. Although there are deficiencies in database availability, it was concluded that the database was sufficient to investigate the issues relevant to the simplification of long-term simulation of reservoir morphology. The following chapter continues with the investigation of modeling techniques using the realization of input data for the Lautrach reservoir.

Chapter 5

Investigation of Modeling Techniques

In this chapter, a preliminary investigation of modeling techniques on the amount and spatial distribution of sedimentation of the Lautrach reservoir is presented. Comparative studies were performed on the aspects of input data aggregation, mesh and time refinement, coupling methods, turbulence modeling etc. On a large-scale and for long-term modeling of reservoir bed evolution, a compromise is necessary between model quality and computational demand. The parameters involved in morphological modeling are too many to treat separately. A joint estimate using calibration-validation procedures are generally adopted. Preliminary model tests which were performed are described in order to propose a simplification with an acceptable uncertainty and a reasonable computational cost as well as data demand. The results of the investigations were used as a preliminary step towards long-term simulation of the bed evolution of the Lautrach reservoir, which is treated in Chapter 6.

A typical one month flow comprising low and peak discharge periods was selected from the flow data of the year 2004, see Figure 4.6. A relation between discharge and suspended sediment concentration based on linear regression was used to estimate the suspended sediment concentration at an interval of 15 minutes. The data were then aggregated on an hourly, daily, in three steps of low and peak flow periods, and on an average monthly basis, as shown in the Figure 5.1. The method of solution used is summarized in Section 2.5.2.

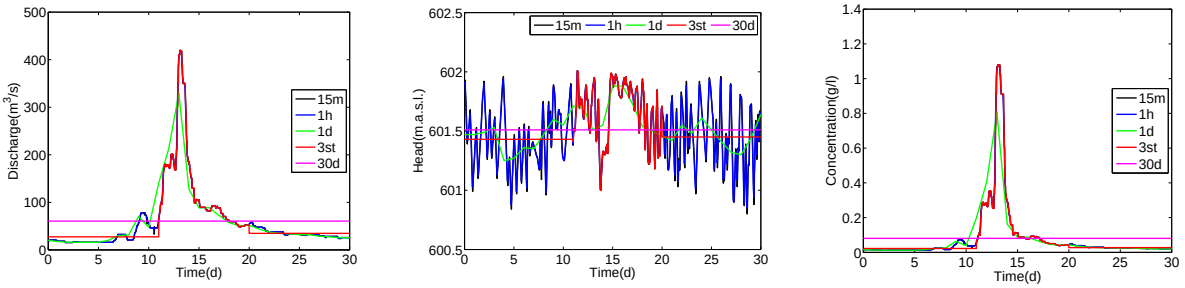

a) Discharge aggregation b) Head aggregation c) SS concentration aggregation

Figure 5.1: Flow, head, and concentration aggregation for a typical flood event

The parameters used in the analysis, unless re-specified are as follows:

- inflow boundary conditions were prescribed discharges; outflow boundary conditions were prescribed water levels; and inflowing suspended sediment concentration were prescribed as shown in Figure 5.1 a), b) and c) respectively.
- the critical shear stress for erosion was taken from studies shown in Table 4.2 & 4.3. The critical deposition velocities were considered as 0.00045, 0.0039, and 0.0049 m/s for the sediment grain d_{16} , d_{50} and d_{84} respectively. The settling velocities were calculated from the grain size in Table 4.1 as 0.000009, 0.0007 and 0.001 m/s for d_{16}, d_{50}

and d_{84} respectively . For the case of uniform sediment assumption, the parameters for d_{50} were considered, in which the settling velocities of 0.0004 - 0.0007m/s, a spatially varying critical erosion shear velocity of 0.02 - 0.04m/s and critical deposition shear velocity of 0.0039 - 0.009 m/s were used in various test cases.

- a spatially varying Manning-Strickler coefficient of 37.6 to 50 $m^{1/3}/s$, an erosion constant of 8E-6 $kg/(m^2 s)$, a bottom concentration (C_{sf}) of 500 kg/m^3 (corresponding to the porosity of 0.8 and sediment density of 2650 kg/m^3), the solver accuracy of 1E-4 to 1E-6 for flow and 1E-6 for the transport, 1E-9 for the k-ϵ, and a maximum erodible depth was fixed to 50 cm for each simulation.

Using MATISSE, a distance criteria-based grid generator, various grids were generated for investigation. Four different mesh refinements were generated for evaluation, with sizes of 8m, 10m, mixed 10m & 20m and 20m, of which the two are shown in Figure 5.2. The number of elements for the meshes are 19279, 12329, 4945 and 3169 for 8 m, 10 m, 10&20 m and 20 m grids respectively, showing large variation which have a direct relation with the computational cost and the quality.

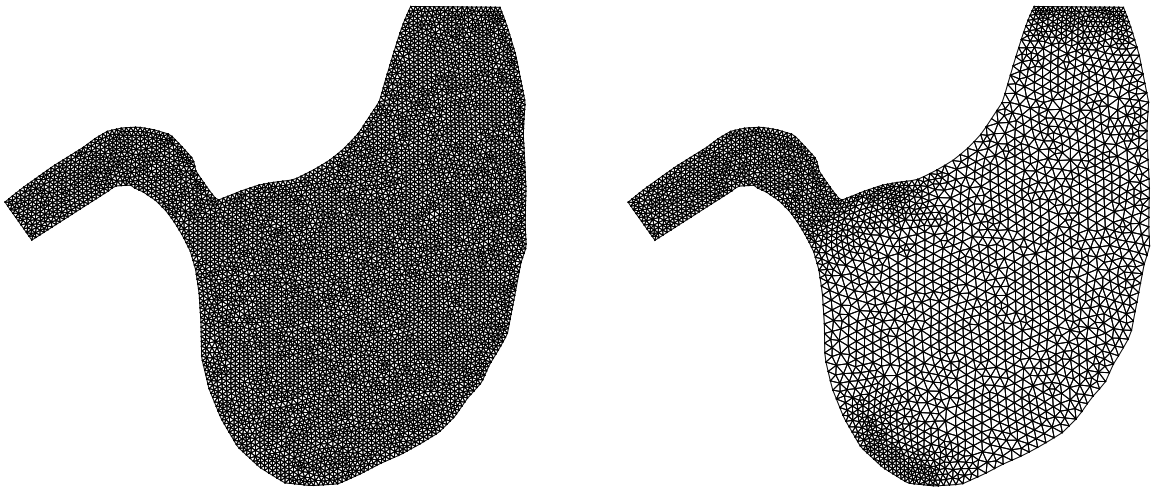

a) 10 m b) 10 & 20 m

Figure 5.2: Some grid refinements of the Lautrach reservoir for evaluation

Comparison in some of the cross sections on the Lautrach reservoir were made between the generated grids and the measured profiles as shown in Figure 5.3. As a result of mesh generation of various refinements involving interpolation, the computed and measured profiles do not show a perfect fit. This indicates the sensitivity of grid generation techniques to density of the digital elevation models interpolated among various cross sections. The problem was especially exaggerated in the cross sections having very complex geometry.

Comparison of reservoir volume for different grid refinements investigated at the crest level are shown in Table 5.1. The volume of reservoirs showed a slight variation with a change in grid refinements.

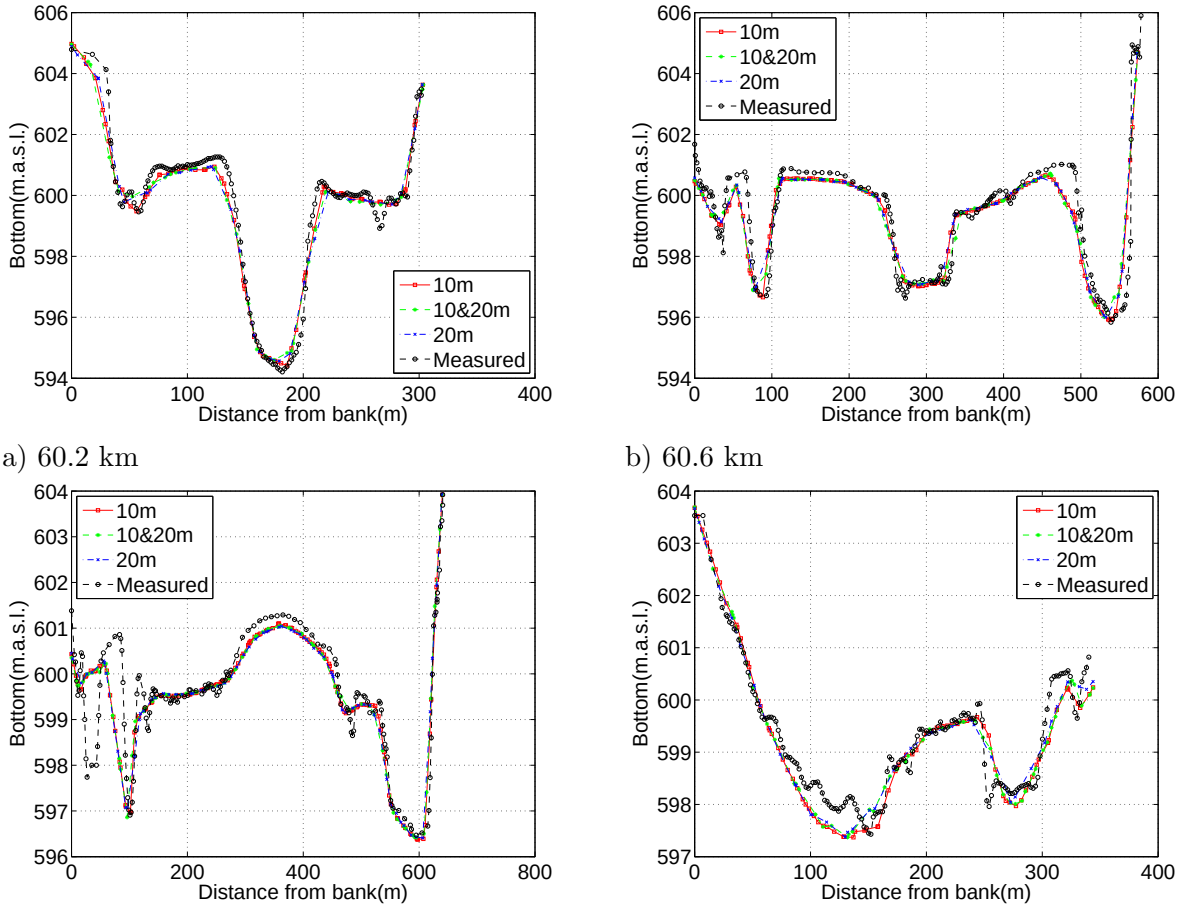

a) 60.2 km b) 60.6 km

c) 60.8 km d) 61.0 km

Figure 5.3: Cross sectional profiles resulting from various grid refinements compared with profiles measured in 1983

Mesh	1983	1988	1992	1996
10m	1,237,640	1,158,250	1,111,250	1,009,300
10-20m	1,242,100	1,163,260	1,114,360	1,013,790
20m	1,240,590	1,160,100	1,112,200	1,014,300

Table 5.1: Water volume for various grid refinements at mean the water level in m^3

5.1 Effect of data aggregation

Numerical experiments were run varying the input aggregation as shown in Figure 5.1 for the duration of one month. A uniform sediment fraction was considered. The rate and cumulative sediment mass deposition is shown in Figure 5.4 a) for the profile of 1988, in b) for the profile of 1996, for the level of aggregations of 15 minutes (15m), hourly (1h), daily (1d), in three steps of low flows and peak flows (3steps) and averaged monthly (30d). Different erosion and deposition parameters were used for the cases a) and b).

The results indicate that:

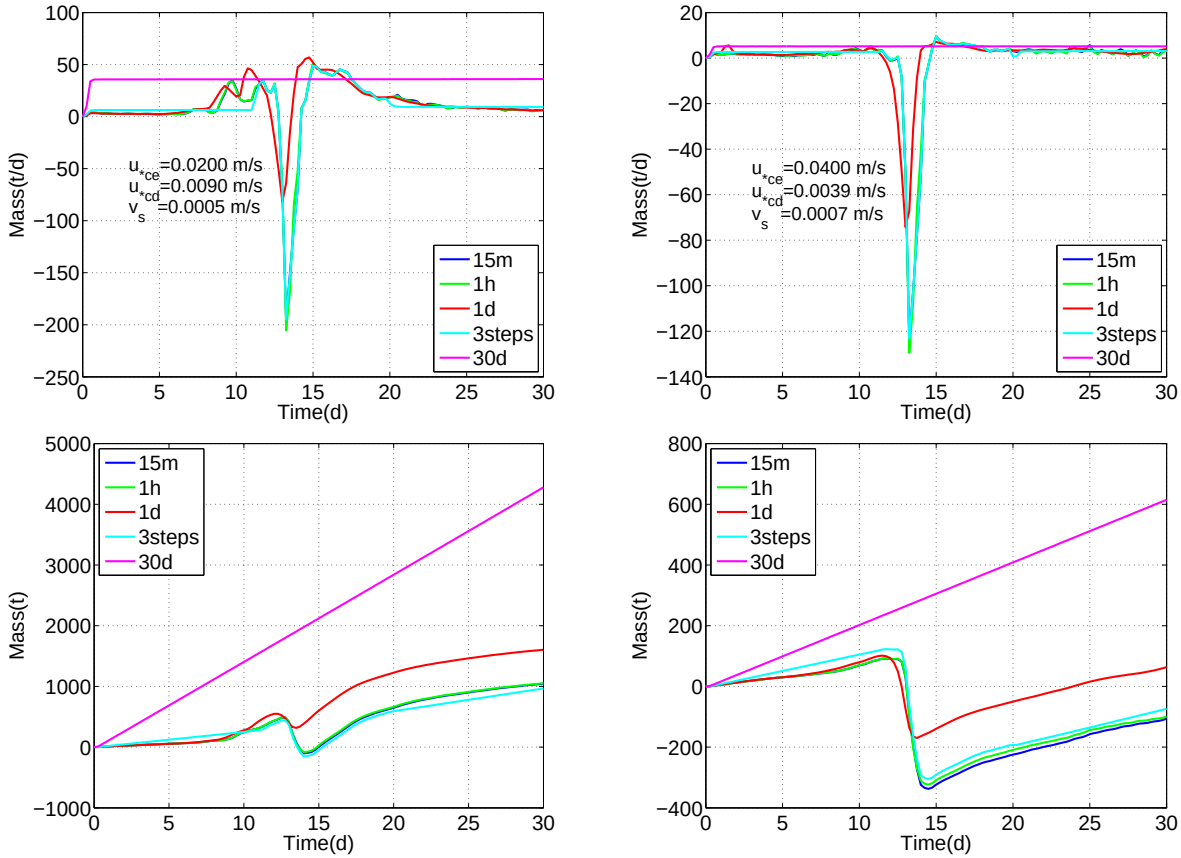

a) Mass deposition, profile 1988

b) Mass deposition, profile 1996

Figure 5.4: Effect of input data aggregation on the mass deposition using different parameters: top daily deposition and bottom cumulative deposition

- most of the variation occurred during peak discharges.
- irrespective of the erosion and deposition parameters, the aggregation showed similar characteristics.
- no significant differences for aggregations of 15 minutes, 1 hour, 1 day, and the three steps (3steps). The case in which the data was aggregated over the whole computational period (30d) yielded distinct results particularly for the peak flow period.
- it was concluded that during the low flow periods; daily, weekly, even monthly averaged data are acceptable with certain degree of uncertainty and flood events must be modeled with the best data resolution available. The daily aggregated data was justified for long-term morphological model calibration and validation.

Gurmessa and Westrich [73], also presented a thorough investigation on the effect of data aggregation on modeling of reservoir sedimentation. Using initial morphological conditions for the years 1983, 1988, 1992 and 1996, aggregation at various levels was analyzed. Cases with constant head and variable head were investigated, making use of various erosion and deposition parameters. The conclusion was that the peak flows must be treated with the most refined data available.

5.1.1 Effect of head aggregation

The water level of the Lautach reservoir is generally kept below the crest level of the barrage, 602 m.a.s.l. For example, for the year 2004, the 15 minutes head data have an average of 601.53, see Figure 4.6 b). The initial morphological boundary conditions of the year 1992 were used. Uniform sediment with u_{ce} of 0.02 m/s, u_{cd} of 0.0039 m/s and v_s of 0.0007 m/s and a spatially varying Manning-Strickler of 37.6 to 41 $m^{1/3}/s$ was used.

Numerical experiments were conducted to compare the effect of daily fluctuating head on deposition for a typical year. Except the head all the other data were kept the same. Figure 5.5 show the spatial distribution of sedimentation at the end of the computational period of one year. The result shows that, no major discrepancy in bed evolution between assuming constant head and the variable head implemented which had a maximum variation of 1m, shown in Figure 4.6 b). For the numerical run, where a variable daily head was

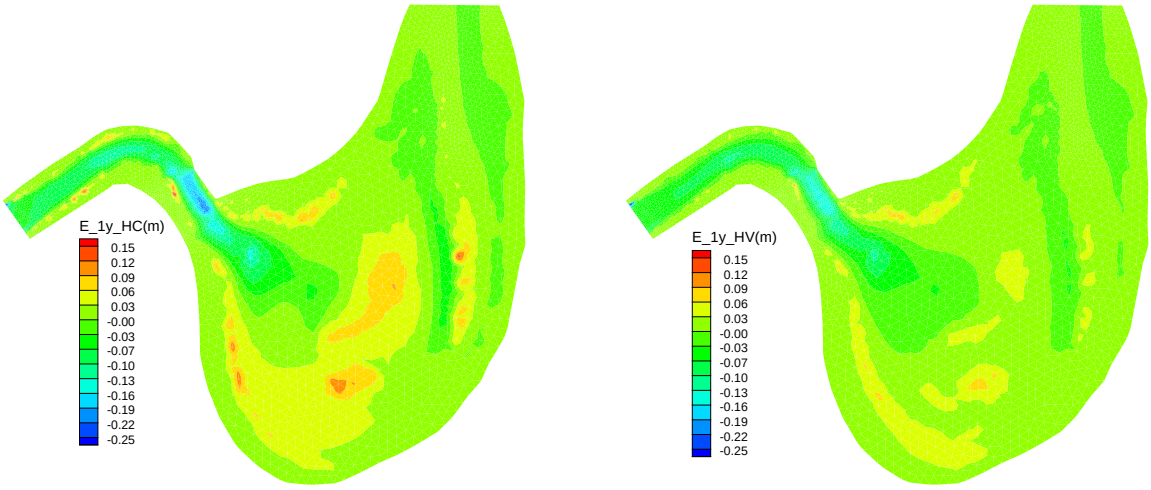

a) Constant head b) Variable head

Figure 5.5: Effect of water head on the spatial distribution of sedimentation, 1992

considered the maximum, minimum, mean and standard deviation of deposition at the end of one year simulation are 0.411, -0.460, -0.001, and 0.069 m respectively. For the numerical run, where constant head was considered the maximum, minimum, mean and standard deviation of deposits at the end of one year simulations are 0.523, -0.348, -0.002 and 0.083 m respectively. The total deposited sediment mass was 9000 tons/year for the variable head and 8000 tons/year for the constant head tests. Similar studies were made to compare head aggregates of 1 hour, 1 day, and 1 year with head varying every 15 minutes. It was concluded to assume a constant head in long-term simulation of the Lautrach reservoir to bridge a gap in the limitation of data availability as well as to facilitate computational effort.

5.1.2 Effect of sediment fraction aggregation

The effect of using multi-fraction and mono-fraction sediment input on the amount and spatial distribution of sedimentation was investigated by assuming d_{16}, d_{50} and d_{84} of the

sediment grains to comprise 25, 50 and 25 % respectively for the multi-fraction assumption and d_{50} to represent the whole sediment input for the mono-fraction computation. The critical erosion shear velocity of 0.02 m/s and a spatially varying Manning-Strickler coefficient of 37.6 to 41 $m^{1/3}/s$ was used.

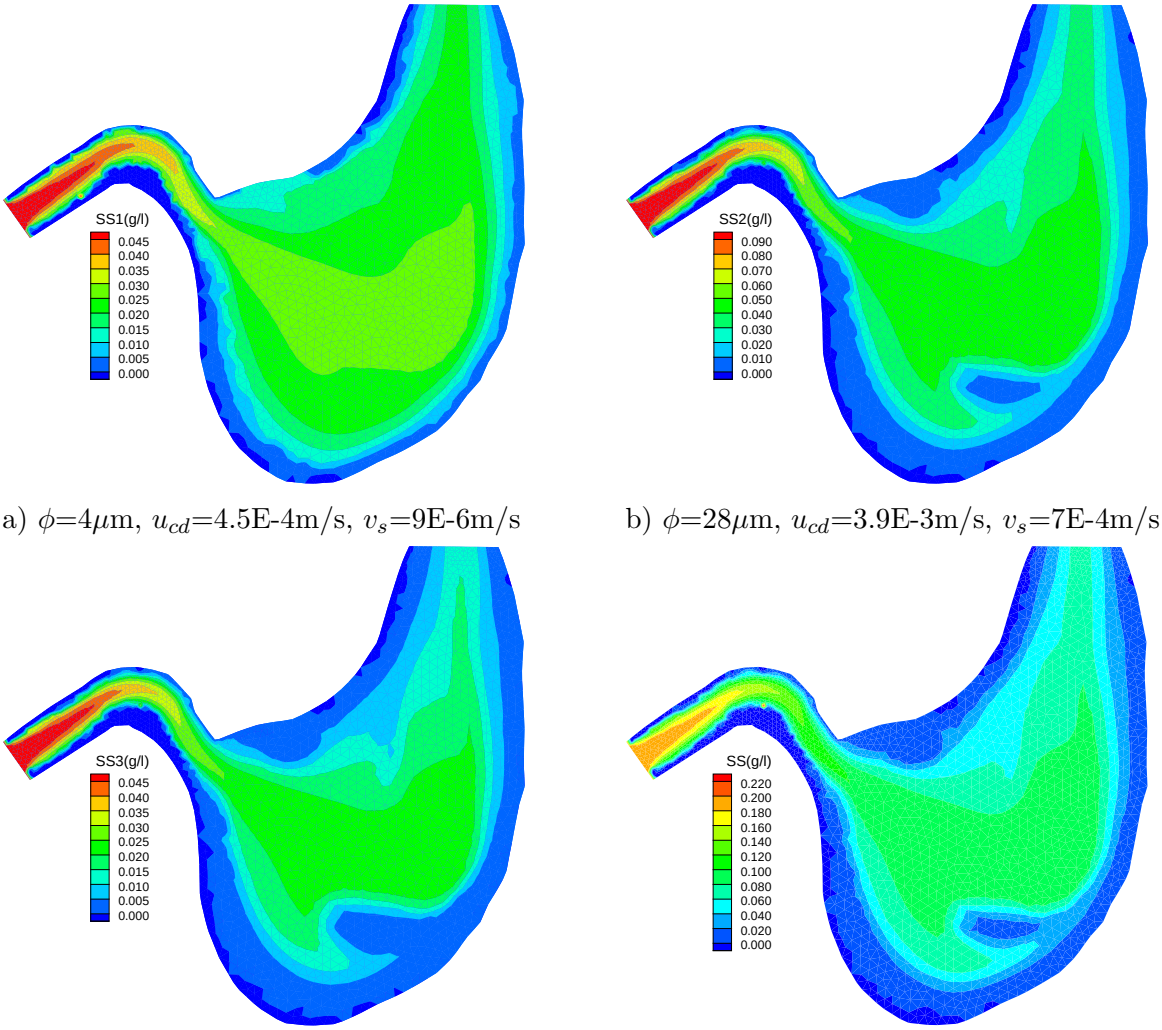

a) ϕ=4μm, u_{cd}=4.5E-4m/s, v_s=9E-6m/s

b) ϕ=28μm, u_{cd}=3.9E-3m/s, v_s=7E-4m/s

c) ϕ=77μm, u_{cd}=4.9E-3m/s, v_s=1E-3m/s

d) ϕ=28μm, u_{cd}=3.9E-3m/s, v_s=7E-4m/s

Figure 5.6: Patterns of the spatial distribution of sediment concentration for different grain size fractions: a), b), c) multi-fractional simulation; d) mono-fractional simulation

The spatial distribution of sedimentation compared at the end of computational period of 5 years between 1983 to 1988 is given in the Figure 5.7 below. The minimum, maximum, mean, and standard deviation of depth of sedimentation/erosion for the multi-fractional sediment is -1.42, 1.93, 4.67E-2, 1.79E-1 m respectively and the corresponding amounts for the mono-fractional sediment is -0.77, 2.12, 6.91E-2 and 1.55E-1 m. The amount of deposited sediment mass were 18500 and 25000 tons for the multi-fractional and mono-fractional assumption respectively. The difference of some 25%, mainly comes from the erosion of the finest particles of the multi-fractional assumption, and can reduce if the erosion shear velocity were assumed higher. For a long-term calibration and validation steps, see Chapter 6, it was decided to consider mono-fractional sediment, neglecting the differences.

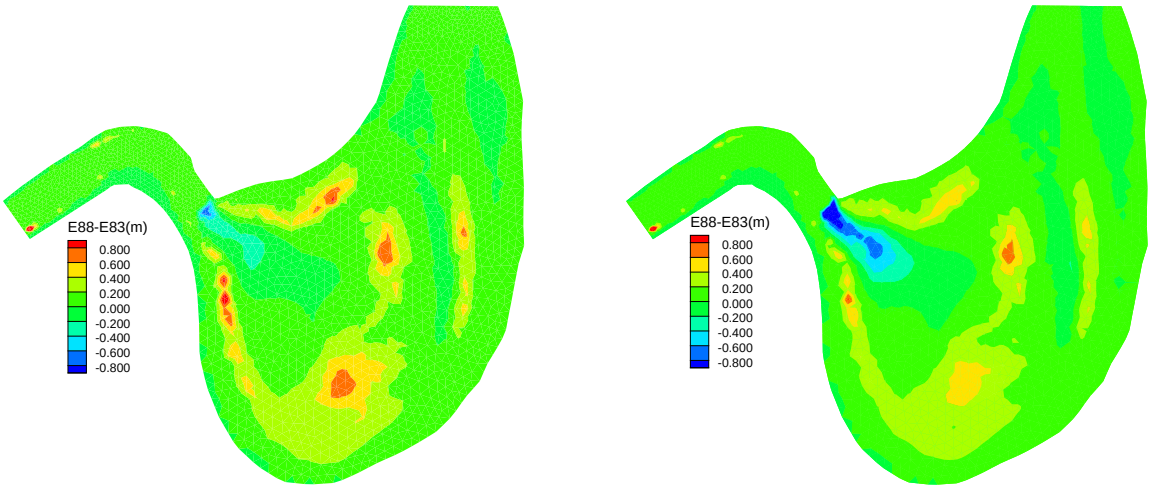

a) Mono-fractional sediment b) Multi-fractional sediment

Figure 5.7: Comparison of the spatial distributions of bed evolution between mono-fractional and multi-fractional sediment assumptions, 1983-1988

5.2 Effects of spatial and temporal refinements

Insufficient spatial or temporal resolution is a common source of errors in numerical solutions for both flow and sediment transport models, see Section 2.5.3. Investigations made on the sensitivity of the sediment mass deposition to grid refinement and numerical time refinements are presented below.

Spatial refinements: The mass of deposited sediment under various grid refinements at initial morphological conditions for the years 1983, 1988, 1992 and 1996 are compared and two cases are shown in Figure 5.8. The grid refinement must be sufficient to represent the reservoir geometry with acceptable approximation requiring a reasonable computational time to allow long-term simulation. It is a very important step in model simplification and must be carefully considered.

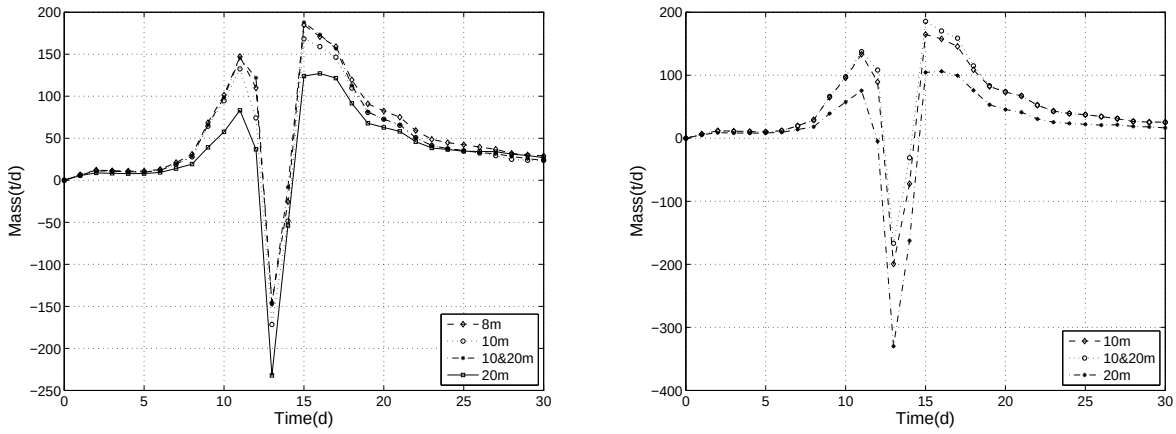

a) Rate of deposition, bed profile 1988 b) Rate of deposition, bed profile 1992

Figure 5.8: Deposited sediment mass under various refinements of numerical grids

Samples of the spatial distribution of sedimentation at the end of simulations for the profiles of 1988 are indicated in Figure 5.9 below. The following points can be concluded from the

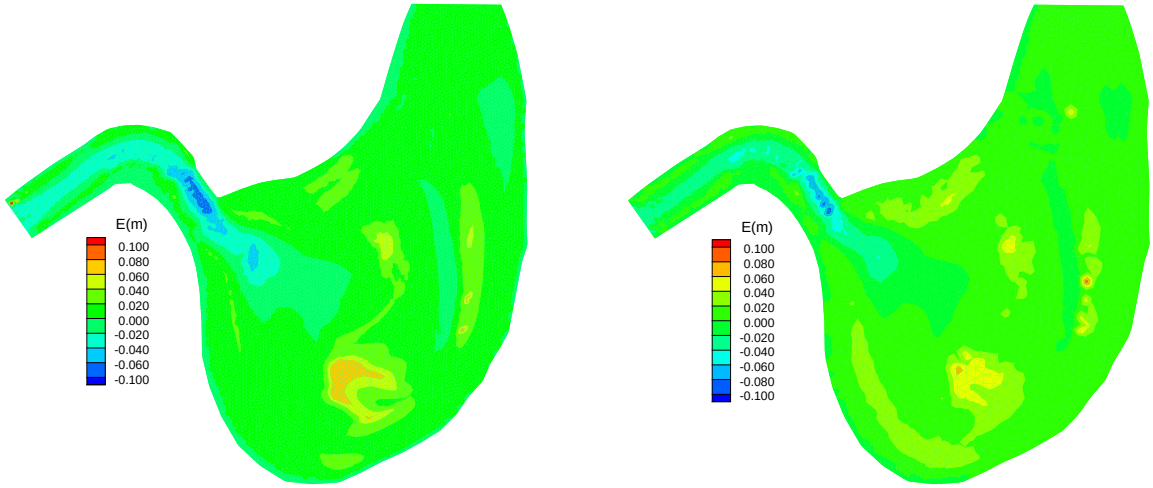

a) Grid size 8 m b) Grid size 10&20 m

Figure 5.9: Spatial distribution of bed evolution for the year 1988 under various spatial discretization

study on grid refinement:

- the initial morphological condition had an influence on the accuracy that various grid refinements showed with respect to the finest grid used in each cases, 1983, 1988, 1992, and 1996.
- the spatial distribution of sedimention/erosion is similar under all refinements investigated.
- for the uniform meshes studied, grid coarsening underestimated the total mass deposition.
- the rate of sediment mass deposition during the low discharge period were less affected by grid refinements.
- the amount of mass deposit for the same boundary conditions used (except the bottom geometry), reduced over time, showing the trend of filling up of the reservoir towards its equilibrium.

The computational time that was used for flow and transport runs on meshes of 8 m, 10 m, 10&20 m and 20 m were 18.2, 6.7 , 3.2 and 1.7 hours, respectively. Time steps of 10 seconds were taken for numerical runs for the whole period of computation of 30 days. Interpreting the results and the computational demand, it was decided to use an adaptive mesh of 10&20 m for the long-term simulation study of Chapter 6.

Temporal refinement: The effect of using different time steps on the computational result were investigated, assuming the initial morphological conditions of the year 1988. A typical results of the effect of temporal discretization on the time step is shown in the

Figure 5.10 for the case of the uniform mesh 10 m and spatially adaptive mesh type 10&20 m. The effect of time steps and spatial discretization in the calculation of total amount

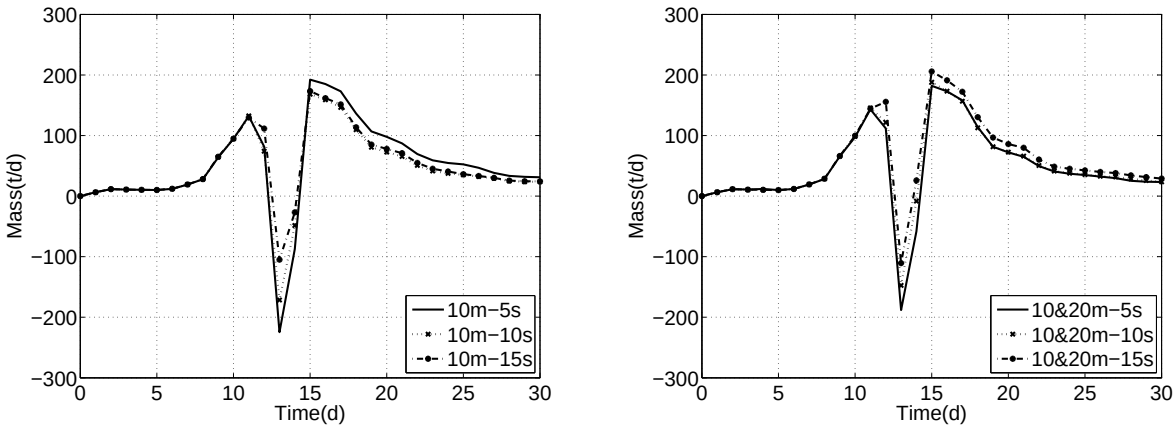

a) Grid 10m b) Grid 10&20m

Figure 5.10: Comparison of rate of sediment mass deposition for various time steps on the profile of 1988

of mass deposited is effected by fluctuations in erosion and deposition fluxes at each node and computational time step. The errors propagated over the whole computational period. Most of the discrepancies occurred at periods of peak flows. It was concluded that the peak flow periods have to be simulated with highly refined temporal resolutions.

For the steady simulations, numerical experiment indicated that the time step resolutions has no effect on the amount and spatial distribution of sedimentation. In general, time steps of 10 s was assumed in the model calibration and validation procedures, unless for the extreme flood events where 5 s were used.

5.3 Flow and transport coupling

An investigation was made on coupling intervals between flow and transport in using a decoupled TELEMAC-SUBIEF model. In this approach, the flow is first simulated and the flow field is stored as an external file at a chosen time interval. The transport model then uses the stored flow fields (velocities, flow depths, and turbulent viscosities) in solving the advection and dispersion of suspended sediment. At each numerical time step of the transport model, the flow field necessary for the solution of sediment transport module is interpolated linearly from the interval at which the flow fields are stored.

Hourly discharge and sediment data were used and the flow model was run for a period of 1 month and the flow field was saved at an interval of 1 hour, 12 hours and 1 day. The transport module was then coupled with the flow field at intervals of 1 hour, 12 hours and 1 day, respectively. Figure 5.11 a) shows the comparison of the amount of daily mass deposited for the three different assumptions indicating the importance of coupling time. Similarly, a daily discharge and sediment data were used, and the flow model was run for a period of 1 month and the flow field were saved at an interval of 1 hour, 6 hours and 1

day, and the transport module was then coupled with the flow model at an interval of 1 hour, 6 hours and 1 day respectively. The results of the effect of coupling is shown in the Figure 5.11 b). From the results it can be seen that the effect of coupling is pronounced

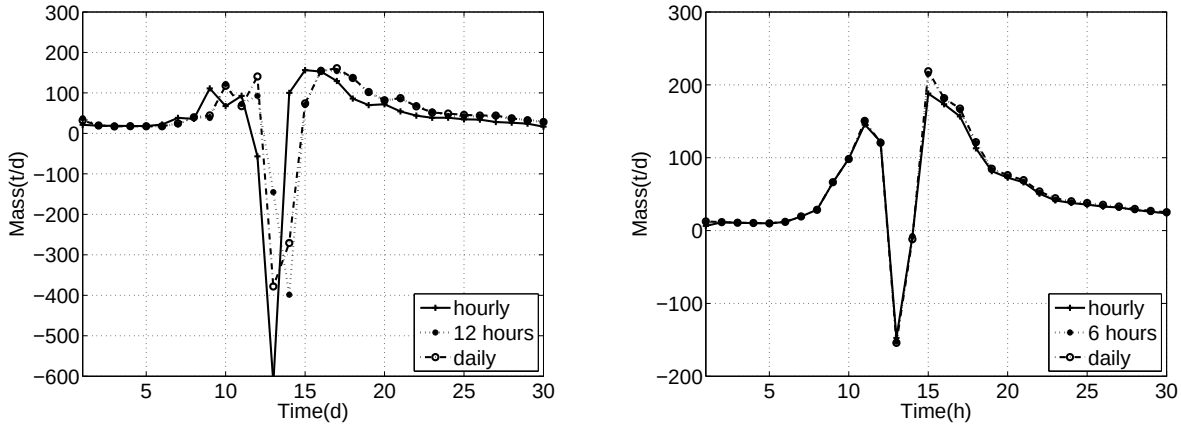

a) Rate of deposition, hourly Q and SS b) Rate of deposition, daily Q and SS

Figure 5.11: Comparison of the rate of sediment mass deposition for various coupling periods using the decoupled simulation

when the data is at higher resolution as shown in a), indicating an hourly data lead to more discrepancy as compared to the daily data.

Comparison was also made between the decoupled modeling approach and a coupling made at numerical time step. Figure 5.12 shows the spatial distribution of sedimentation for the decoupled and coupled approaches at the end of simulation of 1 month for the same inputs. The figure shows that the coupled and the decoupled modeling approach yield similar spatial distribution of sedimentation, however, the decoupled modeling approach overestimates the deposition heights.

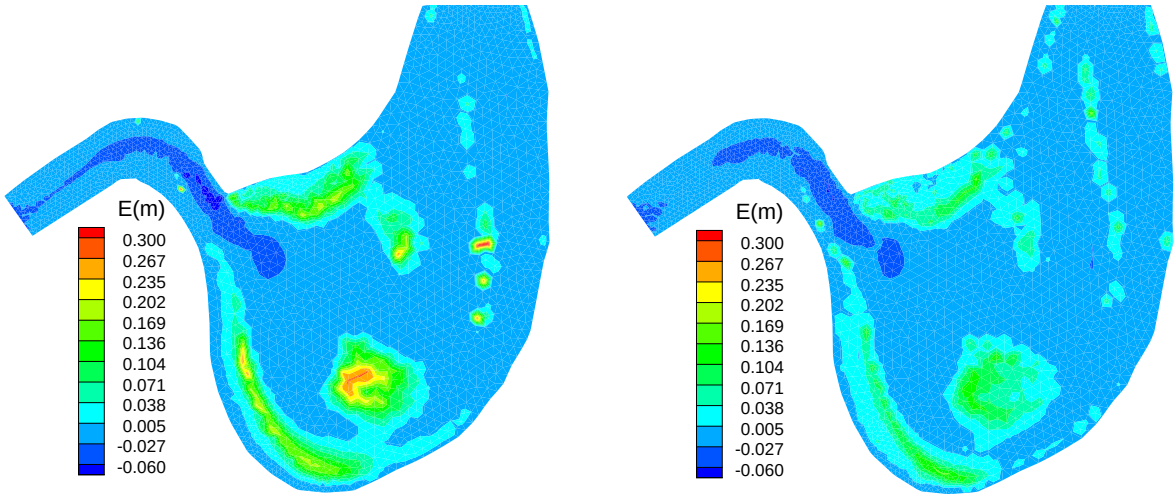

a) Decoupled b) Coupled

Figure 5.12: Spatial distribution of sediment deposition heights using the coupled and decoupled simulations

The study indicates the role of coupling methods in sediment transport simulation. In this

work, the decoupled modeling approach was used. It was also decided to use flow fields saved at an interval of 1 day as an input into the sediment transport module.

5.4 Turbulence models

The turbulence model also plays a significant role in flow and sediment transport modeling. Sophisticated models like the k-ε model, see Section 2.1, can be replaced by simpler models like the Elder model in which longitudinal and lateral dispersion coefficients are calibrated or the constant eddy viscosity model in which constant eddy viscosity is used.

In this study an investigation were made on comparative analysis of the k-ϵ model, the Elder model and the constant eddy viscosity model. Assuming the k-ϵ model as a reference, it was calibrated that Elder model with longitudinal dispersion coefficient of 6 and cross sectional dispersion coefficient of 0.6 has yielded close results. A constant eddy viscosity model was also investigated indicating difficulties in spatial distribution of sedimentation particularly under higher unsteadiness. Figure 5.13 below shows a comparison of total mass deposited using k-ϵ model with Elder model of various coefficients.

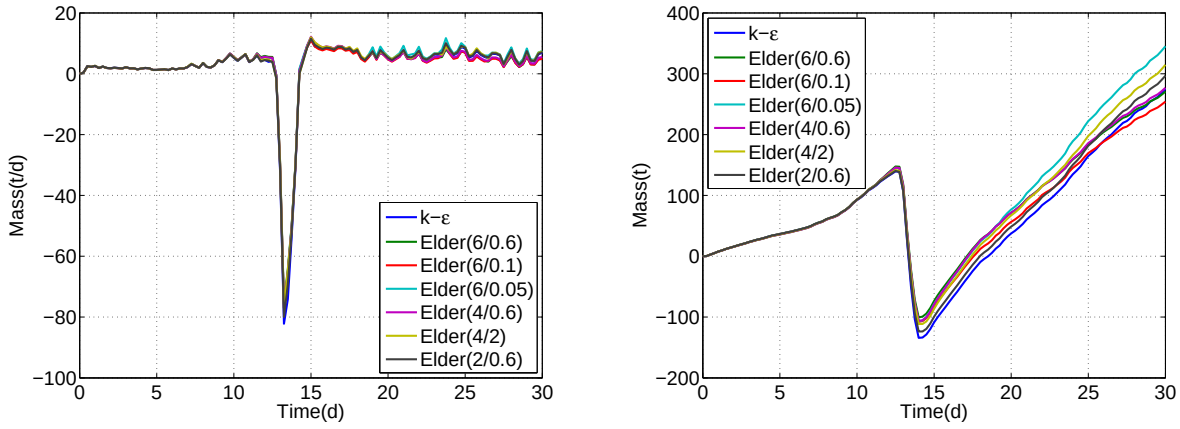

a) Daily rate of mass deposition

b) Cumulative mass deposition

Figure 5.13: Comparison of the use of the k-ϵ and the Elder turbulence models on outcome of daily and cumulative sediment mass deposition

The spatial distribution of sedimentation under various turbulence models indicated the importance of the parameters in dispersing sediment. With the Elder model it was possible to enhance the dispersion across the flow than with the more sophisticated k-ϵ model. The computational demand for the three models indicated the k-ϵ model as the most expensive and the constant eddy diffusivity as the least expensive (20 % lower) solution. The Elder model demanded 17 % lower computational time. For investigation of long-term modeling it was decided to use the k-ϵ model.

5.5 Solver type and accuracy

The effect of methods of solutions and solver accuracies were investigated and shown in Figure 5.14. The models with SA had solver accuracies of 1E-4 for the flow and 1E-6 for the transport models and the models with SA2 had solver accuracies of 1E-6 for the flow and 1E-9 for the transport models. The cumulative mass deposition showed a maximum difference of 6 % for the time step of 15 seconds. The time requirement for computation of SA2 increased by 18-31 %, the highest for the 15 second time step.

Comparison on the method of solver used among GMRES, conjugate gradient, and conjugate residual indicated insignificant change with respect to the amount of mass deposition. The computational time was the cheapest for conjugate gradient and the most expensive for GMRES. The order of difference was 5 %. See Figure 5.14 b). For long-term simulation studies it was decided to use GMRES solver and solver accuracy of the first option, SA. Study made on comparisons of implicit and explicit formulation resulted in insignifi-

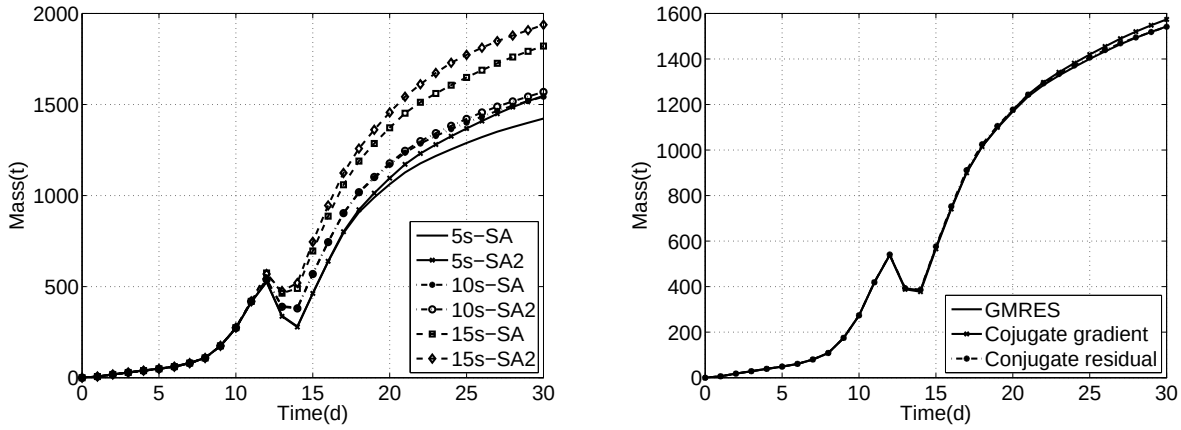

a) Solver accuracies b) Solver types

Figure 5.14: Comparison sediment mass deposition in using various solver accuracies and types

cant discrepancy of the amount and spatial distribution of mass deposition. The implicit formulation were found to be expensive by about 20 % for the numerical experiments made.

Summary

In this chapter preliminary investigations were made on the effects of modeling techniques in order to provide an insight on creating an optimal strategy to be implemented for long-term calibration and validation of bed evolution of the Lautrach reservoir. Numerical tests on using different data aggregation, spatial and temporal discretization, coupling methods and turbulence models, led to simplifications that can be applied for long-term morphological simulation. Chapter 6 follows based on the simplifications and assumptions proposed in this chapter by carrying out, long-term model calibration and validation.